Evaluating the Fatigue and Healing Performance of Asphalt Binders in Base Course Mixtures Using Various Test Protocols

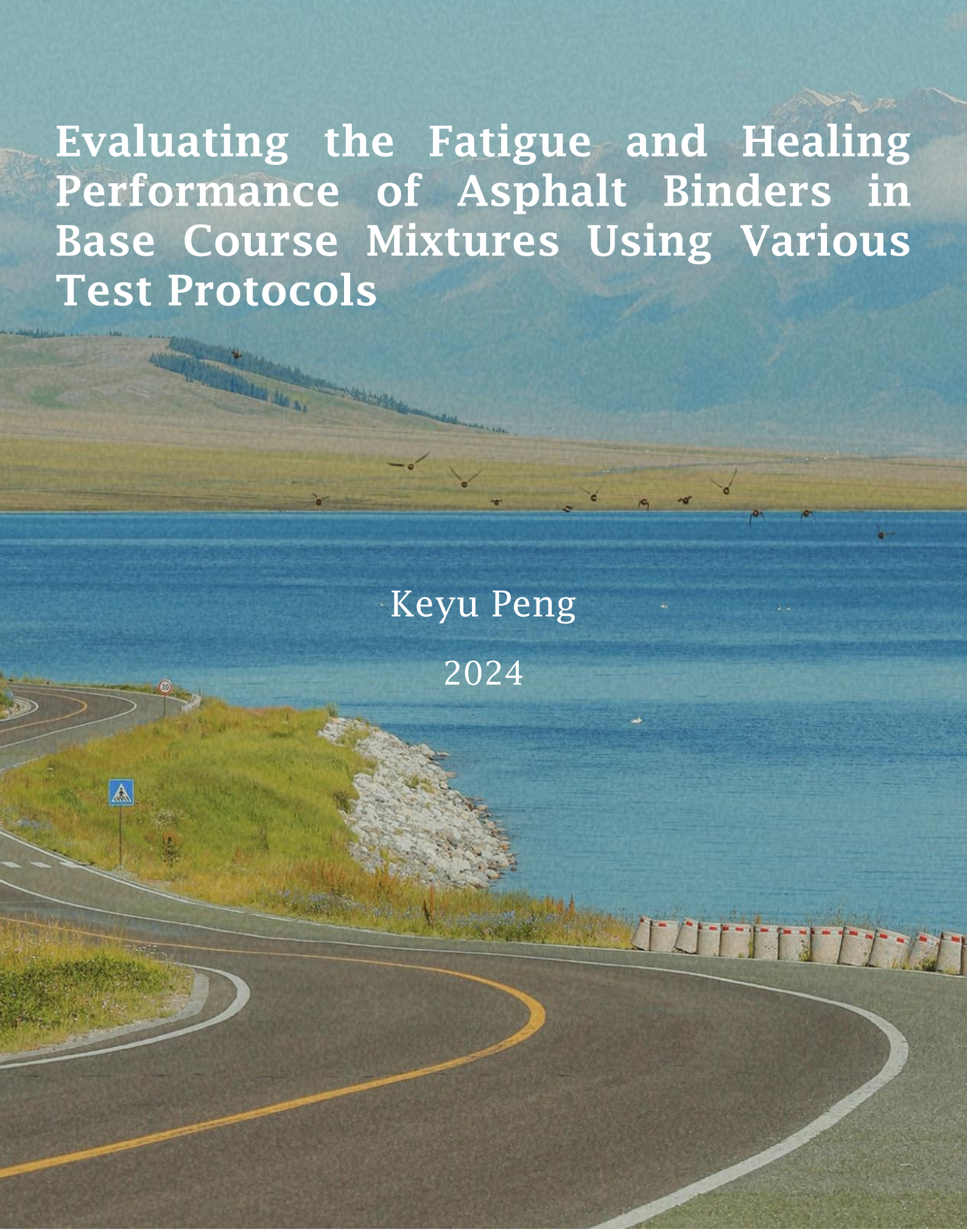

Keyu Peng

2024

TU Delft
TNO innovation for life
Rijkswaterstaat
Ministerie van Infrastructuur en Milieu
DURA VERMEER

MSc thesis in Structural Engineering

Evaluating the Fatigue and Healing Performance of Asphalt Binders in Base Course Mixtures Using Various Test Protocols

Keyu Peng

November 2024

A thesis submitted to the Delft University of Technology in partial fulfillment of the requirements for the degree of Master of Science in Structural Engineering

Keyu Peng: *Evaluating the Fatigue and Healing Performance of Asphalt Binders in Base Course Mixtures Using Various Test Protocols* (2024)

The work in this thesis was carried out in the:
Pavement engineering group
Delft University of Technology

Student number: 5841119

Chair	Dr. Xueyan Liu	(TU Delft)
Daily Supervisor:	Dr.ir. Panos Apostolidis	(TU Delft)
Thesis Committee members:	Prof.dr.ir. Sandra Erkens	(TU Delft)
	Prof.dr.ir. Erik Schlangen	(TU Delft)
	ir. Robbert Naus	(Dura Vermeer))
	ir. G.A. (Greet) Leegwater	(TNO)

Acknowledgements

With the completion of this master's thesis, my journey as a master's student at TU Delft is drawing to a close. Here, I would like to express my heartfelt gratitude to everyone who has supported me along the way.

First, I would like to extend my sincere thanks to Dr. Xueyan Liu, Chair of my thesis committee, for his invaluable guidance throughout my research and even before the thesis began. His expertise and constructive suggestions were instrumental in shaping this thesis, and I deeply appreciate his dedication to my academic and personal development, especially given his busy schedule. His attention to my experiments, research progress and thesis writing, as well as his timely suggestions, provided essential direction. I am also particularly grateful to my daily supervisor, Dr. Panos Apostolidis, for his constant support and encouragement during my thesis journey. Dr. Apostolidis not only helped me overcome the academic challenges I encountered but also gave me the confidence to push through difficult moments. I am very appreciative of his diligent reviews of my thesis and his timely, insightful feedback.

My heartfelt thanks also go to the other members of my thesis committee: Prof.dr.ir. Sandra Erkens, Prof.dr.ir. Erik Schlangen, ir. Greet Leegwater (TNO), and ir. Robbert Naus (Dura Vermeer). Their expertise, insights, and guidance were invaluable in the successful completion of this thesis. I am particularly grateful to them for attending each of my committee progress meetings despite their busy schedules and providing constructive feedback. I would also like to acknowledge the support of Rijkswaterstaat, TNO, and Dura Vermeer in this research.

I would like to express my sincere gratitude to my colleagues in the pavement engineering group, who provided assistance throughout my research. I am grateful to ir. Marco Poot, whose optimistic spirit, knowledge, and experience in asphalt materials helped me overcome numerous challenges in the lab. My thanks also go to ir. Michele van Angelen for his support, particularly in the crucial PAV aging process. Additionally, I would like to acknowledge Dr. Shisong Ren, Dr. Yi Li, Dr. Lili Ma, and ir. Rui Wu for their professional and emotional support.

Special thanks go to my dear friends Pengyi Dai, Yihan Hu, Zhaoyu Yan, and Lu Wang, whose companionship, encouragement, and support made this master's journey at TU Delft an enjoyable experience. Finally, I want to express my deepest gratitude to my parents for their unwavering love, support, and encouragement. Their belief in me has been the foundation of my resilience and success.

Keyu Peng

Delft, November 2024

Abstract

Asphalt pavements play a crucial role in constructing durable and sustainable road infrastructure. In recent years, with the advancement of sustainability and circular economy goals, reclaimed asphalt (RA) has been widely used in road construction. While the use of RA effectively reduces resource consumption and environmental impact, research on the fatigue and healing performance of asphalt mixtures and binders with high RA content remains relatively limited. This study aims to evaluate the healing performance of binder components from three asphalt mixtures commonly used in the base layers of Dutch pavements, employing multiple healing test protocols and healing indices. Two of these binders contain a high proportion of RA bitumen.

To achieve the research objectives, fatigue and healing tests were conducted on three different asphalt binders: Binder 1, composed entirely of fresh bitumen; Binder 2, a blend of high RA content bitumen with softer fresh bitumen; and Binder 3, which includes high RA bitumen content, fresh bitumen, and the rejuvenator. Fatigue performance was evaluated using Time Sweep (TS) and Linear Amplitude Sweep (LAS) tests to determine the fatigue life of each binder. Additionally, healing performance was assessed through single-rest period and multiple-rest period Time Sweep Healing (TS-H) tests, as well as Linear Amplitude Sweep Healing (LAS-H) tests. To evaluate healing performance, two different indices were used: the Healing Shift Factor (SF_h), based on fatigue life extension, and the Healing Index (HI), based on modulus recovery. The TS and TS-H tests were conducted at three different strain levels, followed by fitting to obtain fatigue lines and fatigue equations. The LAS and LAS-H tests were carried out under controlled temperature and frequency conditions. The S-VECD theory was applied to calculate material damage, allowing for fatigue life predictions based on the model.

The test results showed that Binder 3, which contains high RA bitumen content and rejuvenator, exhibited the highest healing performance in half of the cases, particularly in the multiple-rest period TS-H tests. In contrast, Binder 2, also containing high RA bitumen but blended with softer fresh bitumen, showed a more complex response; it showed the highest healing performance in single-rest period tests but displayed lower healing potential in multiple-rest period tests.

The differences between single and multiple rest period tests highlight the limitations of single rest period tests in fully capturing material healing capacity, indicating that more complex loading patterns should be explored for more comprehensive assessments. The variations in healing potential results across different test methods and indices suggest that the healing performance of binders is highly sensitive to test protocol and indices selection.

Based on the described approach, a better understanding of the healing performance of different asphalt binders is achieved. Conclusions and future recommendations for research in this field were provided at the end of this research.

Contents

1. Introduction **2**
- 1.1. Research Context . . . 2
- 1.2. Research Problem . . . 2
- 1.3. Research Objectives . . . 3
- 1.4. Research Scope . . . 3
- 1.5. Research Questions . . . 3
- 1.6. Research structure . . . 4
- 1.7. Research Methodology . . . 5

2. Literature Review **7**
- 2.1. Asphalt Fatigue . . . 7
  - 2.1.1. Fatigue Cracking Principles . . . 7
  - 2.1.2. Fatigue Cracking: Shift Factor . . . 9
- 2.2. Asphalt Healing . . . 11
  - 2.2.1. Asphalt Healing Mechanisms . . . 11
  - 2.2.2. Types of Asphalt Healing . . . 12
  - 2.2.3. Factors Affecting Healing . . . 13
  - 2.2.4. Biasing Effects . . . 14
- 2.3. Introduction and Challenges of Reclaimed Asphalt (RA) . . . 15
- 2.4. Fatigue and Healing Testing Methods of Asphalt Binders . . . 15
  - 2.4.1. Time Sweep (TS) and Time Sweep Healing (TS-H) Tests . . . 16
  - 2.4.2. Linear Amplitude Sweep (LAS) and Linear Amplitude Sweep Healing (LAS-H) Tests . . . 16
  - 2.4.3. Intrinsic Two-Piece Healing (TPH) Test . . . 17
  - 2.4.4. Direct Tension Test (DTT) . . . 18
  - 2.4.5. Binder Bond Strength (BBS) Test . . . 20
- 2.5. Viscoelastic Continuum Damage (VECD) Theory . . . 21
- 2.6. Healing Indices . . . 23
- 2.7. Previous Experience in Healing in Asphalt Binder Materials . . . 25

3. Materials and Methods **28**
- 3.1. Materials . . . 28
- 3.2. Testing protocols . . . 31
  - 3.2.1. TS/TS-H Tests . . . 32
  - 3.2.2. LAS/LAS-H Tests . . . 34
- 3.3. Healing Indices Used In This Study . . . 37
  - 3.3.1. Healing Shift Factor SF_h Interpretation . . . 37
  - 3.3.2. Time Sweep Healing Index HI_{TS} Interpretation . . . 37
  - 3.3.3. Linear Amplitude Sweep Healing Index HI_{LAS} Interpretation . . . 38

4. Fatigue Test Results **40**
- 4.1. Time Sweep Test Results . . . 40

4.2. Linear Amplitude Sweep Test Results . . . 42
4.3. Comparison of TS Measured Fatigue Life with LAS Predicted Fatigue Life . . . 43
4.4. Comparison Between Binder Fatigue Life and Mixture Fatigue Life . . . 46
4.5. Conclusions of the Fatigue Tests . . . 48

5. Healing Test Results **50**
5.1. Time Sweep Healing Test Results . . . 50
5.1.1. Single rest period TS-H test . . . 50
5.1.2. Multiple rest period TS-H test . . . 54
5.2. Linear Amplitude Sweep Healing Test Results . . . 62
5.3. Comparison between TS-H measured fatigue life and LAS-H predicted fatigue life 64
5.4. Conclusions of the Healing Tests . . . 66

6. Conclusions and Recommendations **69**
6.1. Conclusions . . . 69
6.1.1. Main Research Question . . . 69
6.1.2. Sub-questions . . . 69
6.2. Recommendations and Future Work . . . 71
6.2.1. Recommendations . . . 71
6.2.2. Future Work . . . 72

A. Materials and Methods **81**
A.1. Mixture Properties . . . 81
A.2. Binder Composition Calculation . . . 83

B. Fatigue Test Results **85**
B.1. Time Sweep Test Modulus Evolution Curves . . . 86
B.2. Linear Amplitude Sweep Test C-S Curves . . . 95

C. Healing Test Results **97**
C.1. TS-H Single Modulus Evolution Curves . . . 97
C.2. TS-H Multi Modulus Evolution Curves . . . 101
C.3. LAS-H Test Results . . . 107

List of Figures

1.1. Research structure. . . . 5
1.2. Research methodology. . . . 5

2.1. Typical fatigue curve for asphalt concrete (Ragni et al., 2020). . . . 8
2.2. Crack healing model proposed in polymers (Wool and O'connor, 1981). . . . 11
2.3. Three-step mechanism of healing (Qiu, 2012). . . . 12
2.4. Evolution of stiffness modulus under different loading levels (Wang and An, 2024). . . . 14
2.5. DSR set up. . . . 17
2.6. Illustration of the TPH setup using Dynamic Shear Rheometer, (a) Attaching two pieces of bitumen on top and bottom plates; (b) Decreasing the gap width to allow full contact of the two pieces and measuring the change in complex shear modulus over time; (c) Removing the upper plate after the testing (Qiu, 2012). . . . 18
2.7. Illustration of healing test using the DTT (Qiu, 2012). . . . 19
2.8. Schematic representation of the 2-piece healing test method with sequential steps (Leegwater et al., 2018). . . . 19
2.9. The procedure of BBS test (a)–(d) preparation of the sample and (e) appearance of Positest AT-A apparatus and (f) stubs with marks (Zhou et al., 2020). . . . 20
2.10. Damage characteristic curve. . . . 22

3.1. Shortened title for the list of figures . . . 29
3.2. Frequency sweep results of bitumen under various aging conditions. . . . 30
3.3. Shortened title for the list of figures . . . 30
3.4. Frequency sweep results of blended binders. . . . 31
3.5. The loading pattern of the TS test. . . . 32
3.6. The loading pattern of the single rest period TS-H test. . . . 33
3.7. The loading pattern of the multiple rest periods TS-H test. . . . 34
3.8. The loading pattern of the continuous LAS test. . . . 35
3.9. The loading pattern of the LAS-H test. . . . 35
3.10. The typical shear stress-strain response of in the LAS test. . . . 36
3.11. Schematic of the healing index HI_{TS} variables. . . . 37
3.12. Schematic of the healing index HI_{LAS} variables. . . . 38

4.1. Complex modulus evolution of Binder 1 in the strain-controlled TS tests. . . . 40
4.2. Fatigue lines of three binders in the TS tests. . . . 41
4.3. Damage characteristic curves of three binders in the LAS tests. . . . 42
4.4. Predicted fatigue life of three binders in the LAS tests. . . . 43
4.5. Fatigue results from TS and LAS tests. . . . 44
4.6. Comparison between TS measured fatigue life and LAS predicted fatigue life of: (a) Binder 1; (b) Binder 2; and (c) Binder 3. . . . 45

4.7. Shortened title for the list of figures 47

5.1. Modulus evolution curve of Binder 1 at 2.5% strain in TS-H Single test. 50
5.2. Fatigue lines in TS and TS-H Single tests of (a) Binder 1; (b) Binder 2; (c) Binder3. 51
5.3. TS healing index HI_{TS} of three binders in TS-H Single tests 53
5.4. Modulus evolution curve of Binder 1 at 2.5% strain in TS-H Multi test. 54
5.5. Fatigue lines in TS, TS-H Single and TS-H Multi tests of: (a) Binder 1; (b) Binder 2; and (c) Binder 3. 55
5.6. Complex modulus evolution of Binder 2 under (a) 2.5% strain level; and (b) 5% strain level. 59
5.7. Complex modulus evolution of Binder 1 under (a) 2.5% strain level; and (b) 5% strain level. 60
5.8. Complex modulus evolution of Binder 3 under (a) 2.5% strain level; and (b) 5% strain level. 60
5.9. TS healing index HI_{TS} in TS-H Multi tests of (a) Binder 1, (b) Binder 2, and (c) Binder 3. 61
5.10. Healing shift factors of three binders under 100s and 1000s rest period. 62
5.11. LASH Healing Index results of three binders under 100s and 1000s rest period. 63
5.12. Comparison between TS-H Single measured fatigue life and LAS-H predicted fatigue life of (a) Binder 1; (b) Binder 2; and (c) Binder 3. 65

A.1. Aggregate gradation of the asphalt mixtures. 82

B.1. Binder 1 modulus evolution at 1.5% strain in TS test. 86
B.2. Binder 1 modulus evolution at 2.5% strain in TS test. 87
B.3. Binder 1 modulus evolution at 5% strain in TS test. 88
B.4. Binder 2 modulus evolution at 1.5% strain in TS test. 89
B.5. Binder 2 modulus evolution at 2.5% strain in TS test. 90
B.6. Binder 2 modulus evolution at 5% strain in TS test. 91
B.7. Binder 3 modulus evolution at 1.5% strain in TS test. 92
B.8. Binder 3 modulus evolution at 2.5% strain in TS test. 93
B.9. Binder 3 modulus evolution at 5% strain in TS test. 94
B.10. Binder 1 LAS test C-S curve. 95
B.11. Binder 2 LAS test C-S curve. 95
B.12. Binder 3 LAS test C-S curve. 96

C.1. Binder 1 modulus evolution at 2% strain in TS-H Single test. 97
C.2. Binder 1 modulus evolution at 2.5% strain in TS-H Single test. 97
C.3. Binder 1 modulus evolution at 5.0% strain in TS-H Single test. 98
C.4. Binder 2 modulus evolution at 2.0% strain in TS-H Single test. 98
C.5. Binder 2 modulus evolution at 2.5% strain in TS-H Single test. 99
C.6. Binder 2 modulus evolution at 5.0% strain in TS-H Single test. 99
C.7. Binder 3 modulus evolution at 2.0% strain in TS-H Single test. 100
C.8. Binder 3 modulus evolution at 2.5% strain in TS-H Single test. 100
C.9. Binder 3 modulus evolution at 5.0% strain in TS-H Single test. 101
C.10. Binder 1 modulus evolution at 1.5% strain in TS-H Multi test. 101
C.11. Binder 1 modulus evolution at 2.5% strain in TS-H Multi test. 102
C.12. Binder 1 modulus evolution at 5.0% strain in TS-H Multi test. 102
C.13. Binder 2 modulus evolution at 2.0% strain in TS-H Multi test. 103
C.14. Binder 2 modulus evolution at 2.5% strain in TS-H Multi test. 104

C.15. Binder 2 modulus evolution at 5.0% strain in TS-H Multi test. 105
C.16. Binder 3 modulus evolution at 2.0% strain in TS-H Multi test. 106
C.17. Binder 3 modulus evolution at 2.5% strain in TS-H Multi test. 106
C.18. Binder 3 modulus evolution at 5.0% strain in TS-H Multi test. 107
C.19. Binder 1 LASH 100s test C-S curve. 107
C.20. Binder 1 LASH 1000s test C-S curve. 108
C.21. Binder 2 LASH 100s test C-S curve. 108
C.22. Binder 2 LASH 1000s test C-S curve. 109
C.23. Binder 3 LASH 100s test C-S curve. 109
C.24. Binder 3 LASH 1000s test C-S curve. 110

List of Tables

2.1. Empirical shift factors from previous studies. 10
2.2. Studies on healing indices from previous research (Varma et al., 2021). 24

3.1. Binder composition. 29
3.2. Loading frequencies applied in the frequency sweep test. 34
3.3. TS-H and LAS-H test settings. 36

5.1. Healing shift factors for the three binders in TS-H Single test. 52
5.2. TS healing index HI_{TS} of three binders in TS-H Single tests. 53
5.3. Fatigue equations of Binder 1 in TS and TS-H tests. 56
5.4. Fatigue equations of Binder 2 in TS and TS-H tests. 56
5.5. Fatigue equations of Binder 3 in TS and TS-H tests. 57
5.6. Healing shift factors for the three binders in TS-H Single and TS-H Multi tests. . 57
5.7. Healing shift factors of three binders under 100s and 1000s rest period. 63
5.8. Overall healing performance rankings of the three asphalt binders. 66

A.1. Percentages of materials used in the studied asphalt mixtures. 81
A.2. Aggregate gradation of the asphalt mixtures. 82

C.1. LAS Healing index of three binders under 100s and 1000s rest period. 110

Acronyms

Abbreviation	Definition
ISA	International Standard Atmosphere
BBS	Binder Bond Strength
CB	Carbon black
DER	Dissipated Energy Ratio
DSR	Dynamic Shear Rheometer
DTT	Direct Tension Test
HI	Healing Indices
HI_{LAS}	Linear Amplitude Sweep Healing Index
HI_{TS}	Time Sweep Healing Index
LAS	Linear Amplitude Sweep
LAS-H	Linear Amplitude Sweep Healing
LVE	Linear Viscoelastic
MMHC	Methylene-to-Methyl Hydrogen Carbon Ratio
NLVE	Nonlinear Viscoelastic
POTS	Pull-Off Tensile Strength
PSE	Pseudo-Strain Energy
RA	Reclaimed Asphalt
RDEC	Ratio of Dissipated Energy Change
S-VECD	Simplified Viscoelastic Continuum Damage
SBR	Styrene-Butadiene Rubber
SF	Shift Factor
SF_h	Healing Shift Factor
TFOT	Thin Film Oven Test
TPH	Intrinsic Two-Piece Healing
TS	Time Sweep
TS-H	Time Sweep Healing
VECD	Viscoelastic Continuum Damage
...	

1 Introduction

1. Introduction

1.1. Research Context

Fatigue cracking is one of the most common distresses in asphalt pavements, caused by the accumulation of damage due to repeated traffic loading. Initially, microcracks develop within the asphalt matrix, and with continuous traffic loading, these microcracks propagate into macrocracks, ultimately leading to pavement failure. This type of cracking significantly reduces the structural integrity and service life of the pavement. Moreover, fatigue cracking often triggers other forms of deterioration, such as raveling and rutting, exacerbating the overall degradation of the pavement structure (Cheng et al., 2021).

In response to growing demands for more sustainable and cost-efficient road infrastructure, along with the push for circular economy practices, the use of Reclaimed Asphalt (RA) has become increasingly common. In the Netherlands, the incorporation of up to 70% RA in base layer is now standard practice. However, the use of RA introduces variability in the material properties, particularly concerning aging, fatigue, and healing behavior.

Viscoelasticity is a fundamental property when evaluating the fatigue and healing performance of asphalt pavements. The asphalt binder is widely recognized as the primary source of viscoelastic behavior within asphalt mixtures (Zhang et al., 2019), it determines the rheological, cohesive and adhesive behaviors of asphalt mixtures at different material scales (Zhang and Gao, 2021). For asphalt concrete, fatigue cracks typically initiate at weak points such as the asphalt binder and mastic phases or at material interfaces, and then progressively propagate through the mortar phase and, eventually, affect the entire structure (Wang et al., 2023b). Therefore, the capacity of asphalt binders to recover from fatigue damage plays a critical role in prolonging pavement life, especially under repeated traffic loads.

Investigating the impact of incorporating reclaimed asphalt in base layer pavement on its healing and fatigue performance is a crucial task. This study focuses on evaluating the healing performance of three asphalt binders, including two with high RA bitumen content, using various healing test methods and healing indices. The findings of this research will contribute to improving existing pavement design methods and provide theoretical support for the efficient reuse of asphalt materials in the road construction industry, helping to reduce environmental impact.

1.2. Research Problem

Although the use of reclaimed asphalt is becoming increasingly common in road construction, the impact of high RA content on the fatigue performance and healing ability of asphalt mixtures and binders remains uncertain. Specifically, the aging of RA, increased stiffness, and

heterogeneity of the material may lead to a reduction in the fatigue resistance of the mixtures and adversely affect their healing capacity. While existing studies have proposed various healing test methods and evaluation indices, the results are not always consistent, and the understanding of asphalt healing mechanisms remains incomplete. Therefore, further research is needed to investigate the fatigue and healing behavior of high RA content binders under different testing conditions, to improve the accuracy of performance predictions for asphalt materials.

1.3. Research Objectives

This study aims to evaluate the fatigue and healing performance of the binder components of three commonly used asphalt mixtures, among which two contain a high RA content. Through various testing protocols, including single and multiple rest period Time Sweep Healing (TS-H) and Linear Amplitude Sweep Healing (LAS-H) tests, and utilizing different healing indices, this research seeks to analyze the healing performance of these binder components. Additionally, it compares the correlations and distinctions between the results of different healing test methods and indices.

1.4. Research Scope

This study focuses on analyzing the binder performance of three commonly used asphalt mixtures in the base layers of Dutch roads: a mixture containing 100% virgin asphalt aggregates, a mixture containing 70% RA and 30% virgin asphalt aggregates with soft bitumen, and a mixture containing 70% RA with a recycling agent ANOVA 1817. Using two primary healing test methods, Time Sweep Healing (TS-H) and Linear Amplitude Sweep Healing (LAS-H), the fatigue resistance and healing ability of these materials are evaluated under controlled laboratory conditions. The experimental conditions align with Dutch road design standards, aiming to provide scientific evidence on the fatigue and healing performance of RA-containing binders and offer recommendations for improving pavement design.

1.5. Research Questions

Main Question:

What is the healing performance of three asphalt binders used in base layer mixtures, as assessed by various healing test protocols and healing indices?

Sub questions:

1. How are the TS (TS-H) and LAS (LAS-H) tests characterized and what are their differences?
2. Which asphalt binder demonstrates the highest fatigue resistance?
3. What is the correlation between the fatigue test results of asphalt binders and asphalt mixtures?

4. Are there significant differences in the healing performance of asphalt binders between single rest period tests and multiple rest period tests?
5. What are the similarities and differences when evaluating the healing performance of asphalt binders using different healing indices?
6. Are the healing performances of asphalt binders consistent across different testing methods?

1.6. Research structure

This thesis report consists of 6 chapters and appendices, the research structure is shown in **Figure 1.1**.

Chapter 1: Introduction

This chapter introduces the research context, research problem, research objectives, research scope, and research questions, outlining the core topics and framework of this study.

Chapter 2: Literature Review

This chapter reviews studies related to the fatigue and healing performance of asphalt binders, describes common healing test methods and associated healing indices, and presents the background of viscoelastic continuum damage theory, providing the theoretical foundation for this research.

Chapter 3: Materials and Methods

This chapter details the materials and test methods used in the study, covering the preparation of asphalt binders, the testing methods, equipment, and testing procedures, as well as the healing indices selected for evaluating the healing performance.

Chapter 4: Fatigue Test Results

This chapter compares the fatigue results obtained from different testing methods and analyzes the relationship between the fatigue performance of asphalt binders and asphalt mixtures.

Chapter 5: Healing Test Results

This chapter presents the healing performance results of binders using different healing test methods and healing indices and makes a comparison of these results.

Chapter 6: Conclusions and Recommendations

This chapter provides the main conclusion and recommendations for future research.

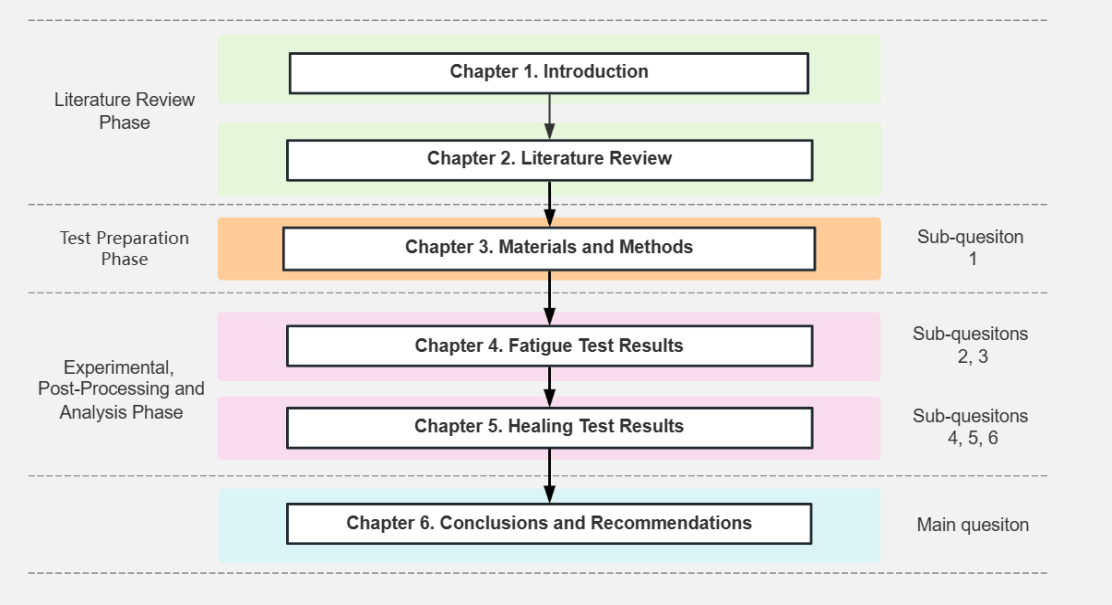

Figure 1.1.: Research structure.

1.7. Research Methodology

The research methodology of this thesis report is shown in **Figure 1.2**.

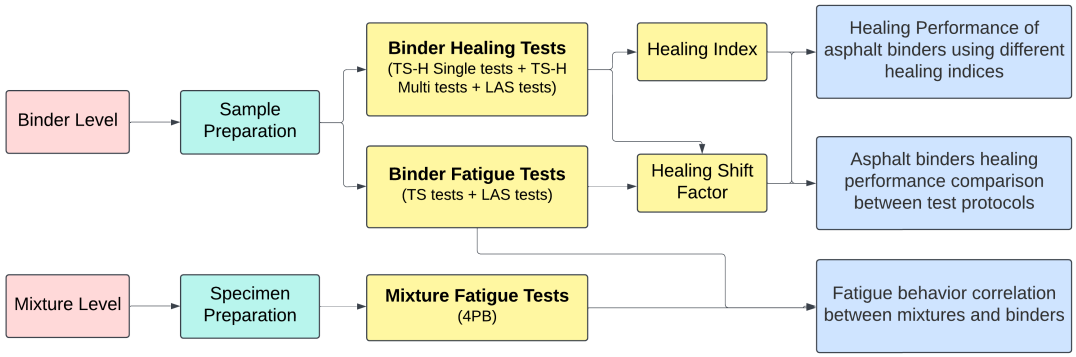

Figure 1.2.: Research methodology.

2

Literature review

2. Literature Review

This chapter provides the conceptual and theoretical foundation of this research. It begins by introducing the fatigue and healing performance of asphalt materials, emphasizing the critical role these properties play in enhancing pavement durability and extending the service life of roads. Following this, section 2.3 discusses the benefits and challenges of using reclaimed asphalt in newly constructed pavement. Section 2.4 provides an overview of commonly used testing methods for evaluating fatigue and healing in asphalt binders, with a focus on the Time Sweep Healing (TS-H) and Linear Amplitude Sweep Healing (LAS-H) tests utilized in this study.

Section 2.5 introduces the fundamental principles of the Viscoelastic Continuum Damage (VECD) theory and its simplified variant, the Simplified Viscoelastic Continuum Damage (S-VECD) model, which is used in LAS-H test analysis to predict fatigue life. Building on these theoretical foundations, section 2.6 explores various healing indices and examines their advantages and limitations in quantifying the healing potential of asphalt binders. Finally, section 2.7 reviews the latest advancements in asphalt binder healing research.

2.1. Asphalt Fatigue

2.1.1. Fatigue Cracking Principles

Fatigue cracking is one of the primary failure mechanisms in asphalt pavements. It refers to the process by which cracks in asphalt materials progressively develop from microcracks to macrocracks due to accumulated damage under repeated cyclic loading. The formation of cracks is related to the viscoelastic properties of the asphalt material. Because stress release in viscoelastic binders is relatively slow, damage tends to accumulate gradually under cyclic loading, ultimately leading to cracking. Fatigue cracking typically initiates at the interface between the asphalt binder and the aggregate, as these areas are relatively weaker and more susceptible to cyclic stresses (Moreno-Navarro et al., 2018).

Fatigue cracking can originate from the surface (top-down cracking) or from the bottom of the asphalt (bottom-up cracking). Top-down cracking begins at the surface of the asphalt pavement and propagates downward, typically induced by horizontal tensile stresses generated under traffic loading. These stresses are most pronounced near the edge of the tire and increase significantly with rising temperatures (Zhao et al., 2018). Additionally, the thickness of the asphalt layer also influences cracking, with thicker asphalt layers being more prone to top-down cracking (Alae et al., 2020).

Bottom-up cracking, on the other hand, occurs when cracks initiate at the bottom of the asphalt layer and gradually propagate upward. This type of cracking is usually generated when

the tensile stress at the bottom of the asphalt layer exceeds the fatigue strength of the material(Cheng et al., 2022). The crack tips are sensitive to the stress concentration, therefore resulting in cracks propagating upwards and forming reflective cracks(Oshone et al., 2019). The type and strength of the base layer, and environmental conditions such as moisture and temperature, are critical factors influencing the formation of bottom-up cracks (Alae et al., 2020).

The typical fatigue cracking process is generally divided into three phases: adaption phase, quasi-stationary phase, and failure phase. **Figure 2.1** shows the typical three phases of asphalt fatigue.

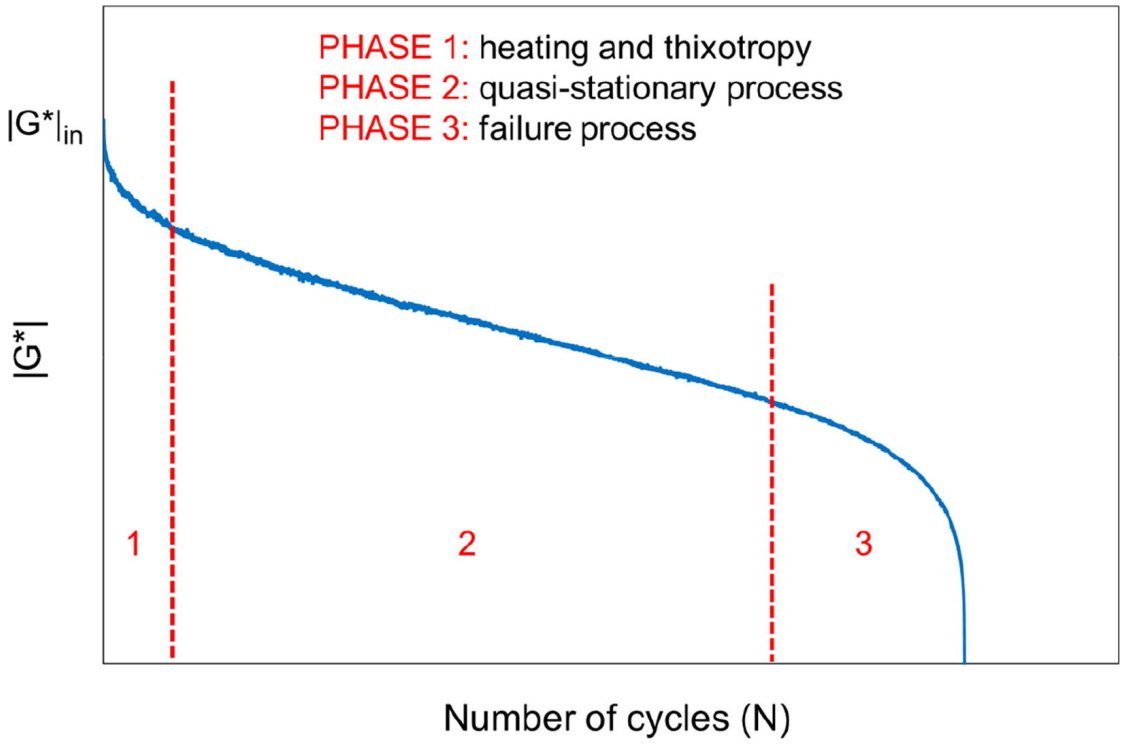

Figure 2.1.: Typical fatigue curve for asphalt concrete (Ragni et al., 2020).

Phase 1 (Adaption Phase): This phase represents the crack initiation process, where the stiffness modulus of the material rapidly decreases due to repeated loading. The damage incurred during this phase occurs at the microscopic level, so there is no significant loss in the material's structural integrity. By the end of this phase, microcracks fully develop in areas of high stress, leading to a reduced rate of new microcrack formation (Venudharan and Biligiri, 2020).

Phase 2 (Quasi-Stationary Phase): In the second phase, the existing microcracks continue to propagate as the number of load cycles increases. The stiffness of the material decreases in an almost linear and stable manner but at a slower rate compared to the first phase.

Phase 3 (Failure Phase): During this phase, the microcracks gradually connect to form macrocracks. Irreversible fatigue damage starts to accumulate, and the material's stiffness begins to decline rapidly, ultimately leading to material failure (Ragni et al., 2020).

Several factors, including aging, environmental conditions, material composition, loading, and construction techniques, influence the fatigue performance of asphalt. Aging negatively impacts fatigue resistance, while environmental factors such as temperature and moisture also play a key role. High temperatures accelerate plastic deformation, and low temperatures cause brittle cracking. The asphalt mixture's composition, including binder viscosity, aggregate gradation, and air void content, can also critically affect fatigue life. Additionally, studies have shown that incorporating modifiers such as polymers and fibers can significantly enhance the fatigue resistance of asphalt mixtures (Moghaddam et al., 2011). Vehicle speed, axle load, and the temporal variation of traffic loading also influence the fatigue behavior of pavements. Manufacturing processes, particularly production temperatures and the selection of additives have a crucial impact on the fatigue performance of asphalt mixtures.

2.1.2. Fatigue Cracking: Shift Factor

Researchers have developed various testing methods to simulate the fatigue behavior of materials, as well as a range of fatigue parameters to characterize the fatigue properties of the materials. However, the actual in-situ service life of asphalt concrete usually exceeds the predictions made by laboratory-based fatigue prediction models. The variance is primarily due to several factors, including the in-situ load spectrum, lateral wandering, environmental conditions, the properties of the material, how specimens are prepared, and the restorative healing processes occurring between sequential traffic loading events. Discrepancies between field and laboratory fatigue prediction results can lead to wasted resources and unnecessary maintenance.

Researchers have introduced the concept of the Shift Factor (SF) to establish a correlation between the actual in-situ service life and the laboratory-predicted service life. The lab-predicted pavement fatigue life is multiplied by the shift factor to estimate the pavement's actual in-situ service life. Over the past few decades, researchers have proposed shift factors ranging from 0.1 to more than 400 based on different evaluation criteria summarized in Table 2.1.

The default shift factor value currently used in the Dutch pavement design method is 4.0. Bitumen's content and penetration grade are taken into account in the equation (**Equation 2.1**) for calculating the shift factor.

$$SF = 1 + 0.0000419 \cdot V_b^{1.06} \cdot \text{pen}^{2.45} \leq 4 \tag{2.1}$$

where V_b is the bituminous binder content (where necessary corrected for the density of the aggregate in accordance with NEN-EN13108-7 Article 5.2.3) [% m/m 'in'], and pen is the penetration value of the bitumen [10-1 mm]. Note that the SF must equal to 1.0 when asphalt mixtures with modified bitumen or additives are used as base pavement layers.

Table 2.1.: Empirical shift factors from previous studies.

Researchers	Year	Shift Factor	Notes
Brown et al.	1985	440	Considering rest period, cracking propagation and wandering
Finn et al.	1986	13.0	10% level cracking
		18.4	45% level cracking.
Gerritsen and Koole	1987	5-25	Considering rest period, wandering and temperature gradient
Pierce et al.	1993	0.1-5.8	Considering asphalt layer thickness (10 cm to 25 cm)
Deacon et al.	1994	10-14	Considering asphalt layer thickness (10.16 cm & 20.32 cm)
Leahy et al.	1995	10	10% level cracking
		14	45% level cracking
Harvey et al.	1997	4-40	Using a Miner's Law approach, the SF is dependent on strain levels of field pavements
Said	1997	10	Using the field data from 11 flexible sections in Sweden, and the laboratory data from indirect tensile fatigue test
Prowell	2010	4.2-75.8	Using the field data from the 4 NCAT road test section
		$<$10	Considering the material properties of SBS-modified asphalt
Mateos et al.	2011	11.4	Using the field data from a full-scale testing track
Yu et al.	2012	1.096	10% level cracking
Biligiri and Said	2015	9.72	Using the field data from the Swedish highway section
Cheng et al.	2018	105.6	Considering the cold central-plant recycling (CCPR) mixture

2.2. Asphalt Healing

2.2.1. Asphalt Healing Mechanisms

The healing capability of asphalt materials refers to the material's ability to spontaneously restore its mechanical properties through intrinsic physical or chemical processes after being subjected to external damage or crack formation. This healing characteristic of asphalt is important for extending pavement service life, particularly under repeated traffic loads. Due to the viscoelasticity and flowability of asphalt binders, cracks can spontaneously heal under certain conditions, thereby slowing the accumulation of damage (Santagata et al., 2015).

Currently, the mechanisms behind asphalt healing are not fully understood, and researchers have proposed various healing mechanisms over the past few decades. Wool and O'Connor developed a healing model for polymers, dividing the process into five stages: surface rearrangement, surface approach, wetting, diffusion, and randomization, as illustrated in **Figure 2.2** (Wool and O'connor, 1981). The fourth stage in this model, diffusion, is considered the most critical, as it governs the development of mechanical properties during the healing process (Varma et al., 2021).

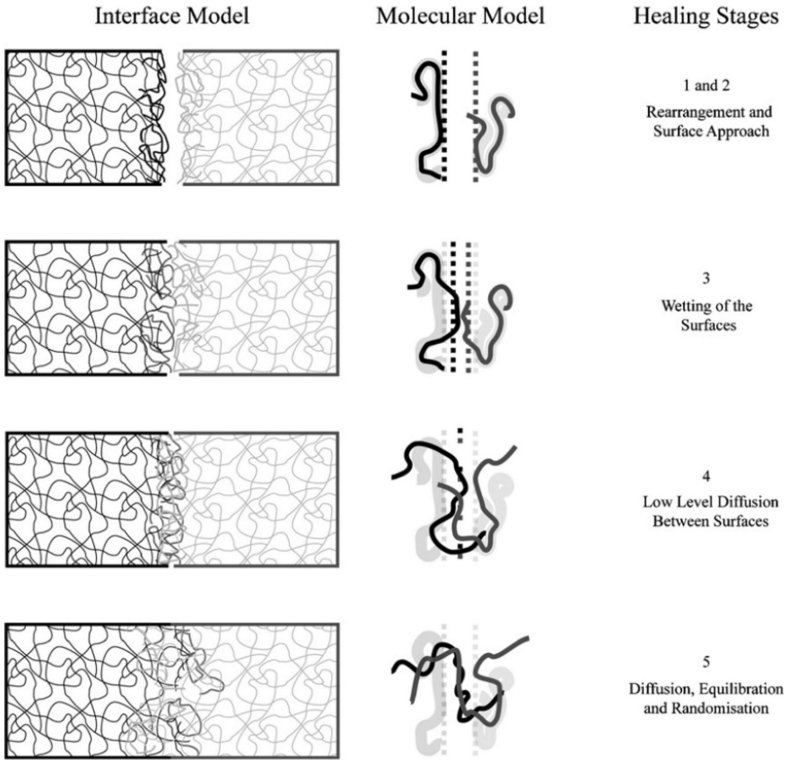

Figure 2.2.: Crack healing model proposed in polymers (Wool and O'connor, 1981).

In 2012, Qiu proposed a new mechanism that considered the competing interactions between fatigue and healing in asphalt, as shown in **Figure 2.3**. Fatigue and healing in asphalt are regarded as two competing mechanisms. Fatigue follows a three-phase model comprising

crack initiation, crack propagation, and eventual failure, while healing is characterized by three stages: flow, wetting, and diffusion (Qiu, 2012). After the flow stage, the stiffness of the material increases, and during the wetting and diffusion stages, the stiffness and strength of the material are restored (Qiu, 2012). In the wetting stage, asphalt with higher surface energy exhibits a higher wetting rate, whereas during the diffusion stage, asphalt containing more molecules with longer chains and fewer branched chains has a stronger diffusion capacity (Sun et al., 2018).

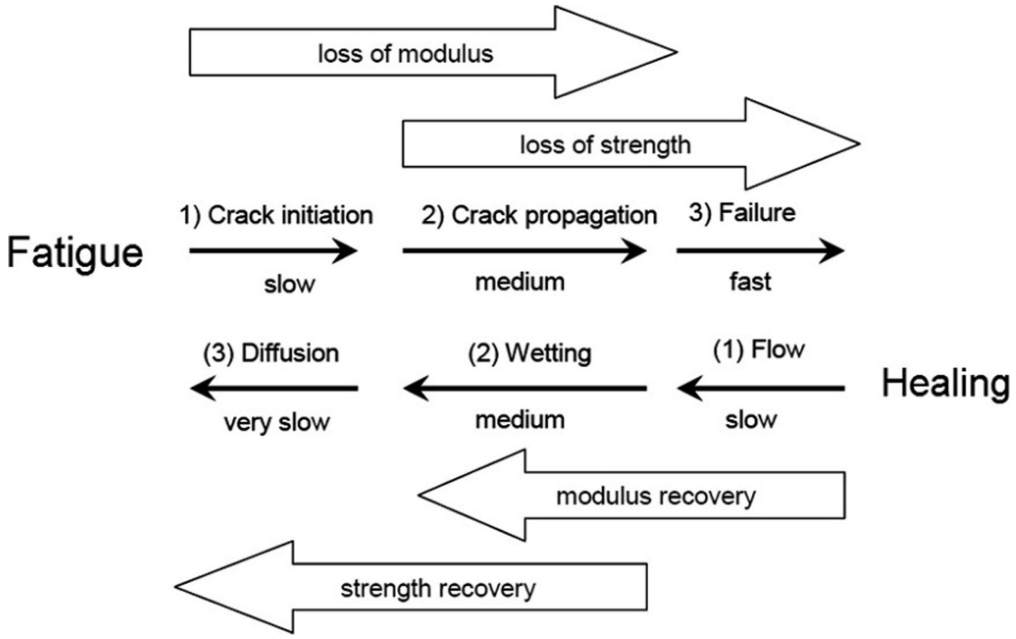

Figure 2.3.: Three-step mechanism of healing (Qiu, 2012).

Sun and Wang, through molecular dynamics simulations, described the self-healing process of asphalt as occurring in two stages. The first stage is a rapid surface-wetting phase, where molecules on the crack surface reconnect through diffusion. The second stage is a slower diffusion phase, during which molecules within the material diffuse more deeply, gradually restoring the material's strength (Sun and Wang, 2020).

2.2.2. Types of Asphalt Healing

Asphalt healing can be classified into intrinsic healing and extrinsic healing. Intrinsic healing refers to the natural recovery process of asphalt without external intervention, primarily driven by the material's inherent chemical and physical properties. In contrast, extrinsic healing involves external interventions to facilitate or enhance the natural healing process. Common examples of extrinsic healing technologies include induction heating and capsule-based healing. In induction heating, electrically conductive and magnetically susceptible particles (e.g., steel particles) are added to the asphalt mixture. When exposed to an external electromagnetic field, these particles generate heat, which helps heal microcracks in the asphalt (Dai et al., 2013). Capsule-based healing method embeds microcapsules containing rejuvenating agents

into the asphalt mixture. When cracks form, the capsules rupture, releasing the agents to restore the binder properties and seal the cracks (Li et al., 2021). This study primarily focuses on the intrinsic healing of asphalt materials.

2.2.3. Factors Affecting Healing

The healing ability of asphalt is influenced by several factors, which are discussed in this section. These factors include chemical composition, aging level, damage level prior to rest periods, temperature, rest time, and the type of additives used.

- **Chemical Composition:** The chemical composition of the asphalt binder affects its healing capacity. Studies have shown that asphalt with higher small-molecule content (e.g., aromatic compounds) and lower large-molecule content (e.g., asphaltenes) exhibits better healing performance (Sun et al., 2017). Additionally, the number of branched chains and the proportion of long-chain molecules in the molecular structure are critical factors influencing the healing capability.
- **Aging Level:** Aging is a key factor that reduces the healing ability of asphalt materials. Research shows that the overall healing capacity of asphalt binders decreases as the aging level increases (Bhasin et al., 2011b).
- **Damage Level Prior to Rest Periods:** As traffic loading increases, damage accumulates within the material. The state of fatigue damage has a significant impact on the low-temperature healing potential of asphalt mixtures, with higher degrees of fatigue damage leading to lower healing potential (Sun et al., 2019). Research shows that the more damage accumulated in asphalt before the healing period, the lower the healing potential (Jayaraman and Padmarekha, 2024).
- **Temperature:** Temperature is one of the most critical factors influencing asphalt's healing ability. Higher temperatures enhance the binder's flowability, making it easier to diffuse into cracks and accelerate the healing process. Research has shown that the healing capacity of asphalt binders increases with rising temperatures (Bhasin et al., 2011b). In contrast, lower temperatures slow down the healing process, in cold conditions, where the viscoelastic behavior of asphalt is diminished.
- **Rest Time:** The length of rest intervals between traffic loadings plays an important role in the healing process. Studies have found a strong correlation between longer rest intervals and higher levels of healing (Jayaraman and Padmarekha, 2024).
- **Additive Types:** Various additives, such as rejuvenators, Carbon black (CB), and Styrene-Butadiene Rubber (SBR), can improve the healing performance of aged asphalt. These additives help restore the flexibility of the aged binder, enhance the repair of microcracks, and reduce permanent deformation under stress (Sarsam and Mahdi, 2020).

2.2.4. Biasing Effects

During fatigue testing of asphalt materials, biasing effects, including nonlinearity, self-heating and thixotropy, can influence fatigue test results, leading to inaccurate assessments of fatigue performance (Mangiafico et al., 2015). These effects arise due to repeated loading and significantly influence the material's mechanical properties, particularly the complex modulus, thereby obscuring the true extent of fatigue damage.

The nonlinearity effect refers to the nonlinear behavior of asphalt materials under varying stress and strain conditions, primarily resulting from the heterogeneity of the materials. The self-heating effect is a phenomenon that the temperature increases within the sample due to energy dissipation during cyclic loading, which subsequently affects the complex modulus. Thixotropy is a characteristic phenomenon in non-Newtonian fluid, which refers to the decrease in viscosity that occurs in the material under shear stress.

Wang and An divided the evolution of the asphalt stiffness modulus into three stages, as shown in Figure 2.4 (Wang and An, 2024). The first stage represents Linear Viscoelastic (LVE) behavior, with increasing load, the stiffness modulus undergoes a reversible decrease due to biasing effects. In the third stage, the material exhibits irreversible damage. Asphalt's self-healing behavior is thought to occur in this third stage.

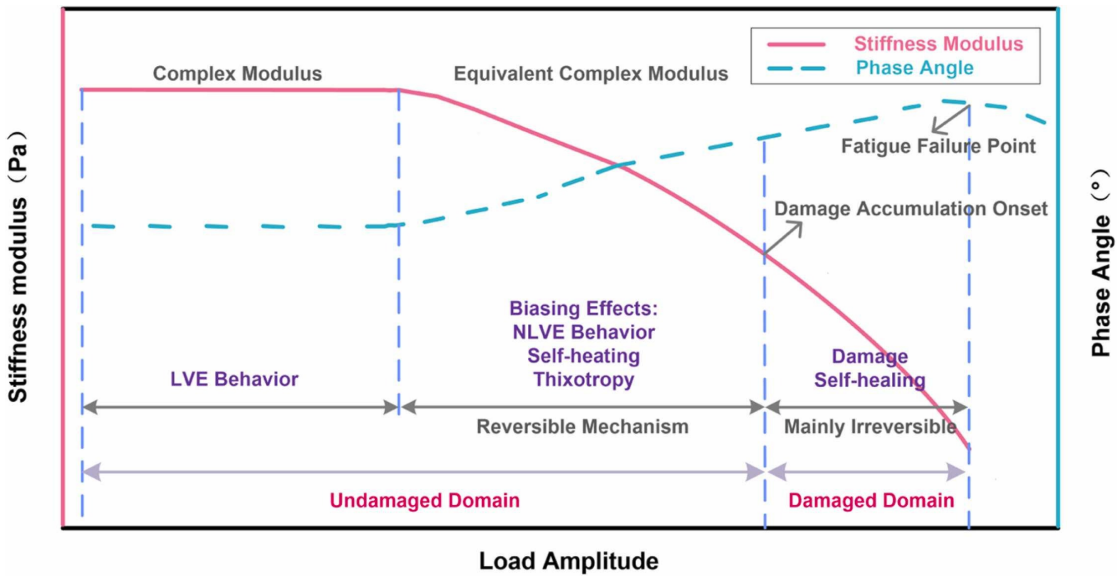

Figure 2.4.: Evolution of stiffness modulus under different loading levels (Wang and An, 2024).

Research indicates that the influence of the self-heating effect in asphalt binder testing is limited, as the specimen size is small, reducing the volume effect (Botella et al., 2020). For asphalt binders, the Nonlinear Viscoelastic (NLVE) effect and self-healing behavior are considered the two primary factors affecting complex modulus evolution and fatigue damage behavior (Wang and An, 2024). However, evaluating biasing effects falls outside the scope of this study.

2.3. Introduction and Challenges of Reclaimed Asphalt (RA)

Reclaimed asphalt (RA) is typically obtained through the removal, milling, and crushing of deteriorated pavements. Aged RA can be modified and reused in the construction of new pavement structures. The use of RA significantly reduces the demand for new asphalt, lowering the costs of road construction and decreasing the environmental burden, while also reducing reliance on petroleum resources. Studies have shown that using 100% RA in new asphalt mixtures can reduce production costs by 50% to 70% (Zaumanis et al., 2015).

However, the high content of RA presents challenges in terms of material performance, with the aged binder in RA being the primary cause of its performance degradation. The aged binder contains a higher proportion of large molecular compounds (such as asphaltenes), which reduce the material's ductility and flexibility (Subhy et al., 2019). The aging process of bitumen involves oxidation and the loss of volatile compounds, leading to changes in its molecular structure. These changes directly affect the viscosity and elasticity of the material, ultimately weakening the fatigue resistance of RA (Zaumanis et al., 2015).

Aged asphalt becomes more brittle and rigid, making it prone to cracking under repeated traffic loads. This issue is exacerbated as the degree of aging increases, causing a rise in stiffness and a significant reduction in fatigue life (Moghaddam and Baaj, 2016). Aging not only reduces the fatigue performance of asphalt but also negatively impacts its healing ability. The reduced viscoelasticity of aged materials means that they are less capable of healing cracks through intrinsic viscous flow.

To improve the performance of asphalt mixtures with high RA content, three recycling strategies are typically employed: the use of softer bitumen, rejuvenators, and polymer modification. Adding rejuvenators can restore the physical, chemical, and rheological properties of aged binders. Rejuvenators reduce the viscosity of aged asphalt, restore its elasticity, and improve both fatigue and crack resistance (Jacobs et al., 2021). Rejuvenators can enhance the flowability of aged asphalt by replenishing the lighter fractions within the binder, thereby improving its healing ability (Elkashef et al., 2018). Some studies have demonstrated that the combination of rejuvenators and softer bitumen can improve the fatigue performance of asphalt mixtures containing high proportions of reclaimed binder, achieving performance comparable to that of virgin binders (Ameri et al., 2018). Additionally, the use of additives such as styrene-butadiene-rubber (SBR) latex in RA mixtures has been shown to enhance low-temperature crack resistance and rutting resistance (Li et al., 2014).

However, different types of rejuvenators vary in their effectiveness at improving fatigue and healing performance. For instance, bio-based rejuvenators, such as those derived from vegetable oils, can quickly enhance the viscoelastic properties of the material, but their long-term effects may accelerate the aging of asphalt (Yaseen and Hafeez, 2020). Therefore, to enable the effective use of high RA content in practical engineering applications, further research is needed to understand how rejuvenators influence the fatigue and healing performance of asphalt materials containing high proportions of RA.

2.4. Fatigue and Healing Testing Methods of Asphalt Binders

Various testing methods have been developed to evaluate the fatigue and healing performance of asphalt binders. The primary testing approaches are classified into two categories: fatigue-

based healing tests and fracture-based healing tests (Ayar et al., 2016).

In fatigue-based healing tests, the sample is subjected to continuous dynamic loading, followed by the introduction of one or more rest periods at specific damage levels. The healing behavior of the asphalt binder is analyzed by recording the mechanical properties (such as complex shear modulus) before and after the rest period or by comparing the changes in fatigue life.

Fracture-based healing tests, on the other hand, are typically performed at the crack interface of asphalt binders or mixtures. These tests evaluate the healing performance by measuring the recovery of mechanical properties after a certain healing time under controlled conditions (Zhou et al., 2020).

2.4.1. Time Sweep (TS) and Time Sweep Healing (TS-H) Tests

The Time Sweep (TS) test is a widely used nonlinear viscoelastic testing method for evaluating the fatigue performance of asphalt binders. Originally proposed in the NCHRP 9-10 project, the TS test can be conducted under either stress-controlled or strain-controlled conditions. In this test, repeated oscillatory sinusoidal shearing is applied to the sample at a constant frequency and temperature, and the modulus decrease is recorded to assess the material's fatigue life. The TS test effectively reflects the damage accumulation of asphalt under actual traffic loads, making it a reliable laboratory simulation method.

However, the TS test has some limitations. It is time-consuming, especially when simulating long-term cyclic loading or under low strain conditions, leading to higher testing time and costs. Additionally, the results are sensitive to test conditions such as temperature and loading frequency, which require strict control over the experimental environment.

The Time Sweep Healing (TS-H) test builds upon the TS test by introducing rest periods to evaluate the material's healing capability. During these rest periods, loading is halted to allow the material to heal through intrinsic physical or chemical processes. After the rest, loading is reapplied, and the recovery of the material's properties or the extension of the fatigue life is measured to assess the healing effect. This test method simulates the healing behavior of asphalt mixtures under real-world conditions, where intermittent traffic, such as during traffic light periods and the nighttime when traffic is lighter, provides sufficient time for self-healing.

Both TS and TS-H tests are the primary methods used in this study. Detailed discussions on the test setup, equipment, and failure criteria are presented in Section 3.2.1.

2.4.2. Linear Amplitude Sweep (LAS) and Linear Amplitude Sweep Healing (LAS-H) Tests

The Linear Amplitude Sweep (LAS) test is a method designed to quickly assess the fatigue performance of asphalt binders by gradually increasing the strain amplitude. The goal of the LAS test is to simulate the stress response of the material under progressively increasing loads, providing a rapid evaluation of its fatigue life (Wang et al., 2019). The LAS test allows for the determination of fatigue properties within a shorter time frame and has become one of the most common methods for evaluating the fatigue resistance of asphalt binders.

The Linear Amplitude Sweep Healing (LAS-H) test extends the LAS test by incorporating healing assessments. It evaluates the healing capacity of the material by recording the recovery of modulus during rest periods introduced between loading stages. The core concept of the LAS-H test is that as strain amplitude increases, the material undergoes partial damage, followed by rest periods where molecular diffusion and rearrangement allow for healing (Lv et al., 2023). Compared to the TS-H test, LAS-H test can assess both fatigue and healing performance in a shorter time, making it suitable for rapid material screening. Its efficiency makes it particularly valuable for large-scale testing in laboratory settings (Wang et al., 2019).

However, a limitation of the LAS-H test is that, due to the loading method of progressively increasing strain amplitude, it may inaccurately estimate the material's fatigue life. Additionally, it has some limitations in accurately simulating the real-world traffic loads experienced by asphalt pavements.

Both LAS and LAS-H tests are the primary methods used in this study. Detailed descriptions of the test setup, equipment, and failure criteria are presented in Section 3.2.2.

The TS, TS-H, LAS, and LAS-H tests are conducted using a Dynamic Shear Rheometer (DSR) (see **Figure 2.5**), which is the most widely used device in current research on asphalt binder performance.

Figure 2.5.: DSR set up.

2.4.3. Intrinsic Two-Piece Healing (TPH) Test

The Intrinsic Two-Piece Healing (TPH) test is a fracture-based healing method used to assess the healing potential of asphalt binders, utilizing the dynamic shear rheometer (DSR) to derive healing function parameters. This method was first proposed by Bhasin and colleagues (Bhasin et al., 2008). In the TPH test, two asphalt specimens with a diameter of 28 mm and a thickness of 3.5 mm are fixed between the two plates of the DSR. The specimens are first heated in an oven, then poured into silicone molds to cool and solidify (Bhasin et al., 2008).

The test is conducted by pressing the two asphalt pieces together using the DSR under appropriate temperature and environmental conditions, simulating the crack healing process. The change in complex shear modulus is monitored during the gap closure and rest periods, and this change serves as a healing index. **Figure 2.6** provides an illustration of the TPH setup. The TPH test effectively reflects the intrinsic healing potential of asphalt binders, particularly in conditions with minimal external loads. It provides direct evidence of molecular rearrangement and diffusion within the material, making it a valuable method for studying self-healing in asphalt binders.

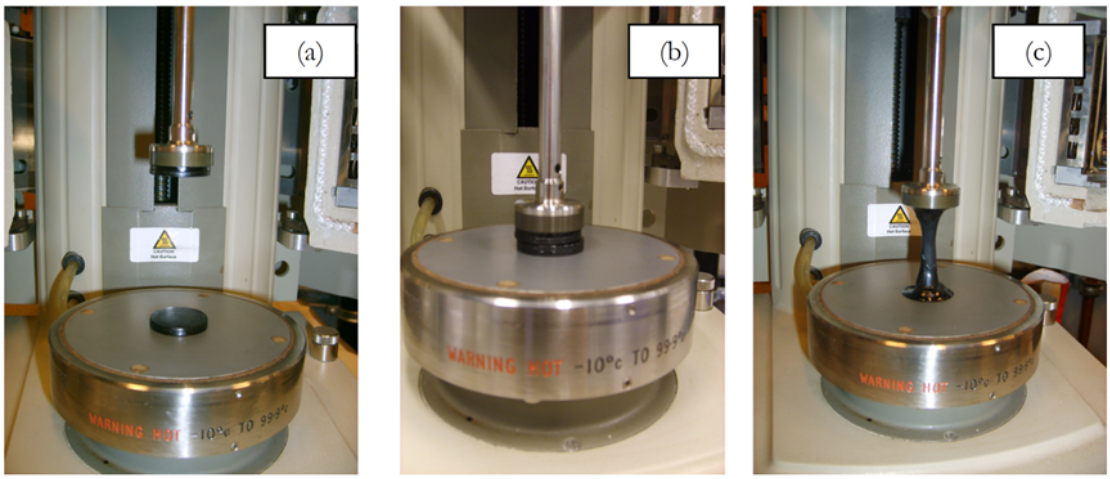

Figure 2.6.: Illustration of the TPH setup using Dynamic Shear Rheometer, (a) Attaching two pieces of bitumen on top and bottom plates; (b) Decreasing the gap width to allow full contact of the two pieces and measuring the change in complex shear modulus over time; (c) Removing the upper plate after the testing (Qiu, 2012).

2.4.4. Direct Tension Test (DTT)

The Direct Tension Test (DTT) is a commonly used method for evaluating the fracture resistance of asphalt binders under low-temperature conditions. In this test, tensile stress is applied to measure the tensile strength of the material before fracture, and the amount of strength recovery after healing is used to assess the material's healing capability. The DTT uses standard dog-bone-shaped specimens for testing. **Figure 2.7** illustrates the setup of the DTT healing test.

The test specimens are first heated and poured into silicone molds, allowed to cool and solidify, and then demolded (Qiu et al., 2012). The specimen is cut into two equal halves at 5°C using a sharp blade, and the cut faces are then placed back together **(Figure 2.7)**. The sample is cured at 22°C for varying duration to allow healing, after which tensile stress is reapplied to evaluate the recovery of strength after healing (Qiu, 2012).

One limitation of the DTT is that it focuses primarily on fracture performance at low temperatures, making it less suitable for evaluating healing at higher temperatures. Additionally, this test simplifies the stress environment by only considering tensile loads, which may not fully

capture the complexity of real-world conditions where asphalt experiences a combination of different stress types.

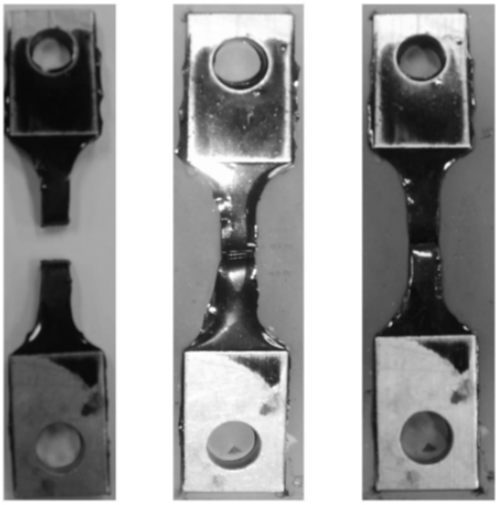

Figure 2.7.: Illustration of healing test using the DTT (Qiu, 2012).

In 2016, Leegwater et al. developed the 2-piece healing test method based on the DSR which combines the two-piece healing test and the direct tension test, to study the healing behavior of asphalt binder under extreme discontinuity conditions, where the binder is fully separated (Leegwater et al., 2016). This method accounts for the recovery of binder strength during the healing period, an aspect not typically considered in other fracture-based healing tests.

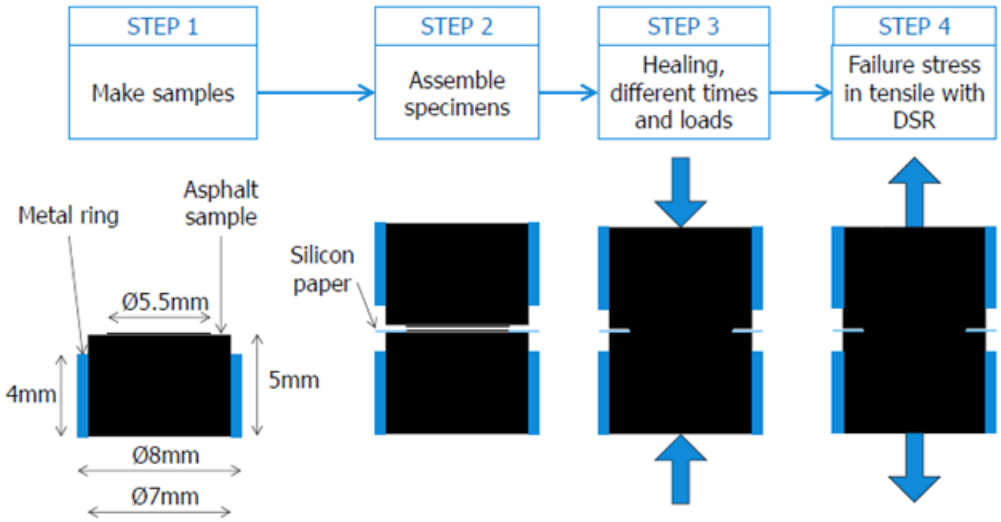

Figure 2.8.: Schematic representation of the 2-piece healing test method with sequential steps (Leegwater et al., 2018).

Figure 2.8 illustrates the schematic and testing procedure for the 2-piece healing test method. At 14°C ± 1°C, the DSR assembles the two sample pieces at a constant displacement speed, followed by a rest period to allow healing. A piece of silicone paper is used to separate the two pieces of samples, controlling the contact area, with a 5.5 mm diameter hole in the silicone paper (Leegwater et al., 2018). After the rest period, a direct tensile test is conducted to determine the failure stress in tension of the healed sample. The ratio of the maximum tensile strength after a healing period to that of a reference sample made of the same binder is defined as the healing ratio, which evaluates the binder's healing capacity (Leegwater et al., 2018).

2.4.5. Binder Bond Strength (BBS) Test

The Binder Bond Strength (BBS) test is a specialized method used to evaluate the adhesive strength between asphalt binder and aggregate, as well as the material's healing capacity. The BBS test assesses the healing ability of the binder by measuring the recovery of bond strength under various temperatures and conditions after fatigue damage. In this test, the healing effect is calculated by dividing the recovered Pull-Off Tensile Strength (POTS) by the initial POTS before healing (Lv et al., 2017). **Figure 2.9** illustrates the procedure for the BBS test.

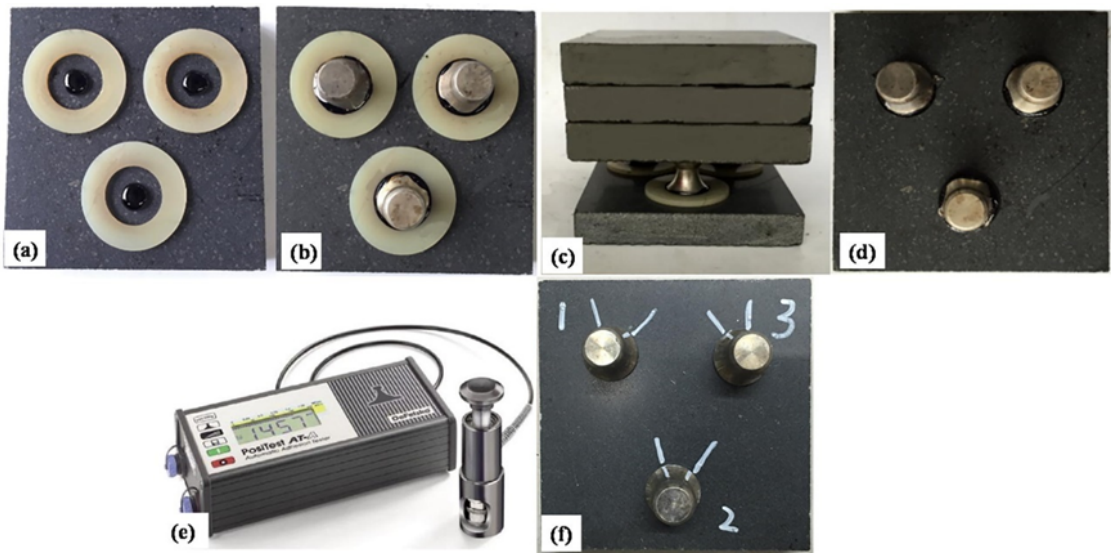

Figure 2.9.: The procedure of BBS test (a)–(d) preparation of the sample and (e) appearance of Positest AT-A apparatus and (f) stubs with marks (Zhou et al., 2020).

This method is particularly useful for understanding how well the binder can recover its bonding strength with aggregate, providing insights into the material's performance after damage in real-world conditions.

2.5. Viscoelastic Continuum Damage (VECD) Theory

The Viscoelastic Continuum Damage (VECD) theory is a mechanical constitutive model used to describe the damage evolution in asphalt materials under fatigue loading. This model integrates viscoelasticity and continuum damage mechanics to capture the time-dependent accumulation of micro-damage in materials subjected to cyclic or long-term loading, thus allowing for predictions of material degradation and fatigue life. The VECD theory is considered to be composed of three fundamental equations: the elastic-viscoelastic correspondence principle, the pseudo-strain energy density equation, and the damage evolution rule (Zhang et al., 2023).

The Simplified Viscoelastic Continuum Damage (S-VECD) model is a streamlined version of the VECD theory, designed to reduce experimental complexity and data processing requirements. The S-VECD model allows for the prediction of fatigue life and damage evolution with fewer experimental data, making it particularly suitable for large-scale laboratory testing or rapid performance evaluations (Klug et al., 2022). Studies have shown that the S-VECD model can accurately predict the fatigue performance of asphalt mixtures and binders under various stress levels.

The concepts of pseudo-strain and pseudo-stiffness are introduced to establish the nonlinear damage evolution rules of materials specifically asphalt binders. These concepts are used to define the damage characteristic curve, commonly known as the C-S curve. The fatigue life of the material is subsequently predicted based on the evolution of these damage characteristics (Zhang et al., 2023). This section provides a brief overview of the key analytical steps and formulas employed in this study.

Pseudo Stiffness (C) reflects the material's capacity to maintain structural integrity during loading, and it can be calculated using **Equation 2.2**:

$$C = \frac{\tau_p}{\gamma_p^R \times DMR} \tag{2.2}$$

$$\gamma_p^R = \gamma_p \times |G^*|_{LVE} \tag{2.3}$$

where γ_p^R is the peak pseudo strain for a given cycle, which is defined in **Equation 2.3**, τ_p is the peak shear stress, γ_p is the peak shear strain for a given cycle, $|G^*|_{LVE}$ is the fitted $|G^*|$ at the testing temperature and loading frequency from the $|G^*|_{mastercurve}$.

Damage Intensity (S) quantifies the accumulation of internal damage in a material during fatigue loading and serves as a key indicator of damage progression. It can be calculated using **Equation 2.4**:

$$S(t) = \sum_{i=1}^{N} \left[\frac{DMR}{2} (\gamma^R)^2 (C_{i-1} - C_i) \right]^{\frac{\alpha}{\alpha+1}} \cdot (t_i - t_{i-1})^{\frac{1}{1+\alpha}} \tag{2.4}$$

where DMR is dynamic modulus ratio = $|G^*|_{fingerprint} / |G^*|_{LVE}$, $|G^*|_{fingerprint}$ is the measured $|G^*|$ of the testing sample, i is the loading time step, α=1/m+1, m is the slope of the dynamic shear stiffness modulus master curve in log space (Safaei et al., 2014).

Based on the calculated values of C and S, the C-S curve can be plotted for each sample. This curve can be fitted using a power law function, as described by **Equation 2.5**, where C_1 and C_2 are the two fitting coefficients that characterize the material's damage behavior.

$$C(S) = 1 - C_1 \cdot S^{C_2} \tag{2.5}$$

The C-S curve is used to describe the evolution of damage in the material during fatigue loading. **Figure 2.10** shows a typical C-S curve for the binder. According to the VECD theory, the C-S curve is considered unique and represents an inherent characteristic of the asphalt binder, independent of the loading conditions (Lee et al., 2000).

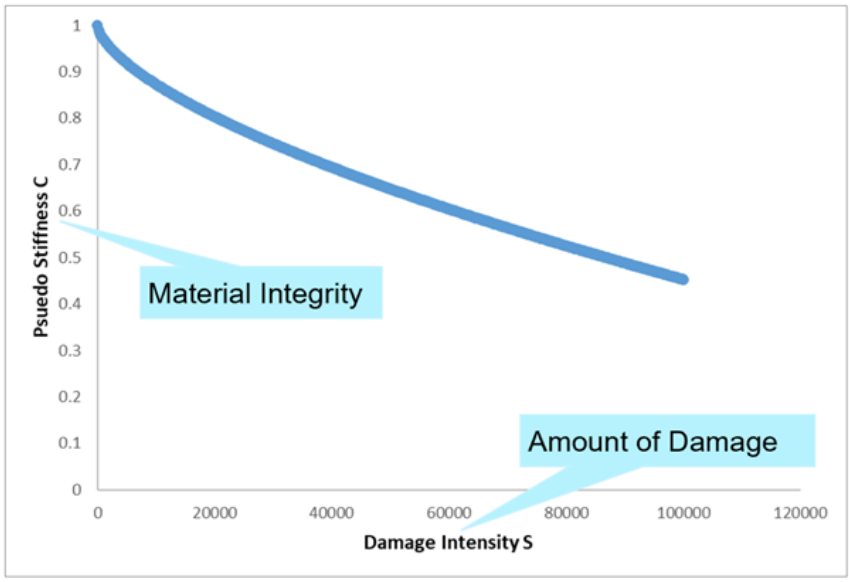

Figure 2.10.: Damage characteristic curve.

According to the aforementioned equations, an expression for the fatigue life N_f can be derived as follows **(Equation 2.5)**:

$$N_f = \frac{f \cdot 2^{\alpha} \cdot S_f^{1-\alpha C_2+\alpha}}{(1-\alpha C_2+\alpha)(C_1 C_2)^{\alpha}(\gamma_p \cdot |G^*|_{LVE})^{2\alpha}} \tag{2.6}$$

Based on S-VECD theory, the results of LAS tests can be analyzed to predict the fatigue life of binders under any strain amplitude. First, the failure point is determined using the selected fatigue failure definition. The damage intensity at the failure point, S_f, is defined by the following equation **(Equation 2.7)**:

$$S_f = \left(\frac{1-C_f}{C_1}\right)^{\frac{1}{C_2}} \tag{2.7}$$

where C_f is the pseudo-stiffness at failure. By substituting **Equation 2.7** into **Equation 2.6**, the relationship between fatigue life N_f and strain amplitude γ_p can be expressed by the following equation **(Equation 2.8):**

$$N_f = A(\gamma_p)^B \tag{2.8}$$

where A is defined by **Equation 2.9**, B= -2α, f is the loading frequency, k = 1 - αC_2 + α

$$A = \frac{f 2^{\alpha} S_f^k}{k(C_1 C_2)^{\alpha} (|G^*|_{LVE})^{2\alpha}} \tag{2.9}$$

2.6. Healing Indices

The healing indices is a parameter used to quantify the healing capacity of asphalt binders or mixtures after fatigue damage. Understanding the healing indices is crucial for assessing the healing characteristics of asphalt materials, improving pavement design, and extending the service life of asphalt pavements. The value of the healing indices is influenced by factors such as the material's viscoelasticity, chemical composition, and external environmental conditions (e.g., temperature, loading mode).

Over the past few decades, researchers have developed various healing indices to evaluate the healing performance of asphalt materials. Verma et al. provide a summary of different healing indices used in asphalt binder healing studies (Varma et al., 2021). However, there is no universally accepted healing indices, primarily due to the lack of a clear understanding of the rest period healing compensation mechanism in asphalt binders (Little et al., 2015).

The existing healing indices for asphalt materials can be broadly classified into three categories (Shan et al., 2013).

- **Properties recovery-based indices**, which measure the recovery of properties such as dynamic modulus, strain, energy, or pseudo-stiffness after a rest period.
- **Fatigue life-based indices**, which evaluate changes in the fatigue life of the material before and after the healing process.
- **Healing rate or damage rate-based indices**, which focus on the rate of healing or damage progression after healing.

Each of these indices offers a different perspective on how asphalt materials recover from damage, with their own advantages and limitations. Properties recovery-based indices are useful for assessing the immediate healing capability of asphalt materials and are easy to implement and calculate in the laboratory. However, they do not reflect the long-term fatigue performance. Fatigue life-based indices measure the extension of fatigue life after healing, providing insights into the long-term effects of healing on fatigue performance. The drawback is that these indices require complex and time-consuming fatigue testing and are sensitive to loading conditions. Healing rate-based indices focus on the speed at which healing occurs and are suitable for dynamic loading conditions. However, these indices often require advanced testing and modeling techniques.

A combination of these approaches can provide a more comprehensive understanding of the healing potential of asphalt materials.

Table 2.2.: Studies on healing indices from previous research (Varma et al., 2021).

Reference	Material	Test Method	Healing Parameter	Healing Indices
(Qiu et al., 2009)	Standard penetration grade bitumen, SBS modified bitumen and hard penetration grade bitumen	Ductility test	Length at break of samples	$\frac{L_{\text{Healed}}}{L_{\text{Original}}} \times 100\%$
		Two-piece healing test using DSR	Shear modulus	$\frac{M_{\text{Healed}}}{M_{\text{Original}}} \times 100\%$
		Direct tension test	Maximum strength	$\frac{S_{\text{Healed}}}{S_{\text{Original}}} \times 100\%$
(Tan et al., 2012)	Bitumen	Fatigue-rest-fatigue test using DSR	Complex modulus	$\frac{\lvert G^* \rvert_{\text{after}}}{\lvert G^* \rvert_{\text{initial}}} \times 100\%$
			Complex modulus and number of cycles	$\left(\frac{\lvert G^* \rvert_{\text{terminal}}}{\lvert G^* \rvert_{\text{initial}}}\right)\left(\frac{N_{\text{after}}-N_{\text{before}}}{N_{\text{before}}}\right) \times 100\%$
(Shan et al., 2013)	Bitumen	Fatigue-rest-fatigue test using DSR	Area under the curve	$\frac{A_{\text{d}}}{A_{\text{before}}}$
(Shen et al., 2013)	Unmodified and modified binder	Fatigue-rest-fatigue test using DSR	Viscofracture strain	$\frac{\Delta\gamma_{vf}^{-}}{\Delta\gamma_{vf}^{+}}$
(Sun et al., 2016)	Unmodified asphalt and SBS modified asphalt	Fatigue-rest-fatigue test using DSR	Complex modulus	$\frac{\lvert G^* \rvert_{\text{healing}}-\lvert G^* \rvert_{\text{terminal}}}{\lvert G^* \rvert_{\text{initial}}-\lvert G^* \rvert_{\text{terminal}}}$
(Lv et al., 2017)	Neat asphalt and SBS modified asphalt	Binder bond strength test	Pull-off tensile strength	$\frac{\text{POTS}_{\text{Ai}}}{\text{POTS}_{\text{I}}}$
(Zhang et al., 2018a)	Asphalt binder	Self-healing ductility test	Ductility	$\frac{L_{\text{Healed}}-L_{\text{Original}}}{L_{\text{Original}}}$

Reference	Material	Test Method	Healing Parameter	Healing Indices
(Liu et al., 2019)	Asphalt base binder and crumb rubber modified binder	Fatigue and healing test (5 fatigue and 4 healing cycles)	Fatigue life	$\frac{\sum N_{fi}}{\sum N_{fl}}$
			Complex modulus	$\frac{\lvert G^* \rvert_i}{\lvert G^* \rvert_{initial}}$
(Xiang et al., 2019)	Bitumen and SBS modified binder	Fatigue-healing-fatigue test using DSR	Energy density	$\frac{\sum E_{after}}{\sum E_{before}}$
(Qiu et al., 2022)	Unaged, short-term aged and long-term aged pen 70 binder	Fatigue-healing-fatigue using DSR	Complex modulus	$\frac{\lvert G^* \rvert_{h0}}{\lvert G^* \rvert_0} \times 100\%$
			Dissipated energy considering number of fatigue loading cycles	$\frac{W_{after}}{W_{before}} \cdot \frac{N_{after}}{N_{before}} \times 100\%$

2.7. Previous Experience in Healing in Asphalt Binder Materials

Since the last century, the healing of flexible pavements has been extensively studied. This section discusses research evaluating the healing potential of asphalt binders, with a particular focus on studies based on TS-H and LAS-H tests.

The healing performance of asphalt binders largely depends on their chemical composition. Studies have shown that the healing capability is closely related to the ratio of saturates to aromatics. A higher content of saturates and a greater saturates-to-aromatics ratio (S/Ar) enhance the molecular diffusion ability, thus improving the healing performance. Conversely, binders with higher asphaltene content exhibit poorer fatigue life and healing capacity, indicating that controlling asphaltene levels can improve fatigue resistance and healing potential (Wang et al., 2018). In another study, chemical composition analyses using techniques such as thin-layer chromatography, gel permeation chromatography, and infrared spectroscopy revealed that binders with higher small-molecule and aromatic content show better healing capabilities (Sun et al., 2017). A specific parameter, the Methylene-to-Methyl Hydrogen Carbon Ratio (MMHC), was proposed in one study to represent molecular mobility in relation to self-healing performance. A lower MMHC value indicates a higher percentage of long-chain molecules, leading to better molecular mobility and, consequently, improved healing performance (Bhasin et al., 2011a).

Polymer modification has been shown to enhance the healing ability of asphalt. One study demonstrated that polymer modifiers (Surlyn, Nylon, PET) effectively improve healing through intermolecular interactions. Adding 5% polymer increased the healing efficiency of the asphalt

binder to 138% (Yang et al., 2014). Another study used the dissipated energy ratio method to assess the viscous healing performance of binders, finding that while the material partially restored its fatigue resistance during the healing period, some irreversible damage remained, particularly at higher damage levels. However, polymer modification significantly improved the healing performance (Santagata et al., 2017).

The healing performance of asphalt binders gradually decreases with aging. As aging progresses, the healing threshold temperature increases and the healing rate declines significantly. For asphalt binders aged to a certain degree, it becomes nearly impossible to recover from fatigue damage (Zhang et al., 2018b).

Shan et al. examined the influence of thixotropy on the fatigue and healing processes of asphalt binders, proposing a set of healing indices to quantify the material's healing capacity (Shan et al., 2010). In another study, Shen et al. explored the mechanisms of adhesive and cohesive healing in asphalt binders, using the dissipated energy method to evaluate healing ability. They observed that healing potential is closely related to binder type, strain level, and temperature (Shen et al., 2010).

Tan et al. conducted a study based on TS-H tests to investigate the healing performance of different types of asphalt binders. They proposed two distinct healing indices and found that the application of rest periods and the microstructural configurations of the binder significantly affected healing capacity (Tan et al., 2012). Other researchers, including (Stimilli et al., 2012) and (Chen et al., 2013), have also evaluated healing by measuring modulus recovery in asphalt materials before and after rest periods, further emphasizing the role of rest intervals in promoting healing.

Kim and Lee introduced a Viscoelastic Continuum Damage (VECD) model capable of differentiating between time-dependent relaxation and self-healing properties in asphalt concrete, and this model has been successfully applied to binder healing analysis (Kim, 1988; Schapery, 1984; Si et al., 2002).

Recently, a healing test protocol based on the Linear Amplitude Sweep (LAS-H) method was proposed, which measures the healing behavior of asphalt binders by applying rest periods before and after cohesive failure (Xie et al., 2017). The LAS-H test protocol, validated through rheological and chemical characterization, offers an alternative method for assessing binder healing potential (Wang et al., 2019). Wang et al. proposed a healing index parameter based on the S-VECD model and developed a healing master curve to assess healing behavior (Wang et al., 2018, 2019).

Ashouri et al. proposed a shift healing model and a simplified characterization test procedure based on the S-VECD theory. This model accounts for rest periods, testing temperature, and the degree of damage, and has been proven effective in predicting the healing behavior of asphalt concrete. It also contributes to more accurate predictions of fatigue cracking, offering a practical tool for assessing the long-term performance of asphalt materials (Ashouri et al., 2021). Fabrizio et al. recently developed self-healing master curves, based on viscoelastic continuum damage theory, to predict binder healing under varying time-temperature conditions (Fabrizio et al., 2023).

3 Materials and Methods

3. Materials and Methods

3.1. Materials

This study evaluated the healing performance of three types of binders, two of which contain RA bitumen. These binders represent the compositions typically used in three mixtures that are commonly applied in the Dutch pavement base layers. The three mixtures are as follows:

- Mixture 1: 100% virgin aggregates (Binder 40/60)
- Mixture 2: 30% virgin aggregates & 70% RA (Binder 160/220)
- Mixture 3: 30% virgin aggregates & 70% RA & agent (Binder 70/100)

The mixtures (M1, M2, and M3) used for the fatigue testing were produced and tested at Laboratorium Ontwikkeling Wegenbouw (Dura Vermeer). The specimens tested in 4PB tests were standard-sized, measuring 455 mm (length) x 50 mm (width) x 50 mm (height). Detailed information on the mixtures is summarized in **Appendix A.1**.

Among the three binders tested in this study, Binder 1 consists of 100% fresh 40/60 bitumen. Its fatigue resistance and healing potential serve as a baseline for comparison, representing the behavior of unaged binders under standard testing conditions. Binder 2 is a blend of fresh 160/220 bitumen and bitumen from RA. The aged binder is generally more brittle and susceptible to fatigue cracking, but the inclusion of soft 160/220 bitumen helps mitigate the brittleness caused by the aged binder. Binder 3 is a blend of fresh 70/100 bitumen, RA bitumen, and the rejuvenator ANOVA 1817. The role of the rejuvenator is to soften the aged binder and restore its viscoelastic properties.

The use of different penetration grade fresh bitumen in these three binders was intentional, as this study aims to find the correlation between mixtures and their binder components' fatigue performance. Therefore, the fresh bitumen in each binder needed to be consistent with the bitumen used in the three mixtures. The three binders are as follows:

- Binder 1: 100% virgin binder 40/60
- Binder 2: virgin binder 160/220 & aged binder in 70% RA
- Binder 3: virgin binder 70/100 & aged binder in 70% RA & ANOVA 1817

The fresh bitumen 40/60 and 160/220 were sourced from Vitol, and the bitumen 70/100 was sourced from Shell. The rejuvenator, ANOVA 1817, was supplied by Cargill. Extracted bitumen from RA, which was utilized for further research, was prepared at TNO. Table 3.1 shows the target composition percentage of three blended asphalt binders, and **Appendix A.2** shows the detailed calculation process.

Table 3.1.: Binder composition.

Binder	Virgin bitumen type	Virgin bitumen percentage [%]	RA bitumen percentage [%]	Agent [%]
1	40/60	100.0	0.0	-
2	160/220	26.7	73.3	-
3	70/100	22.1	73.3	4.6

Only 42.8 g of bitumen was extracted from the RA, which was insufficient for blending Binders 2 and 3. As a result, fresh bitumen was artificially aged to produce binders with properties similar to those of the extracted RA bitumen.

Fresh 70/100 bitumen (AZALT 70/100 DE) from TotalEnergies was selected to prepare aged bitumen with properties (complex shear modulus) similar to those of the extracted RA bitumen. First, the frequency sweep (FS) test was conducted on the extracted RA bitumen sample using DSR to determine its complex shear modulus response across various frequencies. The FS test was performed at 20°C, with oscillatory shear loading applied at a constant strain amplitude of 0.1% across 21 loading frequencies.

Figure 3.1 and Figure 3.3 illustrate the process of bitumen aging and the preparation of new binders. The fresh 70/100 bitumen was subjected to short-term aging using the Thin Film Oven Test (TFOT) (EN 12593) and long-term aging using the Pressure Aging Vessel (PAV) (EN 14769). First, the fresh 70/100 bitumen is placed into six standard PAV containers with a diameter of (140 ± 1) mm, each containing (50.0 ± 0.5) g of bitumen, as shown in **Figure 3.1a**. The aging process involves aging the bitumen in the TFOT at 163°C for 5 hours, followed by aging in the PAV at 100°C for 90 hours, as depicted in **Figure 3.1b**.

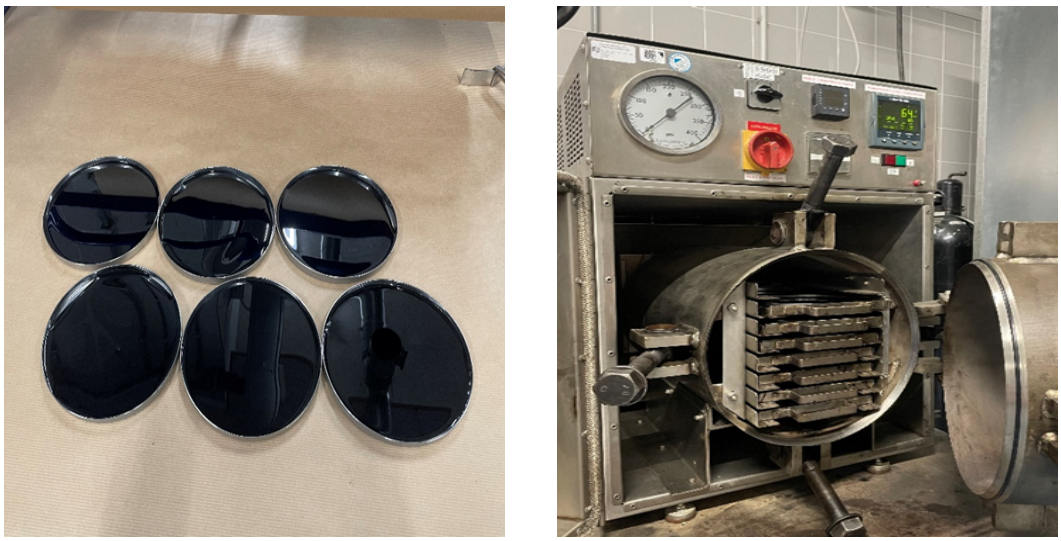

(a) (b)

Figure 3.1.: Bitumen aging process. (a) Sample Preparation; (b) PAV aging.

Long-term PAV aging was conducted on fresh 70/100 bitumen after short-term aging at different temperatures and durations to determine the optimal PAV aging conditions. Figure 3.2 presents the FS results of aged bitumen under various aging conditions compared to the reference bitumen, indicating that the aged bitumen subjected to PAV aging at 100°C for 90 hours most closely matched the complex shear modulus performance of the extracted RA bitumen.

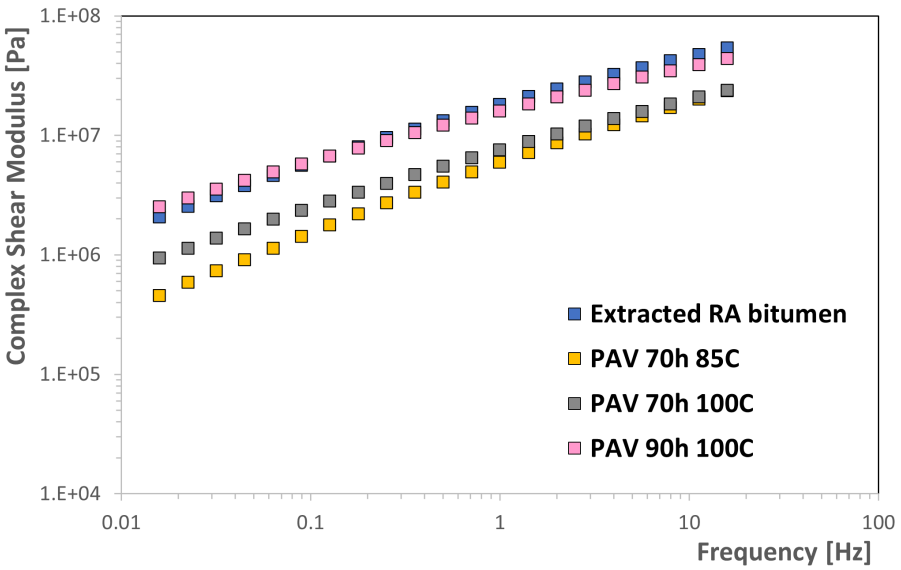

Figure 3.2.: Frequency sweep results of bitumen under various aging conditions.

(a) (b)

Figure 3.3.: Binder preparation process. (a) Blending; (b) Blended Binders.

After the short-term and long-term aging, the aged bitumen was blended with different fresh bitumen. The blending process was carried out using an electric blender to ensure thorough mixing of all components, as shown in **Figure 3.3a**. Finally, the new blended binders are cooled, labelled, and stored for subsequent experiments, as shown in **Figure 3.3b**.

The frequency sweep test was conducted at 20°C on the three blended binders using the DSR, with the complex shear modulus results presented in **Figure 3.4**. At this temperature, B2, the asphalt binder with a high RA bitumen content, exhibited the highest stiffness across all frequencies. In contrast, B3 was the softest of the materials; despite its high RA bitumen content similar to B2, the incorporation of a rejuvenator effectively reduced its stiffness. Thus, among the RA-containing binders, one binder (B2) showed higher stiffness, while the other (B3) demonstrated lower stiffness relative to the reference binder (B1).

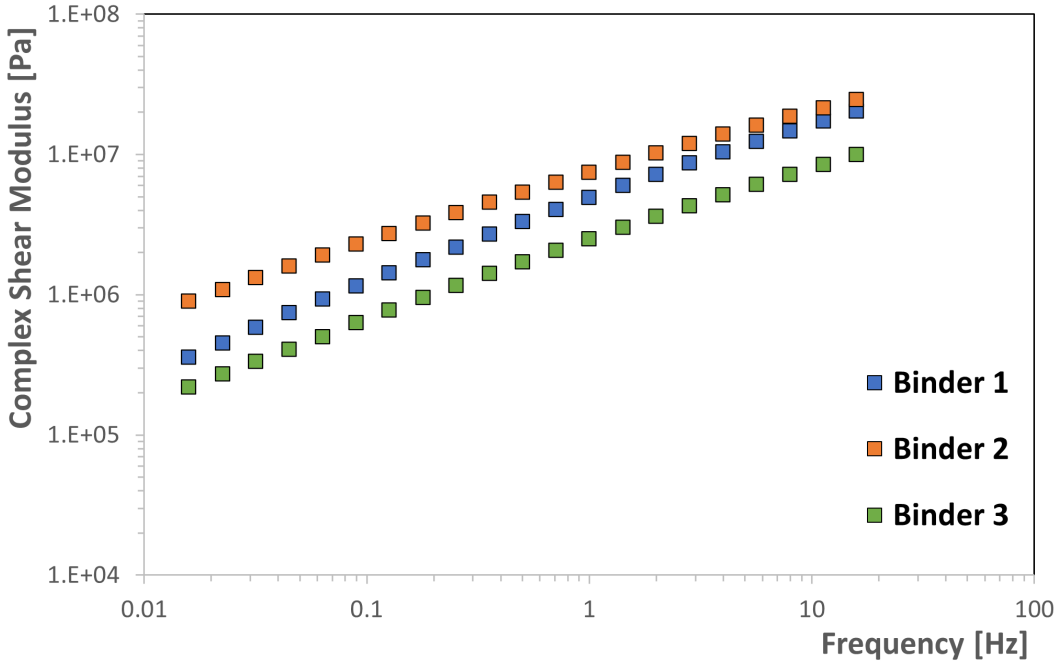

Figure 3.4.: Frequency sweep results of blended binders.

3.2. Testing protocols

In this study, the Dynamic Shear Rheometer (DSR), currently the most widely used equipment for testing the rheological performance of asphalt binders, was employed to conduct both fatigue and healing tests. The tests involved applying oscillatory shear to bitumen samples with a diameter of 8 mm and a thickness of 2 mm. The Time Sweep (TS) and the Linear Amplitude Sweep (LAS) tests were chosen to evaluate the fatigue performance of the asphalt binder, while the Time Sweep Healing (TS-H) and the Linear Amplitude Sweep Healing (LAS-H) tests were used to assess the binder's healing potential.

For each test condition in the TS and LAS tests, three parallel experiments were conducted to ensure consistency. For the TS-H and LAS-H tests, at least two parallel experiments were performed for each condition, with three parallel experiments conducted under certain conditions to further verify the reliability of the results. Since binders can experience adhesive failure or exhibit unstable flow during fatigue, particularly at low or high temperatures (Safaei and Castorena, 2016), the testing temperature in this study was set at 20°C. This temperature was selected to promote cohesive cracking while minimizing flow, ensuring more reliable fatigue and healing assessments.

3.2.1. TS/TS-H Tests

The TS test is the primary method for evaluating the fatigue resistance of asphalt binders. It is typically conducted under either stress control or strain control, where repeated oscillatory sinusoidal shearing is applied to the sample at a constant frequency and temperature. The loading pattern of the TS test is illustrated in **Figure 3.5**. In this study, a sinusoidal load with a frequency of 10 Hz was applied for all TS and TS-H tests.

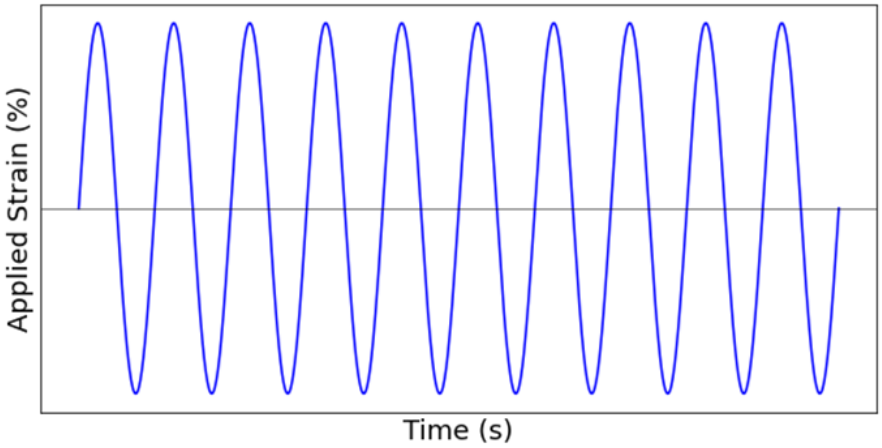

Figure 3.5.: The loading pattern of the TS test.

The traditional fatigue failure criterion for both TS and TS-H tests is based on a 50% reduction in the specimen's stiffness modulus (Bonnetti et al., 2002). Additional criteria include the peak in phase angle, the peak in S × N (stiffness times loading cycles), and energy theory-based definitions, such as the Dissipated Energy Ratio (DER) and the Ratio of Dissipated Energy Change (RDEC) (Bonnetti et al., 2002). Previous studies indicate no significant difference between the results obtained from traditional stiffness reduction (N_{f50}) and energy-based methods like DER (N_{p20}) and RDEC (N_{fl}) in both fatigue and healing tests (Mannan and Tarefder, 2018). Given the difficulty of determining N_{p20} and N_{fl} in healing tests, along with the simplicity and efficiency of the stiffness reduction criterion (N_{f50}), N_{f50} was selected as the failure criterion for the TS and TS-H tests in this study.

There are two main methods for incorporating rest periods in fatigue testing: applying rest intervals and using intermittent loading (Castro and Sánchez, 2006). Applying rest intervals

involves pausing the fatigue test at specific stages for predetermined time intervals before resuming loading. This method may use either a single rest period or multiple rest periods. Intermittent loading, on the other hand, introduces rest periods after each loading cycle, with the rest period potentially being a multiple of the loading duration. This approach is more complex than using rest intervals (Jayaraman and Padmarekha, 2024). In this study, the method of applying rest intervals was used and the duration of rest periods for the various healing tests is detailed in the following sections.

Two types of TS-H tests were designed in this study. The first type incorporates a single rest period during the TS test. In this method, when the bitumen sample is loaded to 50% of its expected fatigue life (50% N_f), a 1000-second rest period is applied, after which the test resumes. To determine the expected fatigue life of the binder, three parallel TS tests are first conducted under three different strain levels. Based on the results, the fatigue equation is used to calculate the expected fatigue life under different strain conditions without rest periods. The loading pattern for the single rest period TS-H test is illustrated in **Figure 3.6**.

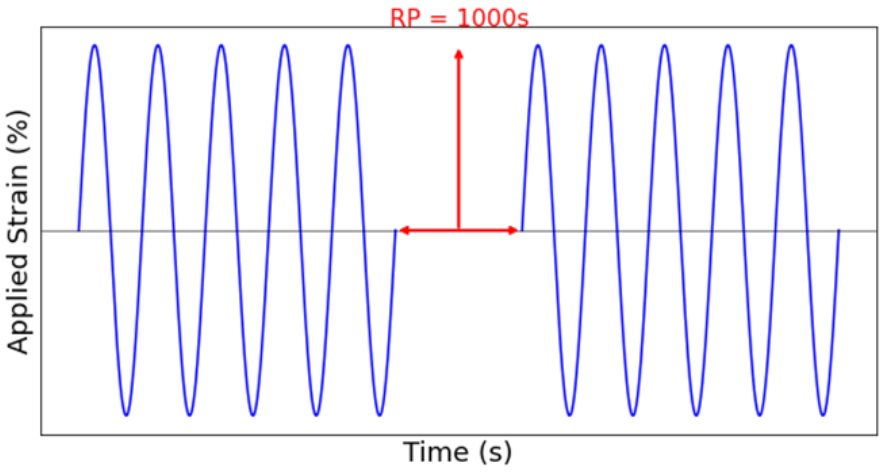

Figure 3.6.: The loading pattern of the single rest period TS-H test.

The second type of TS-H test incorporates multiple rest periods. In this approach, the specimen undergoes alternating loading and resting phases. Initially, the specimen is subjected to continuous loading for 20% of its estimated fatigue life (20% N_f), followed by a 200-second rest period. This cycle of loading and resting is repeated five times, after which the specimen is loaded continuously until failure during the sixth loading. In the TS-H tests with multiple rest periods, a total of five 200-second rest periods were set, resulting in a total rest duration of 1000 seconds, which is identical to the rest duration in the single rest period TS-H tests. The purpose of this setup was to eliminate the potential impact of varying rest durations on the healing performance, thereby focusing on the effect of increasing the number of rest periods on the healing performance.

If no healing effect occurs, the specimen will fail before the completion of the fifth loading-rest cycle, or within the estimated fatigue life. However, if a healing effect is present, the specimen will fail during the sixth loading cycle, extending beyond the estimated fatigue life. The loading pattern for the multiple rest periods TS-H test is depicted in **Figure 3.7**.

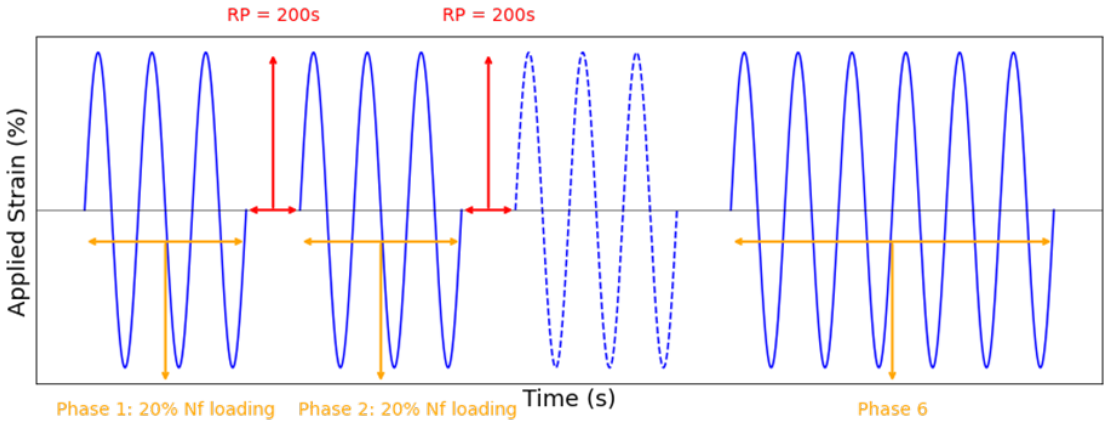

Figure 3.7.: The loading pattern of the multiple rest periods TS-H test.

3.2.2. LAS/LAS-H Tests

The standard LAS test procedure, as defined in AASHTO TP101, consists of two phases: a frequency sweep and a linear strain sweep test. First, a non-destructive frequency sweep test is conducted to obtain the material's rheological properties. The frequency sweep is performed at 20°C, with oscillatory shear loading applied at a constant strain amplitude of 0.1% across 12 unique loading frequencies, shown in Table 3.2.

Table 3.2.: Loading frequencies applied in the frequency sweep test.

Point Number	1	2	3	4	5	6	7	8	9	10	11	12
Frequency (Hz)	0.2	0.4	0.6	0.8	1	2	4	6	8	10	20	30

Then, the sample undergoes a linear strain sweep test, where the strain amplitude is linearly increased from 0.1% to 30%, inducing accelerated fatigue damage. The linear strain sweep phase lasts for 310 seconds, with loading applied at a frequency of 10 Hz. Using the rheological properties obtained from the frequency sweep, along with the results from the strain sweep, the material's fatigue resistance is evaluated through a combination of continuum damage mechanics and predictive modeling techniques. **Figure 3.8** illustrates the loading pattern for the continuous LAS test.

The LAS-H test introduces rest periods into the standard LAS testing procedure. In the LAS-H test, a rest period is introduced when the damage intensity (S) reaches 50% of the failure damage intensity (50%Sf), after which the testing resumes. To determine the specific damage level at failure, a continuous LAS test is first conducted, and the failure damage intensity is established using the S-VECD theory and the selected fatigue failure criterion. In this study, two rest period durations (100s and 1000s) were used to assess the impact of rest period length on the healing performance of asphalt binders. **Figure 3.9** illustrates the loading pattern of the LAS-H test.

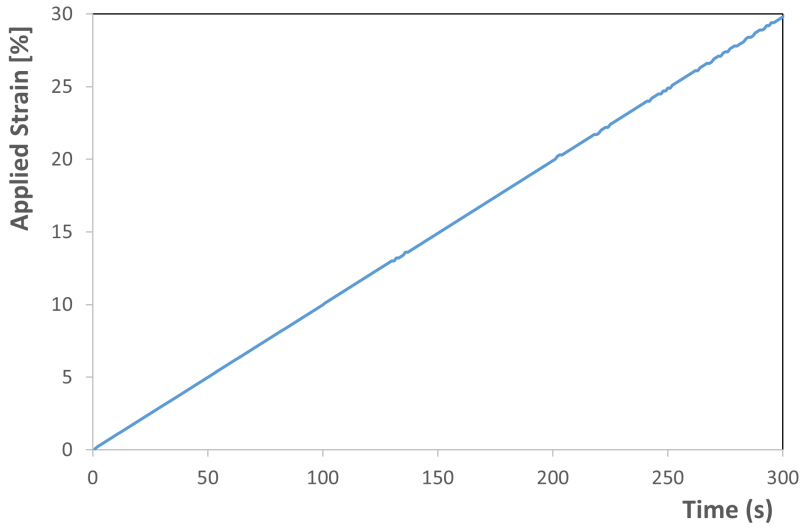

Figure 3.8.: The loading pattern of the continuous LAS test.

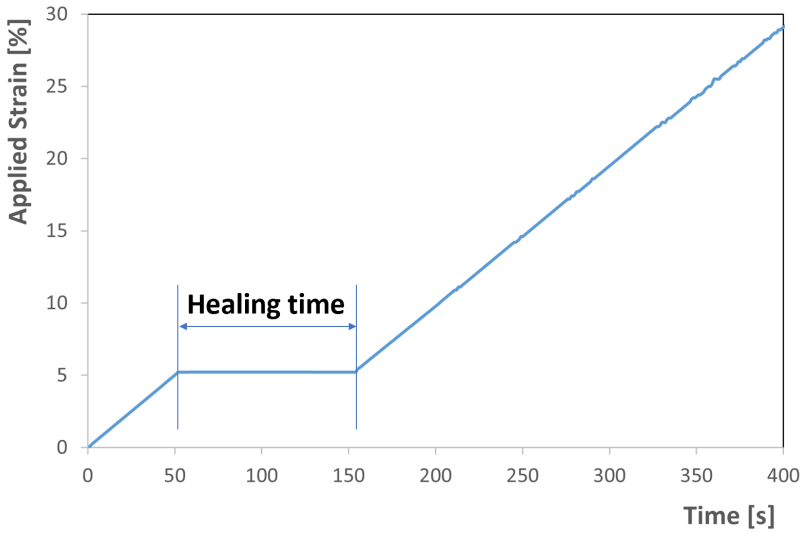

Figure 3.9.: The loading pattern of the LAS-H test.

Common fatigue failure criteria in LAS test include 35% reduction in material integrity (represented by G*·sin δ), the peak in shear stress, the peak in phase angle, the peak of C × N (material integrity times loading cycles), and maximum stored Pseudo-Strain Energy (PSE) (Cao and Wang, 2018). In this study, both LAS and LAS-H tests used the peak in shear stress as the fatigue failure criterion. The fatigue failure point is defined as the moment when the shear stress reaches its maximum. **Figure 3.10** presents a typical shear stress-strain response

for an asphalt binder subjected to a continuous LAS test, illustrating the definition of fatigue failure.

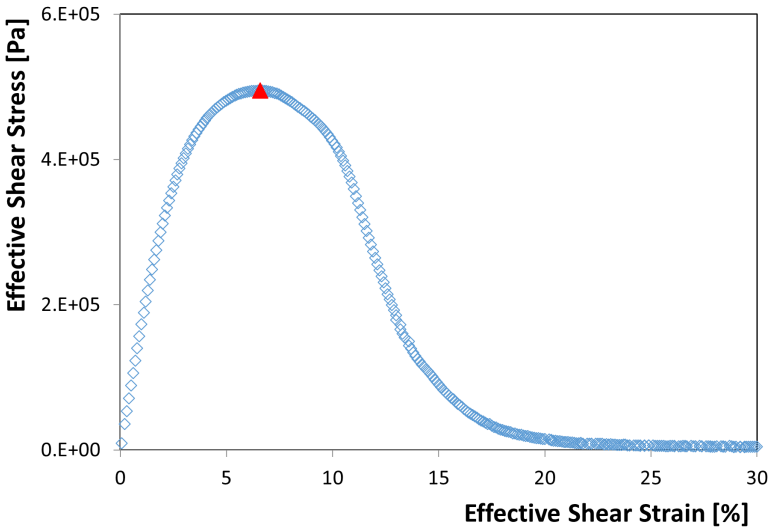

Figure 3.10.: The typical shear stress-strain response of in the LAS test.

Based on the experimental data, the damage characteristic curve, and the selected fatigue failure criterion, the fatigue life predictions for the LAS and LAS-H tests can be calculated using **Equations 2.8 and 2.9**. These calculations allow for the estimation of the material's fatigue life under different loading conditions.

Table 3.3 summarizes all test conditions for TS-H and LAS-H tests in this study.

Table 3.3.: TS-H and LAS-H test settings.

	Strain level (%)	**Rest Period**	**Damage Level**	**Temperature & Frequency**
TS-H Single	2%, 2.5%, 5%	1000s	$50\%N_f$	20°C and 10 Hz
TS-H Multi	2%, 2.5%, 5%	200*5=1000s	20%, 40%, 60% 80%, $100\%N_f$	
LAS-H	0.1% - 30%	100s, 1000s	$50\%S_f$	

3.3. Healing Indices Used In This Study

3.3.1. Healing Shift Factor SF_h Interpretation

In this study, a healing shift factor (SF_h) is used to evaluate the healing effect of the materials, defined by **Equation 3.1**. For the TS and TS-H tests, fatigue life was measured, while for the LAS and LAS-H tests, fatigue life was predicted based on the S-VECD theory. The healing effects were assessed by calculating the ratio of the fatigue life obtained from the tests with rest periods to the fatigue life from continuous loading tests. A higher healing shift factor indicates a greater improvement in fatigue life due to the healing process.

$$SF_h = \frac{N_{\text{f with RP}}}{N_{\text{f without RP}}} \tag{3.1}$$

3.3.2. Time Sweep Healing Index HI_{TS} Interpretation

By selecting the ratio of the complex modulus variation after the rest period to the change before rest as the healing index, the healing response of binders in the TS-H test was assessed using the Time Sweep Healing Index (HI_{TS}), which is defined by **Equation 3.2** (Sun et al., 2016):

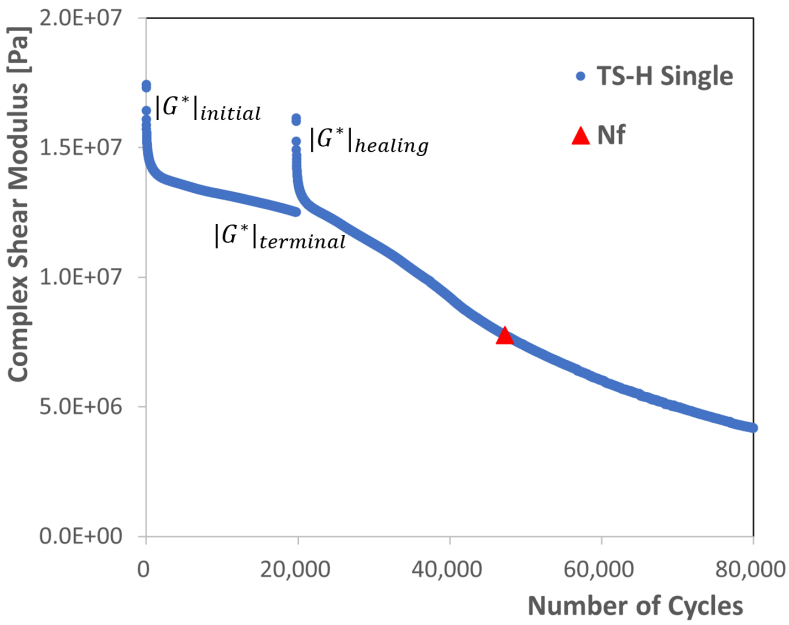

Figure 3.11.: Schematic of the healing index HI_{TS} variables.

$$HI_{TS} = \frac{|G^*|_{\text{healing}} - |G^*|_{\text{terminal}}}{|G^*|_{\text{initial}} - |G^*|_{\text{terminal}}} \tag{3.2}$$

where $|G^*|_{\text{initial}}$ is the initial complex modulus, $|G^*|_{\text{terminal}}$ is the complex modulus before the rest period, $|G^*|_{\text{healing}}$ is the complex modulus after the rest period. **Figure 3.11** presents a schematic of the healing index variables. In this formula, $|G^*|_{\text{initial}}$ represents the average complex modulus over the first 200 cycles after the initial loading applies, while $|G^*|_{\text{healing}}$ is the average complex modulus over the first 200 cycles after reloading.

3.3.3. Linear Amplitude Sweep Healing Index HI_{LAS} Interpretation

For the LAS-H test, the Linear Amplitude Sweep Healing Index (HI_{LAS}) is defined based on S-VECD theory to evaluate the healing effect of binders. This parameter is defined by **Equation 3.3**, where S_1 and S_2 represent the damage intensity before and after the application of the rest period, respectively. The HI_{LAS} quantifies the extent to which the asphalt binder's internal damage evolution is mitigated due to the rest period (Wang et al., 2023a). This parameter allows for a detailed analysis of how rest periods influence the internal healing mechanisms of the binder. **Figure 3.12** presents a schematic of the LAS-H healing index HI_{LAS}.

$$HI_{\text{LAS}} = \frac{S_1 - S_2}{S_1} \times 100\% \tag{3.3}$$

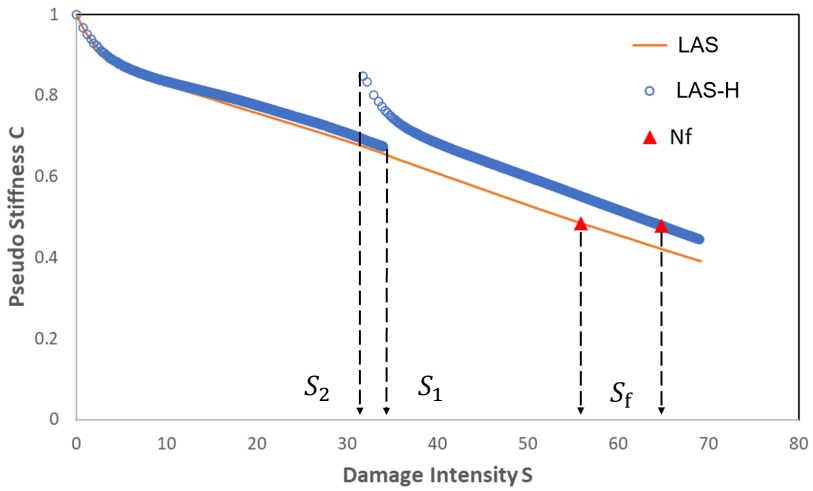

Figure 3.12.: Schematic of the healing index HI_{LAS} variables.

4

Fatigue Test Results

4. Fatigue Test Results

This chapter presents the results of the fatigue tests conducted in this study, including the time sweep fatigue test and linear amplitude sweep test for asphalt binders, as well as the four-point bending test for asphalt mixtures. Additionally, comparisons are made between the TS and LAS test results and between the fatigue performance of binders and mixtures.

4.1. Time Sweep Test Results

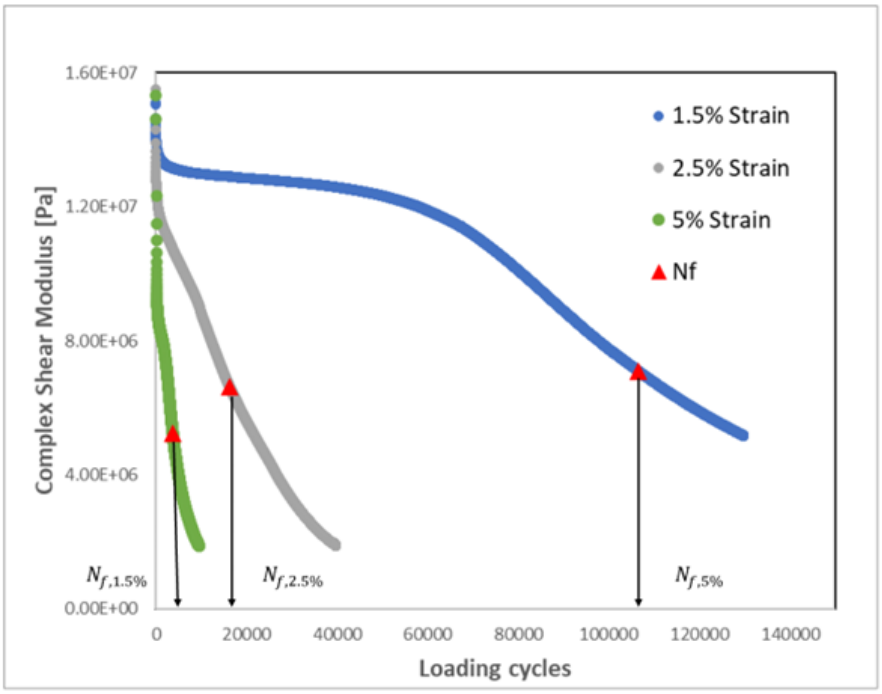

Figure 4.1.: Complex modulus evolution of Binder 1 in the strain-controlled TS tests.

The TS test is designed to assess the fatigue resistance of asphalt binder by monitoring the degradation of material integrity, typically measured through the reduction in modulus, under repeated loading. **Figure 4.1** presents the typical response of Binder 1 in the strain-controlled TS test. The results show that higher strain levels lead to a faster decrease in the binder's complex stiffness modulus, resulting in a shorter fatigue life. In contrast to the 2.5% and 5.0% strain levels, at lower strain levels, the complex stiffness modulus of the sample initially

experiences a prolonged period of gradual decay before entering a phase of rapid degradation. The red triangles in the figure mark the points where the binder's complex stiffness modulus has decreased by 50%, and the number of loading cycles at these points represents the fatigue life at different strain levels. The complex shear modulus evolution curves for the TS test cases are shown in **Appendix B.1**.

The experimental data for the three binders were fitted using a power law model, resulting in fatigue lines for each binder, as shown in **Figure 4.2.** Within the strain range of 1.5% to 5.0%, Binder 3 demonstrates a higher fatigue life compared to Binder 1 and Binder 2, maintaining a relatively high fatigue resistance even at elevated strain levels. Binder 2's fatigue life falls between that of Binder 1 and Binder 3. At lower strain levels, Binder 2's fatigue life N_f is similar to that of Binder 1, but at higher strain levels, its N_f approaches that of Binder 3, the most fatigue-resistant binder. Binder 1 consistently exhibits the lowest fatigue life across all strain levels, with particularly reduced fatigue resistance at higher strain levels compared to the other two binders.

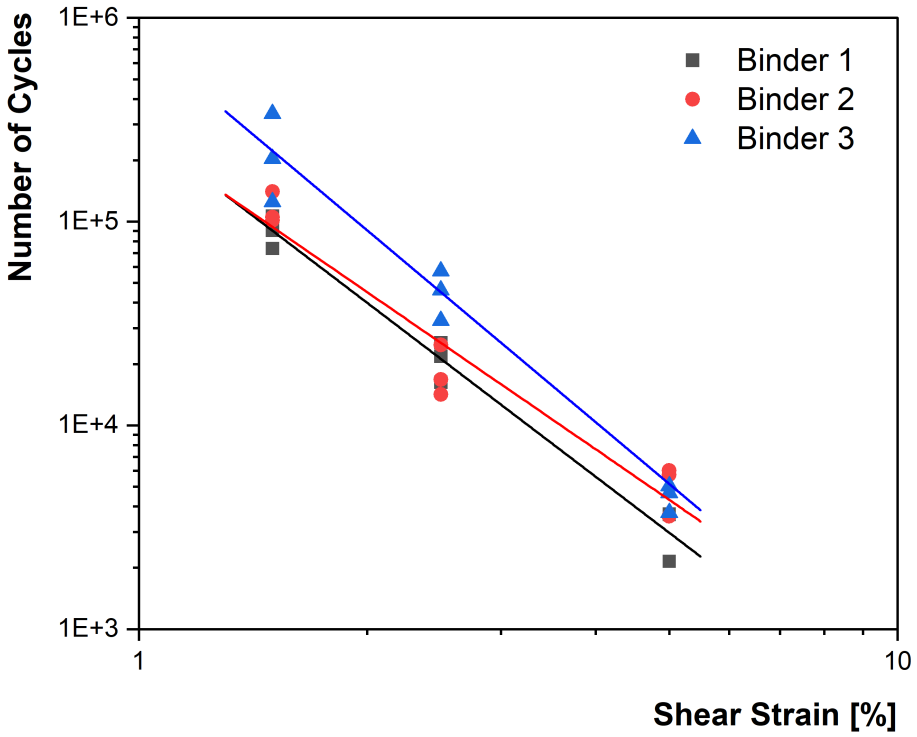

Figure 4.2.: Fatigue lines of three binders in the TS tests.

4.2. Linear Amplitude Sweep Test Results

Based on S-VECD theory, the damage characteristic curves (C-S curves) for the different binders were plotted, as shown in **Figure 4.3**. These curves reveal distinct trends in damage evolution, reflecting the binders' varying levels of fatigue damage resistance. Binder 3 shows higher material integrity at a given damage intensity compared to the other two binders. However, it is important to note that the fatigue performance of binders cannot be fully captured by the damage characteristic curves alone as S-VECD fatigue characterization incorporates three key material functions: Linear Viscoelastic (LVE) properties, damage evolution characteristics and the failure criterion (Wang et al., 2020). Additionally, as shown in Figure 4.3, further evaluation is needed to assess how fatigue life behaves across a broader range of strain levels. Variations in strain could provide more detailed insights into the binders' fatigue resistance. All the C-S curves of the LAS tests are shown in **Appendix B.2**.

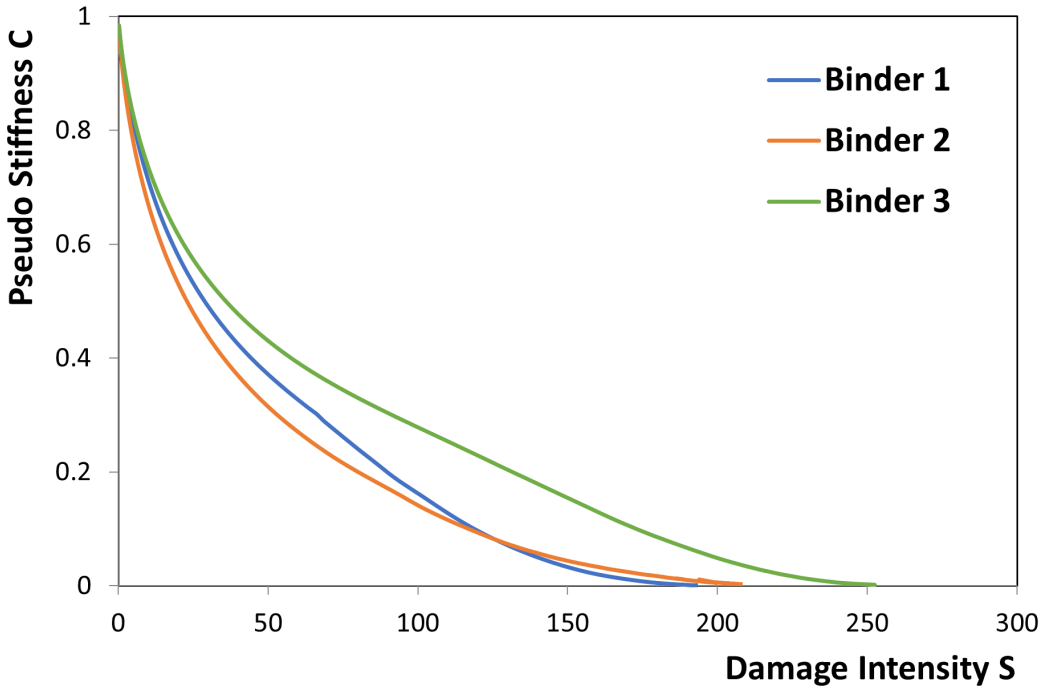

Figure 4.3.: Damage characteristic curves of three binders in the LAS tests.

Using the LAS experimental data, S-VECD theory, and the selected peak in shear stress fatigue failure criterion, the predicted fatigue lives of the different binders at strain levels of 1.5%, 2.5%, and 5.0% were calculated using **Equations 2.8 and 2.9**. The results, shown in **Figure 4.4**, indicate that within the strain range of 1.5% to 5.0%, Binder 3 exhibits significantly higher fatigue life than the other two binders, reflecting its high fatigue resistance across various strain levels. Binder 2 shows better fatigue resistance than Binder 1 at strain levels of 1.5% and 2.5%, but its fatigue life decreases below that of Binder 1 at higher strain levels.

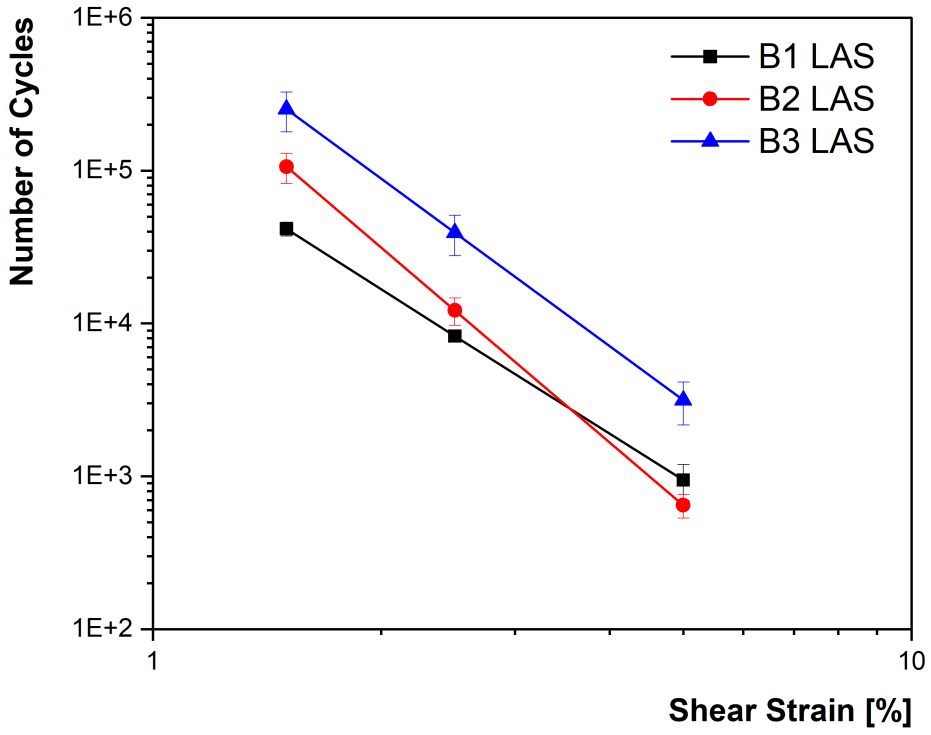

Figure 4.4.: Predicted fatigue life of three binders in the LAS tests.

4.3. Comparison of TS Measured Fatigue Life with LAS Predicted Fatigue Life

Figure 4.5 shows the fatigue lines from the TS and LAS tests, and several similarities and differences can be observed from it. First, the ranking of the fatigue life for the three binders is consistent between the TS and LAS tests, particularly at low and moderate strain levels. Binder 3 exhibits the highest fatigue resistance in both tests, which could be attributed to the effect of the rejuvenator ANOVA 1817. The rejuvenator reduces the stiffness and brittleness of the aged binder from RA, improving its viscoelastic behavior, which allows Binder 3 to exhibit longer fatigue life under both low and high strain conditions. Binder 1 consistently shows lower fatigue resistance in both tests, which could be attributed to the material properties of the fresh 40/60 bitumen used. The hard bitumen (40/60) has poor ductility, making it more prone to brittle failure under high strain conditions.

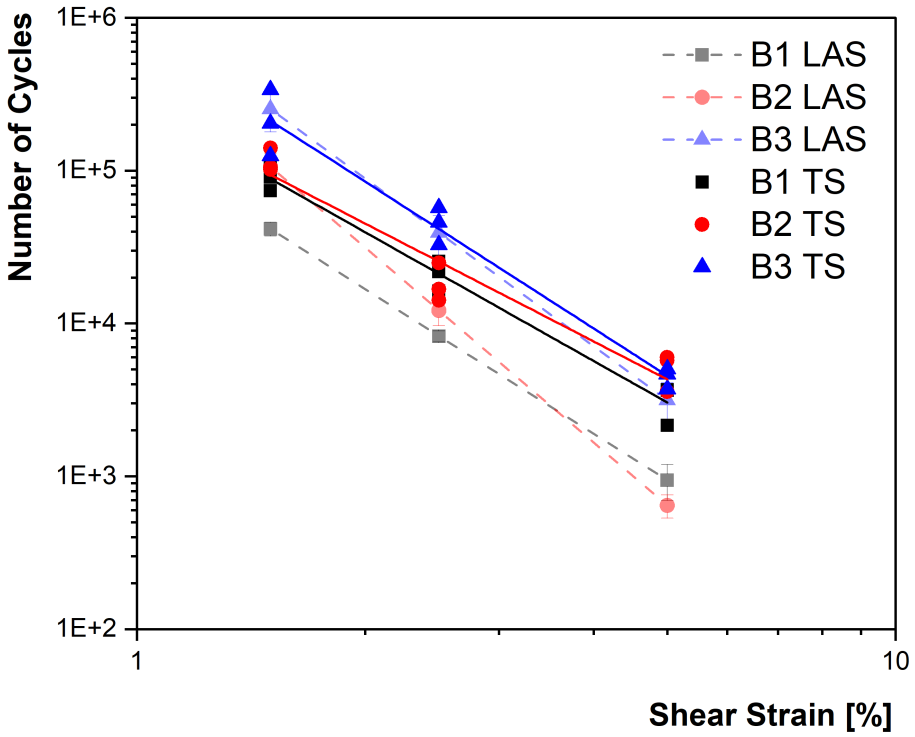

Figure 4.5.: Fatigue results from TS and LAS tests.

The majority of the predicted fatigue life values from the LAS test are lower compared to the fatigue life measured from the TS test. This difference can be attributed to LAS testing being an accelerated fatigue test, utilizing a wider strain range and shorter duration to predict material fatigue resistance. In contrast, the TS test is a more realistic simulation of real-world loading conditions. Consequently, the LAS test may lead to a higher rate of fatigue damage accumulation under higher strain conditions, resulting in lower predicted fatigue life at those strain levels.

Figure 4.6 presents the TS-measured fatigue life and LAS-predicted fatigue life results for the three binders across different strain levels. For Binder 1, a substantial discrepancy is observed between the two methods, with the TS-measured fatigue life consistently exceeding the LAS-predicted fatigue life across all strain levels. In the case of Binder 2, the results align closely at the lower strain level; however, at higher strain (5%), the TS-measured fatigue life is 7.82 times greater than the LAS predictions. Notably, for Binder 3, the fatigue life results from both TS and LAS tests are closely matched across all strain levels. This indicates that Binder 3, which contains a high RA bitumen content and the rejuvenator, exhibited a high level of consistency across both TS and LAS fatigue testing methods.

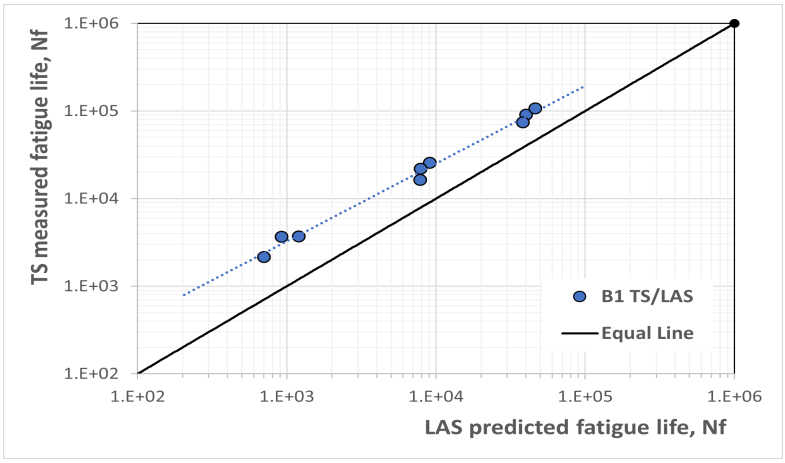

(a)

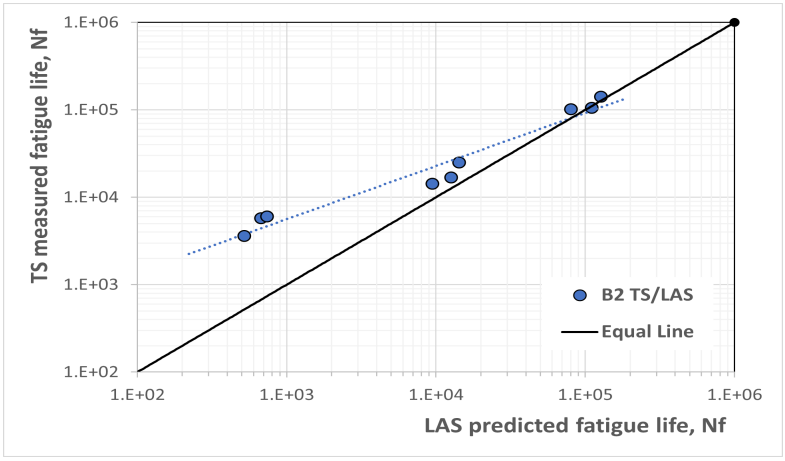

(b)

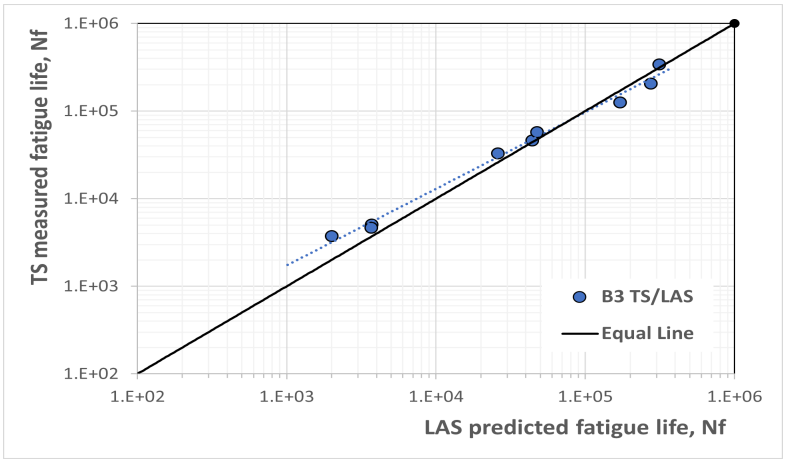

(c)

Figure 4.6.: Comparison between TS measured fatigue life and LAS predicted fatigue life of: (a) Binder 1; (b) Binder 2; and (c) Binder 3.

4.4. Comparison Between Binder Fatigue Life and Mixture Fatigue Life

Fatigue tests were conducted on the three asphalt mixtures using a four-point bending (4PB) machine, the most commonly employed method for asphalt mixture fatigue testing in the Netherlands. Each mixture underwent six parallel tests at high, medium, and low strain levels, with a testing temperature of 20°C. The experimental data for the three mixtures were fitted using a power law model, producing fatigue curves for each mixture as illustrated in **Figure 4.7a**.

Comparing the fatigue lines of the three mixtures (**Figure 4.7a**) with the TS fatigue lines of their corresponding binder components (**Figure 4.7b**) reveals several similarities and differences. The TS test results were selected for comparison rather than the LAS results, as the loading method in the TS test more closely resembles that of the 4PB test, with both employing strain-controlled cyclic loading. This constant-strain loading approach also more accurately reflects real-world traffic loads.

A similar trend is observed in the fatigue performance of both mixtures and binders. Binder 3, which shows the highest fatigue resistance, corresponds to Mixture 3, which also shows significantly higher fatigue life than the other mixtures. Similarly, Binder 1, with the lowest fatigue resistance, corresponds to Mixture 1, which demonstrates the shortest fatigue life. This indicates that the fatigue behavior of the binders plays a crucial role in determining the overall fatigue performance of the mixtures. Previous studies have also shown a strong correlation between the fatigue results from TS tests and the fatigue life measured in mixture tests.

Although the ranking of fatigue life for the binders and mixtures is consistent, there are notable differences in their fatigue lines. This is due to the fact that mixtures are complex systems, with distinct stress distribution and damage accumulation mechanisms. The internal structure and composition of the mixtures also significantly influence their fatigue behavior. Factors, such as aggregate gradation, air void content, and the adhesion between the asphalt binder and the aggregates, play critical roles in determining a mixture's fatigue resistance. As a result, these factors contribute to differences in the fatigue performance of mixtures compared to that of the binders.

The fatigue lines of the binders exhibit a steeper slope under high strain conditions, indicating that the binders are more sensitive to strain compared to the mixtures. This sensitivity could be attributed to the fact that binders, without the structural support provided by aggregates, rely solely on their own ductility and flexibility to endure large deformations. In contrast, the presence of aggregates in the mixtures helps maintain structural integrity under high strain, resulting in a relatively smaller decline in fatigue life. As a result, the mixtures show less strain sensitivity than the binders.

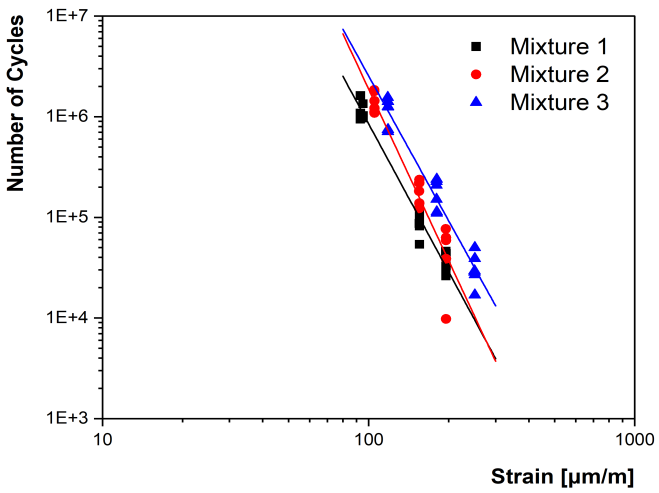

(a)

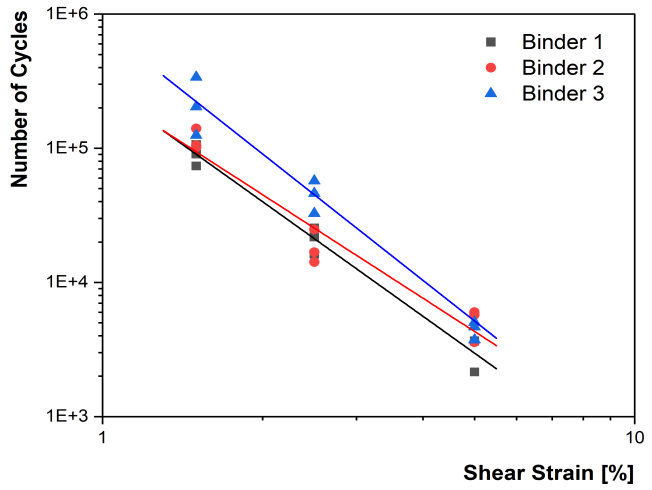

(b)

Figure 4.7.: Fatigue lines of: (a) mixtures from 4PB tests; (b) binders from TS tests.

Additionally, it is noteworthy that at the binder level, Binder 3, which contains the rejuvenator, exhibits significantly better fatigue performance than the other two binders. However, in the mixtures, although Mixture 3 still exhibits the best fatigue life, the gap between Mixture 3 and Mixture 2 or Mixture 1 is not as pronounced as the difference observed between the binders. This disparity may be attributed to the fact that the rejuvenator primarily enhances the binder's viscoelasticity and flexibility, while the overall performance of the mixture also depends on the aggregate distribution and structure. Therefore, the rejuvenator's effects are less direct or pronounced in the mixtures compared to the binders alone.

4.5. Conclusions of the Fatigue Tests

The key findings from the fatigue tests of this research are summarized as follows:

- In the TS tests conducted on asphalt binders, three parallel tests were performed at 20°C on each binder under three different strain levels, and fatigue lines were subsequently plotted. The results indicated that within the strain range of 1.5% to 5%, Binder 3, containing a high RA bitumen content and the rejuvenator, exhibited the longest fatigue life. This was followed by Binder 2, which contained a high RA bitumen content and a softer fresh bitumen, and lastly Binder 1, composed of 100% fresh bitumen.
- In the LAS tests on asphalt binders, the S-VECD theory was used to predict the fatigue life of the binders at various strain levels. The results showed that Binder 3 had the longest predicted fatigue life. Binder 2 showed a longer fatigue life than Binder 1 within the strain range of 1.5% to 2.5%, but it fell below Binder 1 at higher strain levels.
- Although the TS and LAS test results show a high level of consistency in the fatigue life ranking, some differences remain. These discrepancies can be attributed to the differing loading methods of the two tests: the LAS test is an accelerated fatigue test, utilizing a wider strain range and shorter duration to predict material fatigue resistance. Under higher strain conditions, the LAS test may lead to a faster accumulation of fatigue damage, potentially underestimating fatigue life at high strain levels.
- The fatigue life ranking of the asphalt binders' TS fatigue lines aligns with that of the asphalt mixtures' 4PB fatigue lines, revealing that the fatigue behavior of the binders plays a critical role in determining the overall fatigue performance of the mixtures. However, due to the more complex internal structures and composition of asphalt mixtures compared to asphalt binders, some differences in fatigue performance are also observed.

5 Healing Test Results

5. Healing Test Results

This chapter presents the results of the healing tests conducted in this study, including the single rest period Time Sweep Healing (TS-H Single) test, multiple rest period Time Sweep Healing (TS-H Multi) test, and Linear Amplitude Sweep Healing (LAS-H) test. In each test, healing performance was evaluated using healing indices: SF_h, based on fatigue life, and HI, based on the recovery of complex shear modulus after the rest period. This chapter also includes a comparison of the results from the TS-H Single and LAS-H tests.

5.1. Time Sweep Healing Test Results

5.1.1. Single rest period TS-H test

At 20°C, TS-H Single tests with a 1000-second rest period were conducted on different asphalt binders at three strain levels. Two parallel tests were performed for each test condition to ensure the reliability and reproducibility of the results. Two healing indices, SF_h and HI_{LAS}, were then employed to evaluate the healing performance of the asphalt binders. Figure 5.1 illustrates a typical complex shear modulus response of asphalt binders in the TS-H Single test, using the modulus evolution of B1 at 2.5% strain as an example. The complex shear modulus evolution curves for other TS-H Single tests on asphalt binders are provided in **Appendix C.1**.

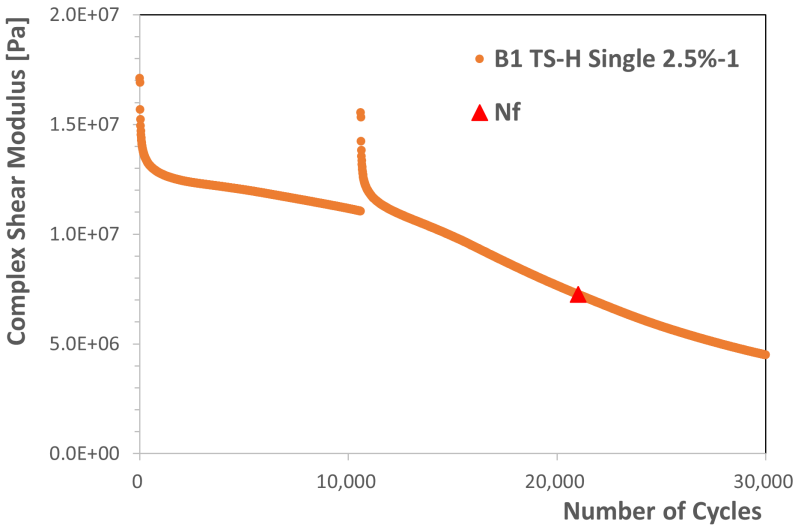

Figure 5.1.: Modulus evolution curve of Binder 1 at 2.5% strain in TS-H Single test.

Healing performance analysis based on healing shift factor SF_h

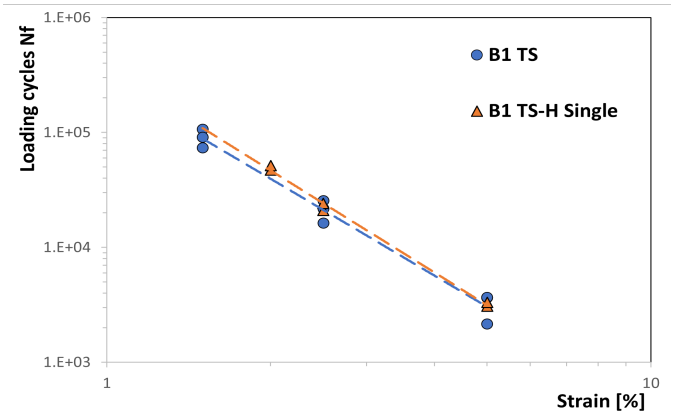

(a)

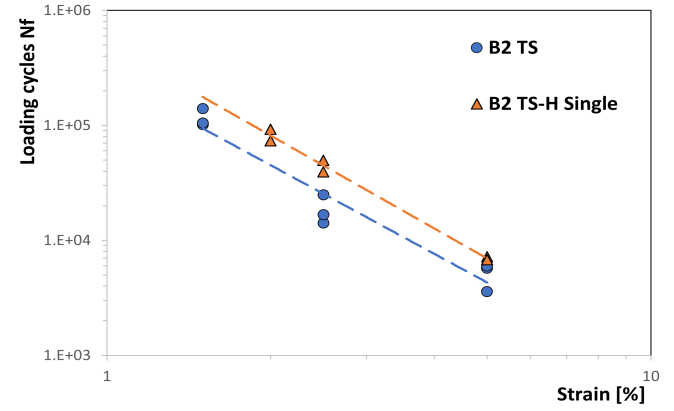

(b)

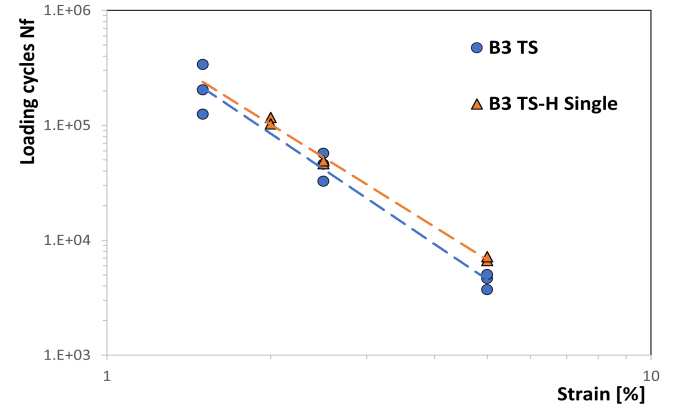

(c)

Figure 5.2.: Fatigue lines in TS and TS-H Single tests of (a) Binder 1; (b) Binder 2; (c) Binder3.

Figure 5.2 shows the fatigue lines from the pure fatigue and the single rest period TS-H tests for the three binders. Due to the introduction of the 1000 s rest period, the fatigue lines for all three binders shifted to varying degrees, with Binder 2 showing the most significant shift. This indicates that including a rest period extends the fatigue life of the binders by allowing some degree of healing to occur during the pauses, resulting in an overall shift of the fatigue curves toward a higher number of loading cycles. The healing effect of Binder 1 is primarily observed under low strain levels. Although the rest period improves its fatigue life, the performance enhancement at high strain levels is limited. In contrast, Binder 3 exhibits higher healing performance under high strain compared to low strain conditions.

Table 5.1 lists the healing shift factors for the three binders under three different strain conditions. For all binders, the shift factors range from 1.03 to 1.81. The SF_h values for all the conditions are greater than 1, indicating that the introduction of a rest period increases the fatigue life of the binder. However, it can be observed that the healing effects of the single 1000s rest period vary among the three binders.

Table 5.1.: Healing shift factors for the three binders in TS-H Single test.

Strain (%)	Binder 1	Binder 2	Binder 3
2.0	1.18	1.81	1.20
2.5	1.14	1.76	1.27
5.0	1.03	1.61	1.49

The SF_h value of Binder 1 shows a decreasing trend with increasing strain, decreasing from 1.18 at 2% strain to 1.03 at 5% strain. Binder 2 exhibits significantly higher SF_h values across all strain levels compared to the other two binders, with a notable value of 1.81 at low strain (2%), indicating a strong healing effect. As strain increases, the SF_h gradually decreases to 1.76 at 2.5% strain and 1.61 at 5% strain. However, even at high strain, the healing effect remains relatively high. In contrast, Binder 3 has a relatively low SF_h value at low strain (1.20 at 2.0%), but the SF_h increases with strain, reaching 1.27 at 2.5% and 1.49 at 5%. This is in contrast to the other two binders, as Binder 3 demonstrates stronger healing ability under higher strain conditions.

Healing performance analysis based on healing index HI_{TS}

Figure 5.3 and **Table 5.2** compares the HI_{TS} results obtained from the TS-H Single test for different asphalt binders at varying strain levels. The healing index of Binder 1 is significantly lower than that of the other two binders across all strain levels, and it shows little variation with increasing strain. Binder 2 maintains a relatively stable healing index at all strain levels, exhibiting the highest healing index at low and moderate strains. Binder 3 shows a gradual increase in healing index from 2.5% to 5% strain, with the healing index exceeding 80% at 5% strain, surpassing both Binder 1 and Binder 2. This indicates that Binder 3 demonstrates the best healing performance under high strain conditions.

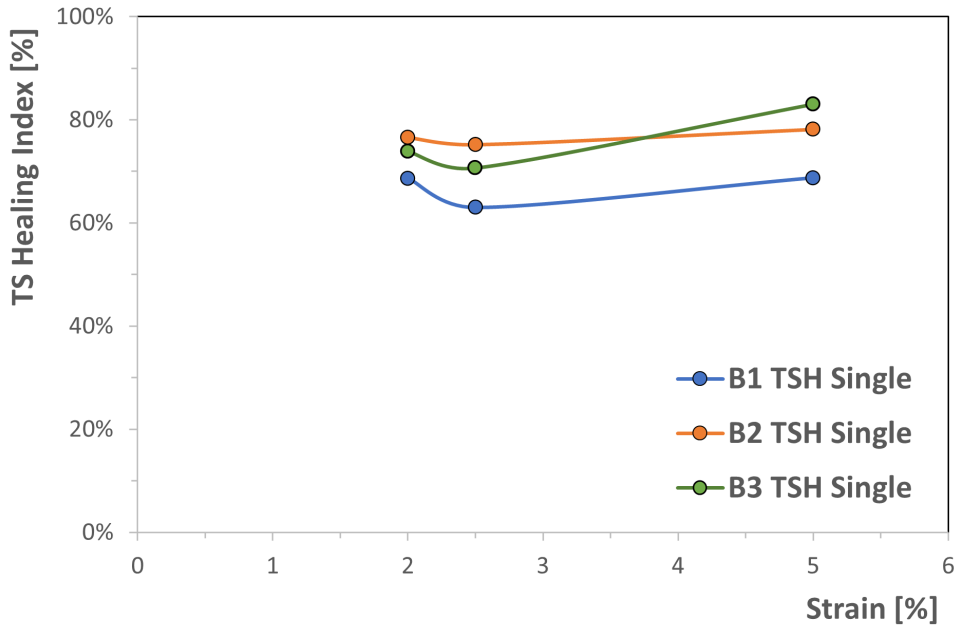

Figure 5.3.: TS healing index HI_{TS} of three binders in TS-H Single tests

Table 5.2.: TS healing index HI_{TS} of three binders in TS-H Single tests.

Strain [%]	Binder 1 [%]	Binder 2 [%]	Binder 3 [%]
2.0	68.64	76.56	73.87
2.5	62.98	75.13	70.66
5.0	68.73	78.15	82.99

The healing shift factor SF_h and the healing index HI_{TS} results from the TS-H Single test exhibit several similarities. First, the healing performance rankings are similar, with Binder 2 demonstrating the highest healing performance at low (2.5%) and medium (5.0%) strain levels in both sets of results, while Binder 1 shows the lowest healing performance at all strain levels. Additionally, for Binder 3, both parameters indicate an improvement in healing capacity as the strain level increases. A plausible explanation is that the rejuvenator becomes more effective at higher strain levels, leading to better healing performance for Binder 3 under high strain compared to low strain conditions.

The healing shift factor SF_h and the healing index HI_{TS} do not always exhibit consistent behavior. For example, Binder 1 shows a clear decreasing trend in the healing shift factor SF_h as strain increases, whereas in the healing index HI_{TS}, its healing capacity remains relatively stable, with a slight increase observed at 5% strain. The discrepancy arises because these two healing indices emphasize different aspects of the healing effect. The healing index HI_{TS} reflects the material's ability to recover its complex shear modulus after a rest period. However, the modulus recovery after the rest period is influenced not only by the material's healing but also by biasing effects. Determining the extent to which the overall modulus recovery is

attributable to material healing versus biasing effects is beyond the scope of this research. In contrast, the healing shift factor SF_h focuses on the actual extension of the material's fatigue life after healing. Even if the stiffness recovery is limited, the SF_h value can still be high if the material successfully delays the propagation of fatigue cracks during the healing process, resulting in a longer fatigue life.

By combining the results of both the healing shift factor and the healing index, a more comprehensive evaluation of the healing potential of different binders can be achieved. This approach captures both the immediate stiffness recovery (healing potential) and the long-term impact of healing on fatigue resistance.

5.1.2. Multiple rest period TS-H test

In addition to the TS-H Single tests, the multiple rest periods TS-H test (TS-H Multi) were also conducted in this study. In the TS-H Multi test, the total rest duration remains consistent at 1000 seconds, as in the TS-H Single test. The primary difference is that, instead of a single rest period, five rest periods of 200 seconds each are introduced throughout the test. This alternating pattern of multiple loading and rest periods more closely simulates real-world traffic conditions experienced by pavements.

To ensure reliability and reproducibility, at least two parallel experiments were conducted for each test condition. Two distinct healing indices, SF and HI, were then used to evaluate the healing performance of the asphalt binders. Figure 5.4 illustrates a typical complex shear modulus response of asphalt binders in the TS-H Multi test, using the modulus evolution of Binder 1 at 2.5% strain as an example. The complex shear modulus evolution curves from other TS-H Multi tests on asphalt binders are presented in **Appendix C.2**.

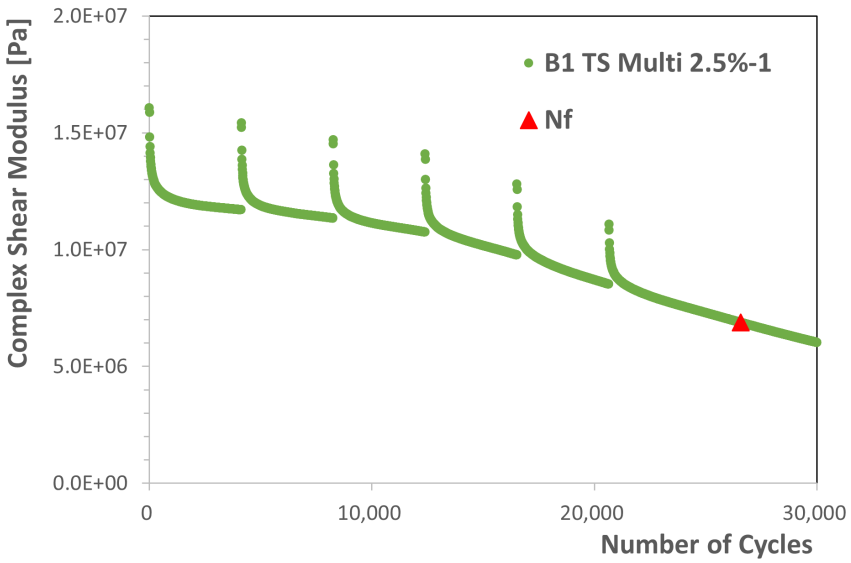

Figure 5.4.: Modulus evolution curve of Binder 1 at 2.5% strain in TS-H Multi test.

Healing performance analysis based on healing shift factor SF_h

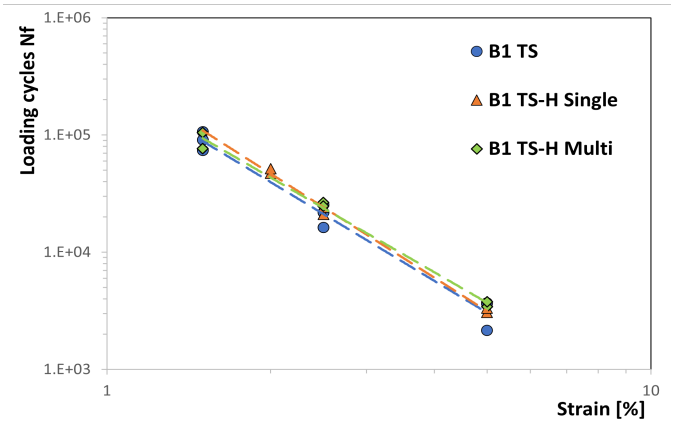

(a)

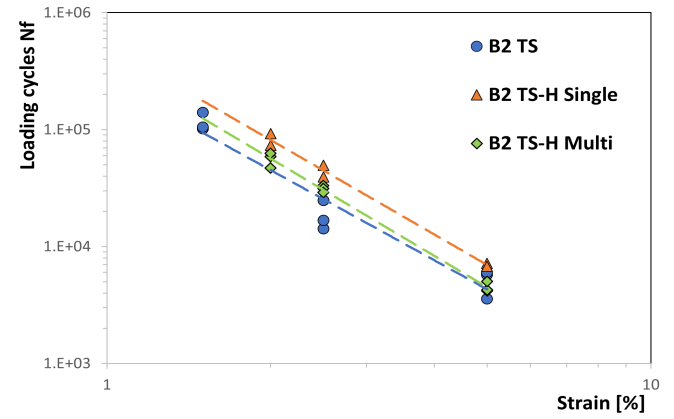

(b)

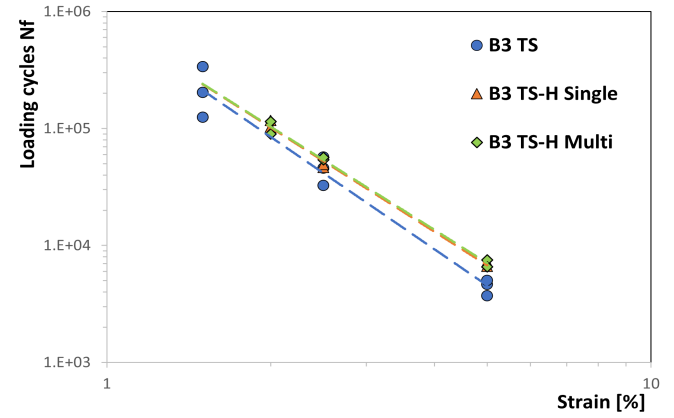

(c)

Figure 5.5.: Fatigue lines in TS, TS-H Single and TS-H Multi tests of: (a) Binder 1; (b) Binder 2; and (c) Binder 3.

Figure 5.5 shows the fatigue lines for the three binders from the TS, TS-H Single, and TS-H Multi tests. Due to the introduction of five rest periods in the TS-H Multi test, all three binders exhibit different degrees of shifts in their fatigue lines. This shift indicates that the inclusion of rest periods increases the fatigue life of the binders, causing the overall fatigue curves to move toward higher loading cycles.

In the classical fatigue analysis of asphalt materials, the fatigue line in the double logarithmic coordinate system is defined by **Equation 5.1**.

$$N_f = k_1 \left(\frac{1}{\varepsilon}\right)^{k_2} \tag{5.1}$$

where N_f is the number of cycles to failure, ε represents the applied cyclic strain, and k_1 and k_2 are coefficients related to the material properties.

Table 5.3 to **5.5** list the fatigue equations and key parameters obtained from TS, TS-H Single, and TS-H Multi tests for the three types of binders. k_1 is a coefficient related to the material's fatigue performance, while k_2 represents the linear gradient of the fatigue line, reflecting the sensitivity of the material's fatigue life to strain levels.

Table 5.3.: Fatigue equations of Binder 1 in TS and TS-H tests.

Test Type	**Fatigue Equation**	**Fatigue Parameters**		R^2
		k_1	k_2	
B1 TS	$N_f = 2.75 \times 10^5 \left(\frac{1}{\sigma_0}\right)^{2.798}$	2.75×10^5	2.798	0.956
B1 TS-H Single	$N_f = 3.60 \times 10^5 \left(\frac{1}{\sigma_0}\right)^{2.948}$	3.60×10^5	2.948	0.988
B1 TS-H Multi	$N_f = 2.78 \times 10^5 \left(\frac{1}{\sigma_0}\right)^{2.683}$	2.78×10^5	2.683	0.9525

Table 5.4.: Fatigue equations of Binder 2 in TS and TS-H tests.

Test Type	**Fatigue Equation**	**Fatigue Parameters**		R^2
		k_1	k_2	
B2 TS	$N_f = 2.66 \times 10^5 \left(\frac{1}{\epsilon}\right)^{2.561}$	2.66×10^5	2.561	0.9445
B2 TS-H Single	$N_f = 5.24 \times 10^5 \left(\frac{1}{\epsilon}\right)^{2.685}$	5.24×10^5	2.685	0.9607
B2 TS-H Multi	$N_f = 3.83 \times 10^5 \left(\frac{1}{\epsilon}\right)^{2.762}$	3.83×10^5	2.762	0.9646

Table 5.5.: Fatigue equations of Binder 3 in TS and TS-H tests.

Test Type	Fatigue Equation	Fatigue Parameters		R^2
		k_1	k_2	
B3 TS	$N_f = 7.75 \times 10^5 \left(\frac{1}{\epsilon}\right)^{3.192}$	7.75×10^5	3.192	0.7739
B3 TS-H Single	$N_f = 7.95 \times 10^5 \left(\frac{1}{\epsilon}\right)^{2.961}$	7.95×10^5	2.961	0.9803
B3 TS-H Multi	$N_f = 7.90 \times 10^5 \left(\frac{1}{\epsilon}\right)^{2.930}$	7.90×10^5	2.930	0.9669

In the fatigue equations for Binder 1, k_1 and k_2 show some variation across the three test types, but the changes are relatively small. Under single rest period healing test conditions, Binder 1 exhibits higher fatigue resistance and greater sensitivity to strain. The fatigue equation for Binder 2 reveals a different trend. Under the single rest period healing condition, it shows a significantly higher fatigue life compared to the other two test conditions, and under the multiple rest period healing condition, it has the highest sensitivity to strain. For Binder 3, both single and multiple rest periods healing conditions improve fatigue resistance compared to the TS test. Under the TS-H Single condition, the k_1 value is higher, and it also shows a greater sensitivity to strain.

Table 5.6 summarizes the healing shift factors SF_h obtained from the TS-H Single and TS-H Multi tests for the three binders. For all binders, the range of shift factors due to the introduction of multiple rest periods is between 1.04 and 1.55, all greater than 1, indicating that the introduction of multiple rest periods effectively increases the fatigue life of the binders. For Binders 1 and 3, the SF_h values increase with increasing strain, suggesting that these binders are well-suited for high strain conditions. In contrast, for Binder 2, the SF_h values decrease as strain increases, indicating that the healing benefits decrease at higher strain levels.

Table 5.6.: Healing shift factors for the three binders in TS-H Single and TS-H Multi tests.

Strain [%]	TS-H Single			TS-H Multi		
	Binder 1	Binder 2	Binder 3	Binder 1	Binder 2	Binder 3
2.0	1.18	1.81	1.20	1.10	1.25	1.22
2.5	1.14	1.76	1.27	1.12	1.20	1.30
5.0	1.03	1.61	1.49	1.22	1.04	1.55

In the TS-H Multi test, Binder 1 also exhibited the lowest healing performance. Its SF_h results were very similar between the TS-H Single and TS-H Multi tests, showing a slight increase from a range of 1.03 to 1.18 in the TS-H Single test to 1.10 to 1.22 in the TS-H Multi test. Notably, the trend of SF_h values with strain level differed between the two tests: in the TS-H Single test, the SF_h value decreased as strain level increased, whereas in the TS-H Multi test, it increased with higher strain levels. Binder 1 exhibited only a limited extension of fatigue life in both the TS-H Single and TS-H Multi tests, which can be attributed to its composition of 100% fresh, unaged 40/60 bitumen.

For Binder 2, which uses a soft binder (160/220) to mitigate the brittleness of the aged RA binder, the fatigue life under multiple rest periods was lower than that observed in the single rest period test, particularly at higher strain levels. To exclude the possibility of experimental randomness, three parallel TS-H Multi tests were conducted for Binder 2, confirming that its fatigue life does not benefit as much from multiple rest periods, especially under high strain conditions.

Overall, Binder 3 demonstrated the highest healing performance in the TS-H Multi test. Across all strain levels, its SF_h results in the TS-H Multi test were slightly higher than those in the TS-H Single test, increasing from a range of 1.20 to 1.49 to a range of 1.22 to 1.55. The introduction of multiple rest periods gives binders more opportunities to heal microcracks at different stages of damage, which contributes to Binder 3's enhanced fatigue life. The high healing performance of B3 could be attributed to its rejuvenator component, which softens the aged binder and restores its viscoelastic properties to allow effective healing during each rest period.

Notably, Binder 3 exhibited high healing performance in both the TS-H Single and TS-H Multi tests, in contrast to Binder 2, which showed greater sensitivity to the number of rest-reload cycles.

To analyze the reduction in fatigue life of Binder 2 during the TS-H Multi test, the complex shear modulus evolutions of Binder 2 were plotted. Figure 5.6 compares the evolution of the complex modulus of Binder 2 when tested with Single and Multiple rest periods at 2.5% and 5.0% strain levels.

The figure shows that although the complex modulus partially recovers after each rest period, the rate of modulus decline accelerates significantly with increasing rest-reload cycles for Binder 2, which contains a high proportion of RA bitumen and softer binder components. To quantify this phenomenon, the slope of the complex modulus curve for each loading phase during the TS-H Multi test was calculated for Binder 2 at 2.5% and 5% strain. To avoid the sharp modulus drop at the beginning of each loading phase, the slope was calculated based on the last 20% of data in each phase. For the 2.5% strain test, the slopes of the complex modulus curves were 154, 125, 176, 284, 317, and 438, respectively, while for the 5% strain test, the slopes were 1061, 1098, 1301, 1438, 1489, and 1664. These results indicate that the repeated rest periods and reload cycles accelerated the accumulation of damage in Binder 2, leading to earlier failure.

This indicates that the damage incurred during each reload surpasses the recovery gained during rest periods, leading to further accelerated modulus decline. Similar accelerated degradation phenomena have also been observed by other researchers in TS-H tests with multiple rest periods (Jayaraman and Padmarekha, 2024).

Figure 5.7 and Figure 5.8 compare the evolution of the complex modulus of Binder 1 and 3 when tested with Single and Multiple rest periods at 2.5% and 5.0% strain level. For Binder 1 and 3, no accelerated modulus degradation was observed as a result of multiple rest periods or repeated loading. Both binders maintained a similar trend in the slope of the complex modulus curves in the TS-H Multi test compared to the TS-H Single test or even demonstrated improved performance.

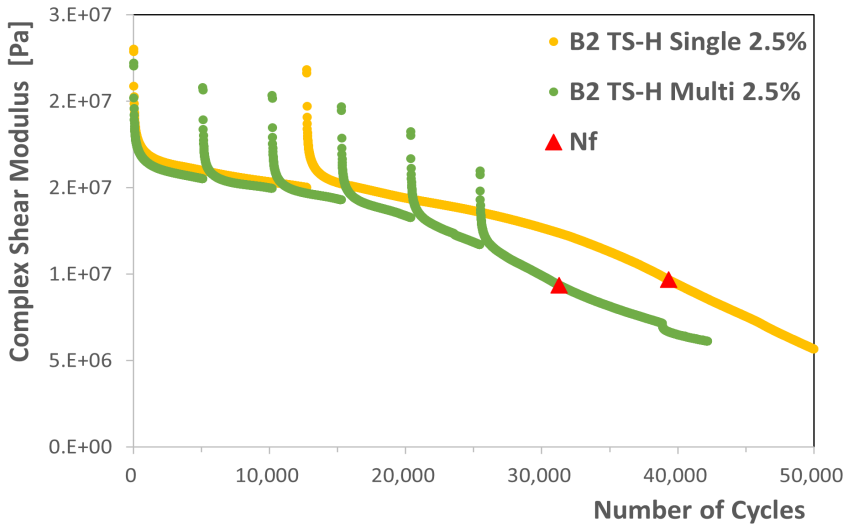

(a)

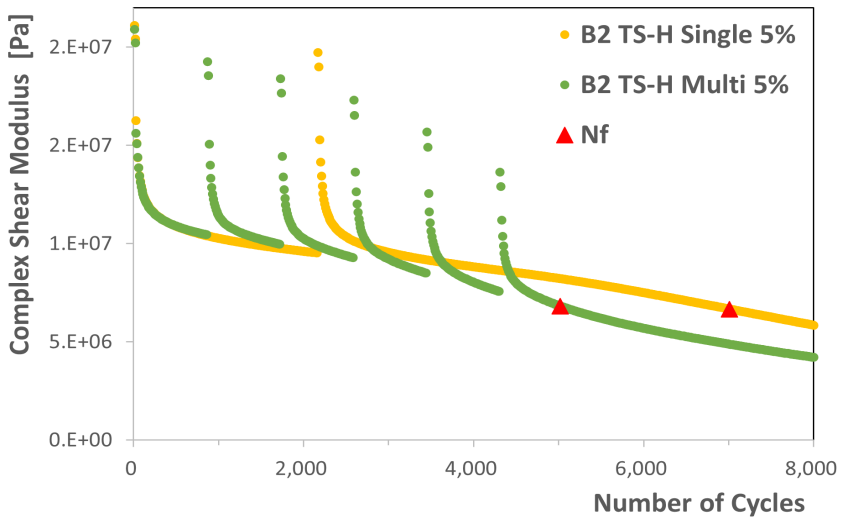

(b)

Figure 5.6.: Complex modulus evolution of Binder 2 under (a) 2.5% strain level; and (b) 5% strain level.

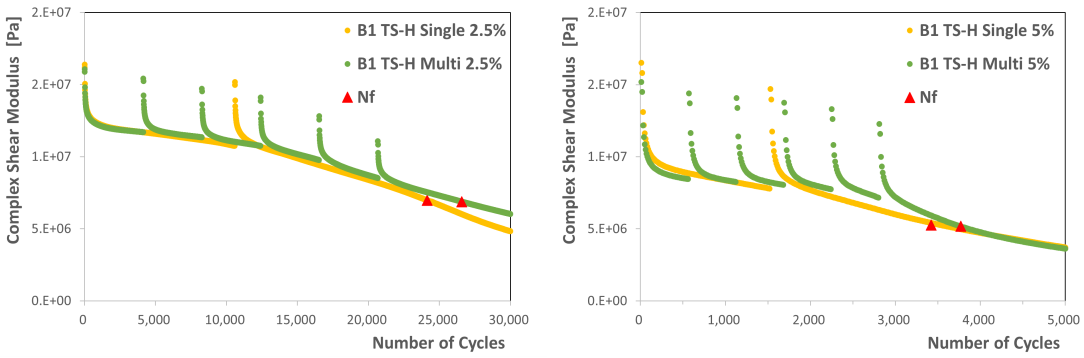

(a) (b)

Figure 5.7.: Complex modulus evolution of Binder 1 under (a) 2.5% strain level; and (b) 5% strain level.

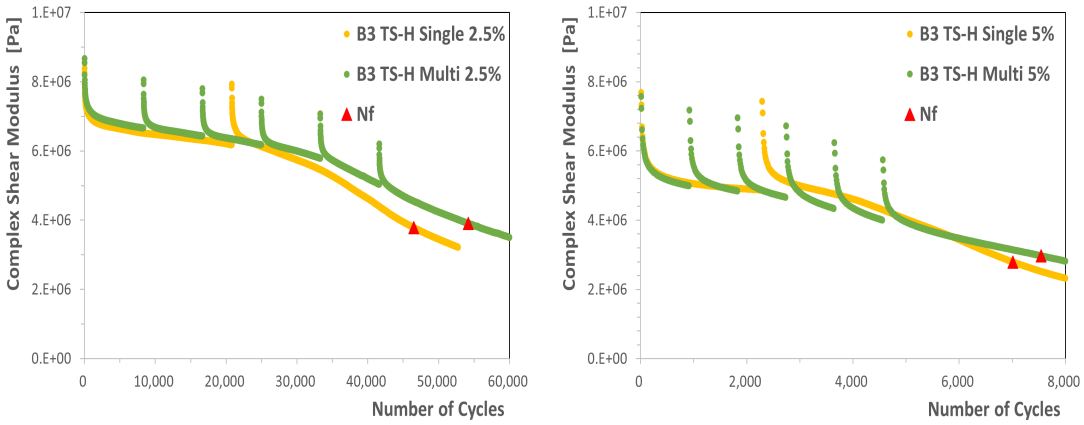

(a) (b)

Figure 5.8.: Complex modulus evolution of Binder 3 under (a) 2.5% strain level; and (b) 5% strain level.

Healing performance analysis based on healing index HI_{TS}

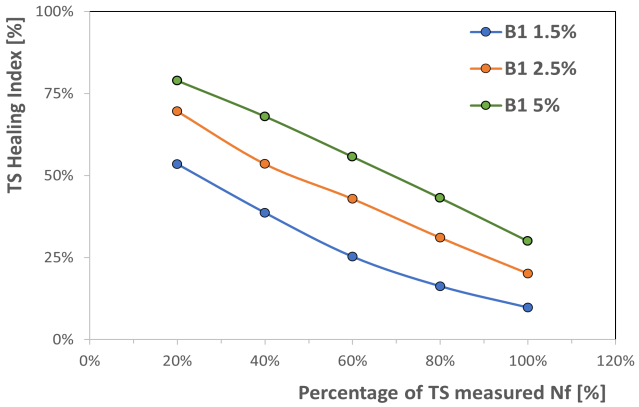

(a)

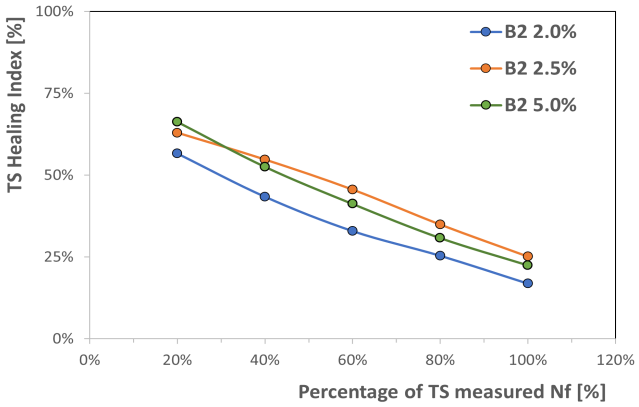

(b)

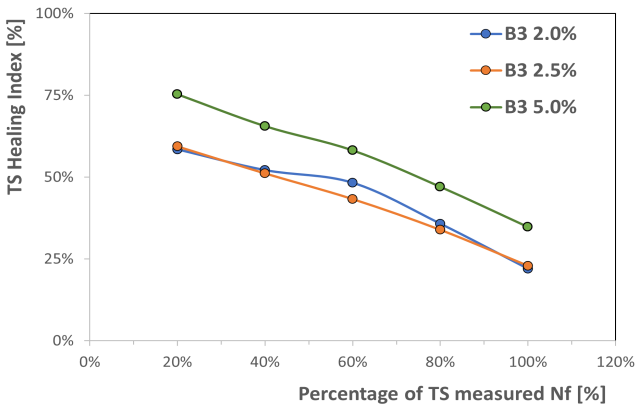

(c)

Figure 5.9.: TS healing index HI_{TS} in TS-H Multi tests of (a) Binder 1, (b) Binder 2, and (c) Binder 3.

Figure 5.9 shows the HI_{TS} results obtained from the TS-H Multi test for different asphalt binders at varying strain levels. The healing index for all three binders gradually decreases with an increasing number of rest periods, particularly during the fifth rest period (at 100% N_f), where the healing effect is significantly reduced. This indicates that the greatest healing benefits are achieved during the first rest period, while the binders' healing capacity decreases progressively with additional rest periods.

In the TS-H Multi test, Binder 1's healing capacity progressively increases with strain, consistent with the trend observed in its healing shift factor (SF_h). For Binder 2, the healing index at 2.5% and 5.0% strain levels is higher than at low strain (2.0%). However, overall, when the strain increases from 2.5% to 5.0%, the healing index slightly decreases, indicating that Binder 2's healing potential is constrained at higher strain levels. Notably, under high strain conditions, Binder 2's healing index is significantly lower than that of the other two binders, which aligns with the trend shown by the healing shift factors (SF_h), indicating that the healing potential of Binder 2 is limited during TS-H Multi tests at high strain. For Binder 3, the healing index is similar at 2.0% and 2.5% strain levels. However, at high strain (5.0%), Binder 3's healing index increases significantly, which corresponds with the upward trend in its healing shift factors (SF_h) as strain increases.

5.2. Linear Amplitude Sweep Healing Test Results

In the LAS-H test, two different rest periods, 100s and 1000s, were considered to evaluate the impact of rest duration on the healing effect. To ensure reliability and reproducibility, two parallel experiments were conducted for each test condition. All the C-S curves of the LASH tests are shown in **Appendix C.3**.

Healing performance analysis based on healing shift factor SF_h

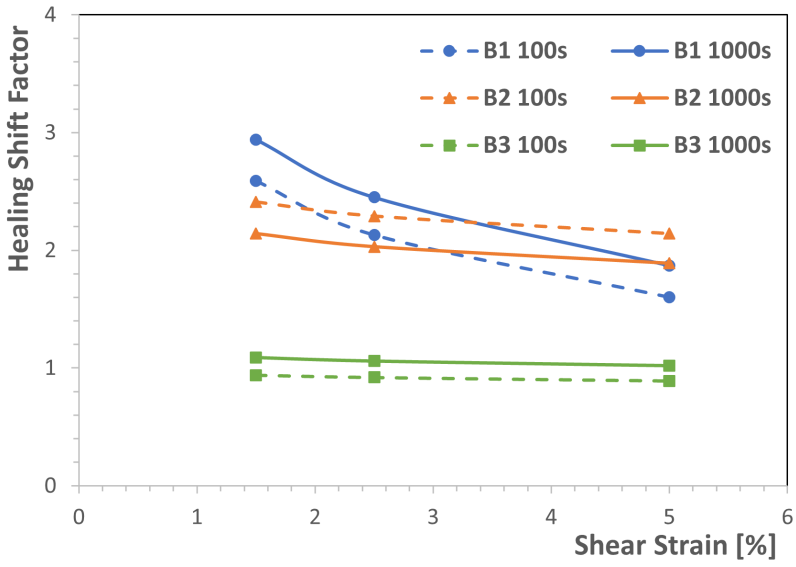

Figure 5.10.: Healing shift factors of three binders under 100s and 1000s rest period.

The healing shift factors SF_h for asphalt binders under different rest periods were calculated and are presented in **Figure 5.10**. Additionally, the results of these healing shift factors are summarized in **Table 5.7**.

Table 5.7.: Healing shift factors of three binders under 100s and 1000s rest period.

Strain [%]	100s RP			1000s RP		
	B1	B2	B3	B1	B2	B3
1.5	2.59	2.41	0.94	2.94	2.14	1.09
2.5	2.13	2.29	0.92	2.45	2.03	1.06
5	1.60	2.14	0.89	1.87	1.89	1.02

According to the predicted fatigue life results based on S-VECD modeling, Binder 1 shows significant healing effects under both the 100s and 1000s rest periods, especially under low strain conditions. However, as the strain increased, the healing effect decreased.

For Binder 2, the healing effect was notable under both rest periods, with minimal differences in healing performance across the various strain levels. As the rest period increased from 100 to 1000 seconds, the predicted fatigue life decreased, indicating that extended rest periods may not always benefit this binder and could potentially lead to accelerated damage accumulation.

Binder 3 showed poor healing performance under both rest periods, with SF_h values close to 1.0. This indicates that, regardless of strain level, the binder's ability to heal was quite limited, and the rest periods did not contribute significantly to extending the fatigue life.

Healing performance analysis based on healing index $HI_{\mathbf{LAS}}$

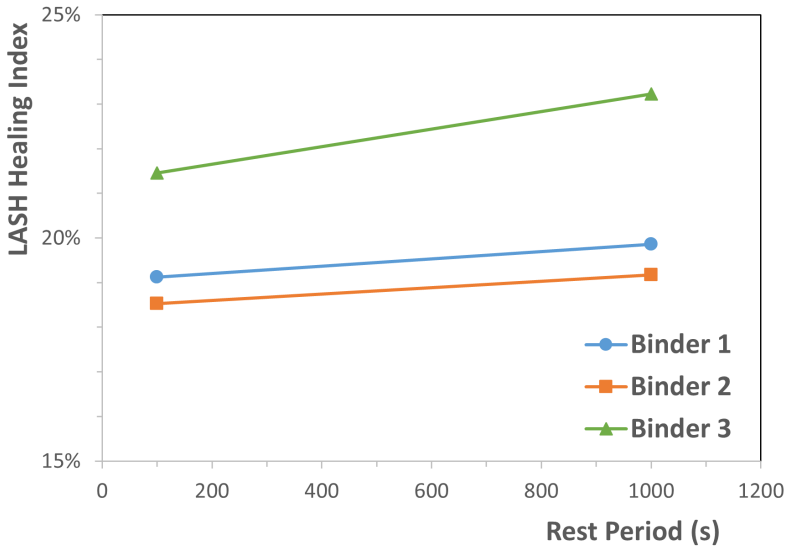

Figure 5.11.: LASH Healing Index results of three binders under 100s and 1000s rest period.

Figure 5.11 shows the healing index HI_{LAS} results for the three binders with healing times of 100 seconds and 1000 seconds, and the results are also summarized in **Table C.1** in the Appendix. Binder 3 showed higher HI_{LAS} values compared to the other two binders, with Binder 1 ranked second, having results very close to those of Binder 2. In contrast, Binder 2, which contains a high proportion of RA bitumen and softer bitumen (160/220), exhibited the lowest healing potential. The healing performance rankings of the three binders, as indicated by the Healing Index HI_{LAS}, are consistent with the rankings obtained from the healing shift factor (SF_h) in the TS-H Multi test.

Additionally, it can be observed that the HI_{LAS} for all binders increases as the rest period is extended, indicating that the healing performance improves with longer rest periods, which is consistent with findings from previous studies (Wang et al., 2019). However, the increase in HI_{LAS} was quite limited for all binders. In particular, for Binder 1 and Binder 2, when the rest period duration was increased tenfold, their HI_{LAS} only grew by 0.74% and 0.65%, respectively. In contrast, Binder 3 showed a more noticeable improvement in HI_{LAS}. This could be attributed to the rejuvenator in Binder 3, which effectively restored the viscoelastic properties of the aged binder, allowing the material to heal more.

Research has shown that providing rest periods before extensive damage occurs yields the most significant healing effects (Planche et al., 2004). Once extensive damage forms, increasing the rest period no longer improves the healing performance. This is because asphalt's intrinsic healing is more effective at addressing micro-cracks, while it has limited effectiveness in healing macro-cracks. In the current tests, the samples had already undergone continuous loading, with damage levels reaching 50% before the rest periods began. As a result, the healing effect of the rest periods was limited, as much of the damage had already progressed beyond the micro-crack stage.

5.3. Comparison between TS-H measured fatigue life and LAS-H predicted fatigue life

Figure 5.12 presents the TS-H Single measured fatigue life and LAS-H (1000s RP) predicted fatigue life results for the three binders. For Binders 1 and 3, the fatigue life measured in the TS-H test shows strong agreement with the fatigue life predicted by the LAS-H test at low and moderate strain levels. However, at the higher strain level of 5%, the fatigue life measured by the TS-H test of B1 and B3 is 1.81 and 2.16 times the predicted values from the LAS-H test, respectively. For Binder 1, composed of 100% fresh bitumen, and Binder 3, containing high RA bitumen content and a rejuvenator, the LAS-H test can accurately predict the fatigue life at low to moderate strain levels. However, at high strain (5%), it tends to underestimate fatigue life.

However, for Binder 2, while the results are similar at low strain levels, a notable discrepancy appears at high strain levels, where the TS-H measured fatigue life is significantly higher than the LAS-H predicted fatigue life. At moderate and high strain levels, the fatigue life measured by the TS-H test is 1.85 and 5.73 times the predicted values from the LAS-H test, respectively.

The results indicate that the current VECD-based model, which uses LASH test data to predict the fatigue life of binders, may not be suitable for Binder 2. This model was originally developed without accounting for healing effects and was intended to predict fatigue life similar to that obtained from TS tests using LAS data. To improve the correlation between LAS-H and

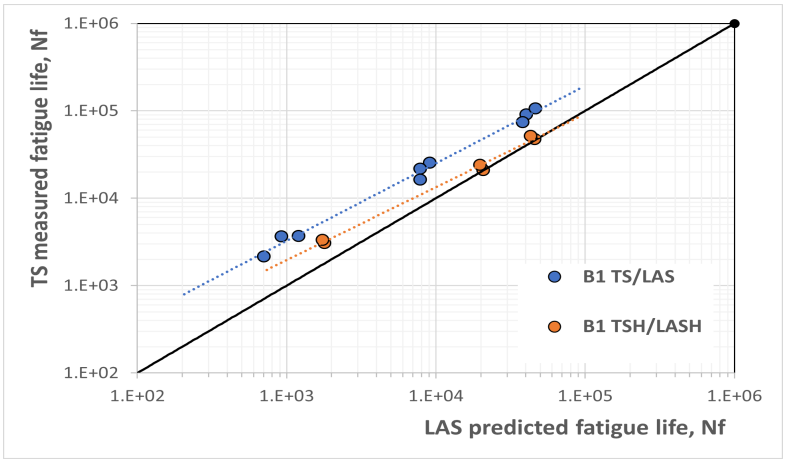

(a)

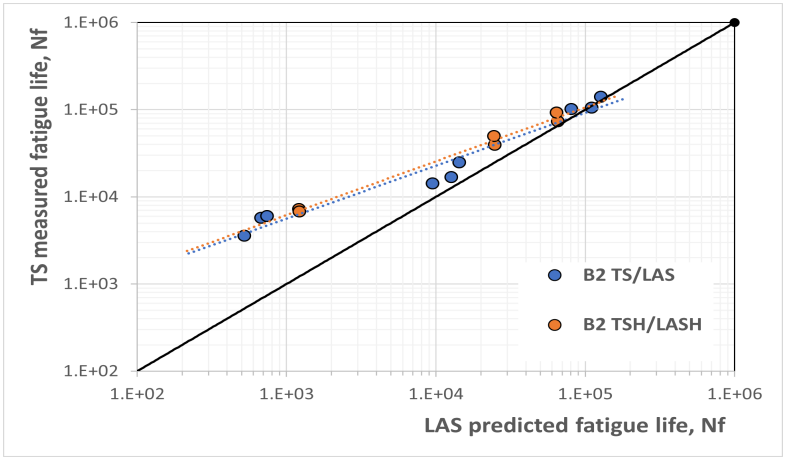

(b)

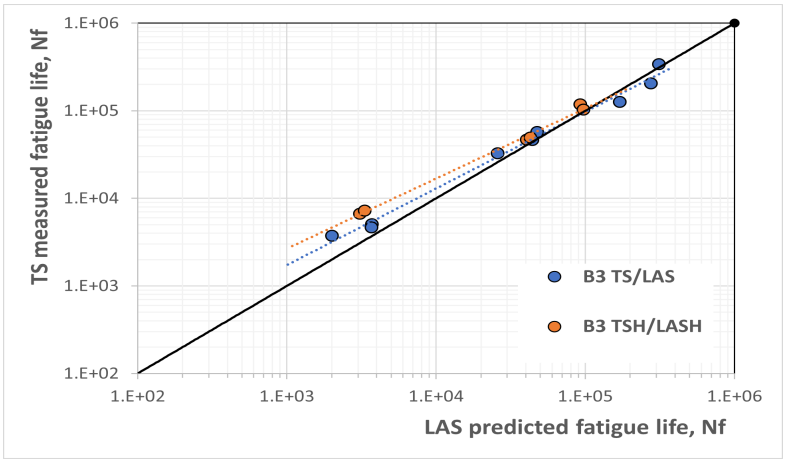

(c)

Figure 5.12.: Comparison between TS-H Single measured fatigue life and LAS-H predicted fatigue life of (a) Binder 1; (b) Binder 2; and (c) Binder 3.

TS-H test results, further research is needed to develop a model that is more appropriate for healing evaluation. For the LAS-H test, incorporating the healing index HI_{LAS} to assess the healing performance of materials could be a more effective approach.

5.4. Conclusions of the Healing Tests

The key findings from the healing tests of this research are summarized as follows:

- **Table 5.8** summarizes the overall healing performance rankings of the three asphalt binders based on various testing methods and healing indices. Binder 3, containing high RA bitumen content and the rejuvenator, demonstrated the highest healing capacity in half of the cases and ranked lowest in only one instance. In contrast, Binder 1, composed entirely of fresh bitumen 40/60, exhibited the lowest healing performance in half of the cases, particularly in the TS-H tests.

Table 5.8.: Overall healing performance rankings of the three asphalt binders.

	Highest Performance	**Medium Performance**	**Lowest Performance**
TS-H Single SF_h	B2	B3	B1
TS-H Single HI_{TS}	B2	B3	B1
TS-H Multi SF_h	B3	B2	B1
TS-H Multi HI_{TS} **(5%)**	B3	B1	B2
LASH SF_h	B1	B2	B3
LASH HI_{LAS}	B3	B1	B2

- It is observed that the healing performance of asphalt binders is sensitive to the choice of healing test protocols and healing indices. Different testing methods or healing indices may yield varied, and sometimes even contradictory, conclusions.
- Inconsistencies were observed in the evaluation of healing performance when using different healing indices within the same testing method. This discrepancy arises because the healing shift factor (SF_h) and healing index (HI) emphasize different aspects of the healing effect. The SF_h focuses on the overall extension of the material's fatigue life, specifically reflecting the influence of rest periods on the degradation rate of the asphalt binder's complex modulus. In contrast, the HI captures modulus recovery after rest periods, a measure that may be influenced by the biasing effects inherent to asphalt materials.
- Comparing the SF_h results from the TS-H Single and TS-H Multi tests reveals that for Binder 1 and Binder 3, increasing the number of rest-reload cycles slightly enhances their healing performance. However, a significant difference was observed for Binder 2, which contains a high RA bitumen content and softer bitumen (160/220). In the TS-H Single test, Binder 2 exhibited superior fatigue life extension capabilities, whereas in the TS-H Multi test, its healing performance declined sharply. Binder 2 showed sensitivity

to the number of rest-reload cycles, with repeated rest and loading cycles accelerating its modulus degradation rate.

- In the LAS-H test, all binders showed increased healing potential with extended rest periods. However, the improvement in healing performance from extending the rest period from 100 seconds to 1000 seconds was limited, particularly for Binder 1 and Binder 2.
- A comparison between the TS-H Single measured fatigue life and the LAS-H predicted fatigue life revealed that Binders 1 and Binder 3 showed high consistency between the two methods at low and medium strain levels, while Binder 2 exhibited this consistency only at low strain. For all binders, the TS-H measured fatigue life was consistently higher than the LAS-H predicted fatigue life at high strain levels, indicating that the LAS-H test tends to underestimate fatigue life under high strain conditions.

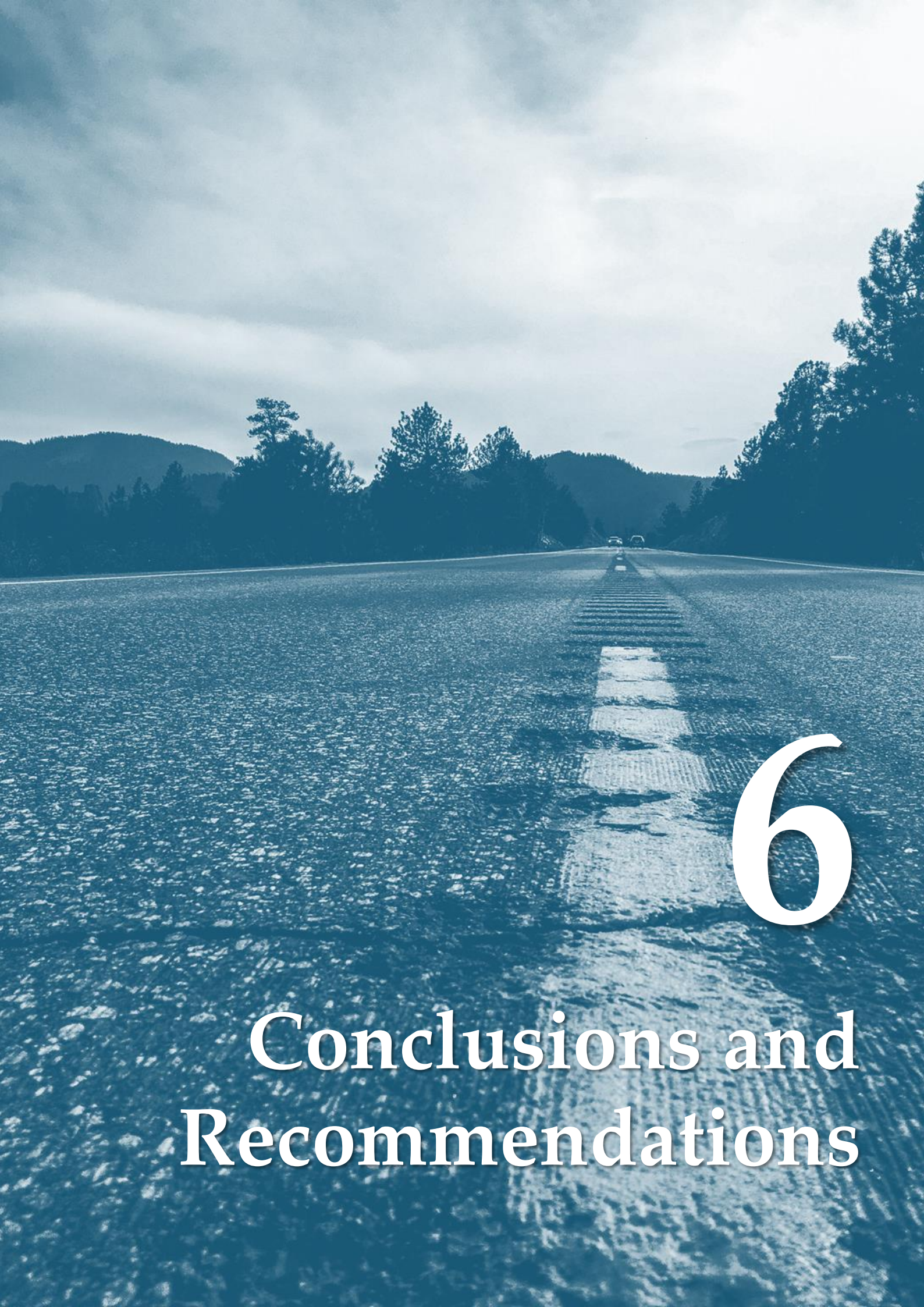

6

Conclusions and Recommendations

6. Conclusions and Recommendations

6.1. Conclusions

6.1.1. Main Research Question

In this research, an answer was sought to the following question:

What is the healing performance of three asphalt binders used in base layer mixtures, as assessed by various healing test protocols and healing indices?

The healing performance of the three asphalt binders used in base layer mixtures varies significantly depending on the test protocols and healing indices applied. By employing multiple test methods, including single and multiple rest period TS-H and LAS-H tests, along with healing indices based on fatigue life extension and modulus recovery, the study provides an assessment of the binders' healing potential under different conditions.

Binder 3, containing a high RA bitumen content and the rejuvenator, exhibited the highest healing potential in half of the conditions, particularly under repeated rest-reload cycles. Its healing performance was strong in both the TS-H Single and TS-H Multi tests, suggesting that its healing potential is minimally affected by the number of rest-reload cycles. In contrast, Binder 2, which also contains high RA bitumen but is blended with softer fresh bitumen rather than the rejuvenator, demonstrated a more complex response. Binder 2 showed the highest healing performance in the TS-H Single test, but experienced a notable decline with increased rest cycles, indicating a higher sensitivity to test conditions. As the reference binder in this study, Binder 1, composed entirely of fresh bitumen, exhibited the lowest healing potential in half of the conditions and moderate performance in the remaining cases.

The healing performance of asphalt binders is highly sensitive to the choice of healing test protocols and indices. Researchers should carefully select healing test methods and indices, as these choices yield varied insights into the healing behavior of asphalt binders.

6.1.2. Sub-questions

- **Sub-question 1: How are the TS (TS-H) and LAS (LAS-H) tests characterized and what are their differences?**

Section 2.4 provides a detailed description of the TS (TS-H) and LAS (LAS-H) tests. The primary difference between the two methods lies in their loading approaches. The TS (TSH) test simulates cumulative damage under long-term, sinusoidal shear loading, closely reflecting fatigue performance under real traffic conditions. However, this test is time-intensive and requires strict control over experimental conditions such as temperature and strain amplitude. In contrast, the LAS (LAS-H) test employs a gradually increasing strain amplitude to rapidly

assess fatigue performance within a shorter timeframe, making it suitable for large-scale material testing. However, due to its loading approach, LAS testing may result in less accurate fatigue life estimates.

Overall, the TS (TS-H) test is better suited for precise evaluations of long-term fatigue and healing behavior, while the LAS (LAS-H) test is ideal for quick assessments and large-scale testing.

- **Sub-question 2: Which asphalt binder demonstrates the highest fatigue resistance?**

According to the TS and LAS test results, Binder 3 demonstrated the highest fatigue resistance. Within the strain range of 1.5% to 5.0%, the fatigue life of Binder 3 was significantly higher than that of Binder 1 and Binder 2. Even under high strain conditions, Binder 3 maintained relatively high fatigue resistance. This superior performance is primarily attributed to the use of the rejuvenator ANOVA 1817 in Binder 3, which effectively reduced the stiffness and brittleness of the aged binder from the RA. The rejuvenator enhanced the viscoelastic behavior of the binder, allowing Binder 3 to exhibit longer fatigue life under both low and high strain conditions.

- **Sub-question 3: What is the correlation between the fatigue test results of asphalt binders and asphalt mixtures?**

The fatigue test results indicate a clear correlation between the fatigue performance of asphalt binders and asphalt mixtures. Specifically, Binder 3 exhibited the highest fatigue resistance in the binder tests, correspondingly, Mixture 3 also showed a significantly longer fatigue life. Similarly, Binder 1 had the lowest fatigue performance in the binder fatigue tests, correspondingly, Mixture 1 also displayed the shortest fatigue life. This trend suggests that the fatigue behavior of the binder substantially influences the overall fatigue performance of the asphalt mixture.

However, despite the consistent ranking in fatigue life between binders and mixtures, differences exist in the slopes and details of their fatigue curves. Asphalt mixtures are complex systems, where internal stress distribution and damage accumulation mechanisms differ from those in binders. Factors such as aggregate gradation, air voids, and the adhesion between binder and aggregate play a critical role in the mixture's fatigue behavior, leading to variations in performance despite similar trends.

- **Sub-question 4: Are there significant differences in the healing performance of asphalt binders between single rest period tests and multiple rest period tests?**

Significant differences in healing performance were observed between single rest period tests (TS-H Single) and multiple rest period tests (TS-H Multi) for asphalt binders. In general, binders with rejuvenators and high RA content bitumen (Binder 3), maintained high healing performance across both test types, showing minimal sensitivity to the number of rest-reload cycles. In contrast, Binder 2, which contains a high RA content and softer bitumen but no rejuvenator, exhibited a more complex response. While Binder 2 demonstrated strong healing performance in the TS-H Single test, its performance declined considerably in the TS-H Multi test, where the increased number of rest-reload cycles accelerated its complex modulus degradation rate. These findings highlight the importance of test methods selection when evaluating the long-term healing potential of different asphalt binders.

- **Sub-question 5: What are the similarities and differences when evaluating the healing performance of asphalt binders using different healing indices?**

The study employed two different healing evaluation parameters: the Healing Factor (SF_h) and the Healing Index (HI). In some cases, both parameters showed similar ranking trends when assessing the healing performance of the binders. However, they were not always entirely consistent in their evaluations. The healing index (HI) primarily reflects the short-term stiffness recovery of the binder after a rest period, while the healing shift factor (SF_h) focuses on the actual extension of the material's fatigue life after healing, considering the long-term impact. Combining the results of both parameters provides a more comprehensive evaluation of the binders' healing potential.

- **Sub-question 6: Are the healing performances of asphalt binders consistent across different testing methods?**

The healing performance of binders showed differences across various testing methods. Binder 3 exhibited different healing results in the TS-H and LAS-H tests. In the LAS-H test, the Healing Displacement Factor (SF_h) indicated that Binder 3 had limited healing capacity. However, in both the TS-H Single and TS-H Multi tests, Binder 3 demonstrated excellent healing ability, with no decline in healing capacity as the load-rest cycles increased. Similar findings have been reported in other studies, where different healing rankings were observed in TS-H Single, TS-H Multi, and LAS-H tests (Baglieri et al., 2022).

These differences can be attributed to the distinct loading methods and testing procedures used in the two test types. The fatigue life in the TS-H test is directly measured during the experiment, while in the LAS-H test, fatigue life is predicted based on a model. This difference in approach may lead to variations in the observed healing capacities across the tests.

6.2. Recommendations and Future Work

6.2.1. Recommendations

- In this study, various healing test methods and indices were utilized to evaluate the healing performance of asphalt binders, yielding valuable insights. However, there remain areas for refinement and further exploration. In this section, recommendations and future work are outlined, aiming to address limitations and propose potential future research in this field.
- In this study, only a limited amount of bitumen could be extracted from reclaimed asphalt, making it impractical to use for blending binders B2 and B3 or to conduct penetration grade tests. Consequently, the complex shear modulus response in the frequency sweep test was employed to evaluate whether the artificially aged bitumen properties aligned with those of the extracted RA bitumen. Access to more extracted RA bitumen would have allowed for direct blending into new binders, potentially enhancing the accuracy and reliability of the research findings.
- After blending the new binders, this study utilized complex shear modulus responses from frequency sweep tests to evaluate binder stiffness. If sufficient binder quantities were available, additional penetration tests on these binders would offer more comprehensive insights into their characteristics.

- In this study, the TS tests were first applied at three strain levels: 1.5%, 2.5%, and 5.0%. However, due to time constraints, the subsequent TS-H tests were conducted at a low strain level of 2.0% instead of 1.5%, as TS testing is particularly time-intensive at lower strain levels. Testing at 2.0% strain allowed for substantial time savings without significantly impacting results, as the fatigue lines were fitted from multiple parallel experiments across three strain levels. Further research could explore the effects of varying low-strain thresholds on TS-H test outcomes. With sufficient time, maintaining consistency in the selected strain levels across all tests would enhance the reliability of the results.

6.2.2. Future Work

- In this study, several fatigue-based macroscale healing tests were conducted on asphalt binders. To further explore the reasons for performance differences observed across various healing test methods, microscale studies, such as Scanning Electron Microscopy (SEM) and Atomic Force Microscopy (AFM), or mesoscale studies, such as Fluorescence Microscopy and X-ray computed tomography, should be conducted.
- In this study, the healing performance of the binder components in three types of asphalt mixtures was investigated. The subsequent research could be conducting mastic (the mixture of bitumen and fillers) tests using DSR testing or three-point bending tests. It may offer a more representative correlation between binder properties and mixture behavior. These tests offer better cohesion representation, which plays a key role in both fatigue and healing resistance at the mixture level.
- The LAS fatigue life prediction model was originally developed without accounting for healing effects. To improve the correlation between LAS-H and TS-H test results, further research is needed to develop a model that is more appropriate for healing evaluation.
- TS-H test with intermittent loading (each loading cycle is followed by a rest period) should be considered, which is closer to the real traffic loading phenomenon.
- A significant challenge in understanding healing mechanisms in asphalt pavements is establishing a robust link between the healing properties of binders and the fatigue/healing behavior of asphalt mixtures. Mixture tests using the dog-bone-shaped samples can be explored. These specimens localize damage to a predictable area, allowing for a more precise analysis of healing behavior. Using such specimens with the VECD model could provide more reliable insights into the material's recovery properties and improve the overall evaluation of healing in base layer asphalt mixtures.
- Identifying the influence of biasing effects on modulus recovery and actual healing is an area that may be of interest for future research, particularly when using modulus recovery-based healing indices. Especially for the LAS test, where strain amplitudes can reach up to 30%, making it difficult to ignore the nonlinear responses induced by high-intensity loading. Understanding and quantifying these biasing effects is crucial for accurately evaluating the fatigue life and healing performance of asphalt materials. Therefore, future research could explore optimized testing protocols to better isolate and control these effects, enabling more precise assessments of healing performance.

Bibliography

Alae, M., Zhao, Y., Zarei, S., Fu, G., and Cao, D. (2020). Effects of layer interface conditions on top-down fatigue cracking of asphalt pavements. *International Journal of Pavement Engineering*, 21(3):280–288.

Ameri, M., Mansourkhaki, A., and Daryaee, D. (2018). Evaluation of fatigue behavior of high reclaimed asphalt binder mixes modified with rejuvenator and softer bitumen. *Construction and Building Materials*, 191:702–712.

Ashouri, M., Wang, Y., Choi, Y.-T., and Kim, Y. (2021). Development of healing model and simplified characterization test procedure for asphalt concrete. *Construction and Building Materials*, 271:121515.

Ayar, P., Moreno-Navarro, F., and Rubio-Gámez, M. C. (2016). The healing capability of asphalt pavements: a state of the art review. *Journal of Cleaner Production*, 113:28–40.

Baglieri, O., Baaj, H., Canestrari, F., Wang, C., Hammoum, F., Tsantilis, L., and Cardone, F. (2022). Testing methods to assess healing potential of bituminous binders. In *Proceedings of the RILEM International Symposium on Bituminous Materials: ISBM Lyon 2020 1*, pages 55–62. Springer.

Bhasin, A., Bommavaram, R., Greenfield, M. L., and Little, D. N. (2011a). Use of molecular dynamics to investigate self-healing mechanisms in asphalt binders. *Journal of Materials in Civil Engineering*, 23(4):485–492.

Bhasin, A., Little, D. N., Bommavaram, R., and Vasconcelos, K. (2008). A framework to quantify the effect of healing in bituminous materials using material properties. *Road Materials and Pavement Design*, 9(sup1):219–242.

Bhasin, A., Palvadi, S., and Little, D. N. (2011b). Influence of aging and temperature on intrinsic healing of asphalt binders. *Transportation research record*, 2207(1):70–78.

Biligiri, K. P. and Said, S. H. (2015). Prediction of the remaining fatigue life of flexible pavements using laboratory and field correlations. *Journal of Materials in Civil Engineering*, 27(7):04014201.

Bonnetti, K. S., Nam, K., and Bahia, H. U. (2002). Measuring and defining fatigue behavior of asphalt binders. *Transportation Research Record*, 1810(1):33–43.

Botella, R., Perez-Jimenez, F. E., Lopez-Montero, T., and Miro, R. (2020). Cyclic testing setups to highlight the importance of heating and other reversible phenomena on asphalt mixtures. *International Journal of Fatigue*, 134:105514.

Brown, S., Brunton, J., and Stock, A. (1985). The analytical design of bituminous pavements. *Proceedings of the Institution of Civil Engineers*, 79(1):1–31.

Cao, W. and Wang, C. (2018). A new comprehensive analysis framework for fatigue characterization of asphalt binder using the linear amplitude sweep test. *Construction and Building Materials*, 171:1–12.

Castro, M. and Sánchez, J. A. (2006). Fatigue and healing of asphalt mixtures: discriminate analysis of fatigue curves. *Journal of transportation engineering*, 132(2):168–174.

Chen, Y., Simms, R., Koh, C., Lopp, G., and Roque, R. (2013). Development of a test method for evaluation and quantification of healing in asphalt mixture. *Road materials and pavement design*, 14(4):901–920.

Cheng, G., Zheng, Y., Yu, J., Liu, J., and Hu, X. (2022). Investigation of the fatigue life of bottom-up cracking in asphalt concrete pavements. *Applied Sciences*, 12(23):12119.

Cheng, H., Liu, J., Sun, L., Liu, L., and Zhang, Y. (2021). Fatigue behaviours of asphalt mixture at different temperatures in four-point bending and indirect tensile fatigue tests. *Construction and Building Materials*, 273:121675.

Cheng, H., Sun, L., Liu, L., and Li, H. (2018). Fatigue characteristics of in-service cold recycling mixture with asphalt emulsion and hma mixture. *Construction and Building Materials*, 192:704–714.

Dai, Q., Wang, Z., and Hasan, M. R. M. (2013). Investigation of induction healing effects on electrically conductive asphalt mastic and asphalt concrete beams through fracture-healing tests. *Construction and Building Materials*, 49:729–737.

Deacon, J., Tayebali, A., Coplantz, J., Finn, F., and Monismith, C. (1994). Fatigue response of asphalt-aggregate mixes, part iii—mix design and analysis. *Strategic Highway Research Program Report: No. SHRP-A*, 404.

Elkashef, M., Williams, R. C., and Cochran, E. W. (2018). Physical and chemical characterization of rejuvenated reclaimed asphalt pavement (rap) binders using rheology testing and pyrolysis gas chromatography-mass spectrometry. *Materials and Structures*, 51:1–9.

Fabrizio, M., Underwood, B. S., Lucia, T., Orazio, B., and Ezio, S. (2023). Self-healing master curves of bituminous binders: a non-linear viscoelastic continuum damage framework. *Road Materials and Pavement Design*, 24(sup1):124–144.

Finn, F., Saraf, C., Kulkarni, R., Nair, K., Smith, W., and Abdullah, A. (1986). *Development of pavement structural subsystems*. Number 291.

Gerritsen, A. and Koole, R. (1987). Seven years' experience with the structural aspects of the shell pavement design manual. In *Proceedings Sixth International Conference on Structural Design of Asphalt Pavements, Ann Arbor, Michigan, USA*.

Harvey, J. T., Deacon, J. A., Taybali, A. A., Leahy, R. B., and Monismith, C. L. (1997). A reliability-based mix design and analysis system for mitigating fatigue distress. In *Eighth International Conference on Asphalt PavementsFederal Highway Administration*, number Volume I.

Jacobs, G., Margaritis, A., Hernando, D., He, L., Blom, J., et al. (2021). Influence of soft binder and rejuvenator on the mechanical and chemical properties of bituminous binders. *Journal of Cleaner Production*, 287:125596.

Jayaraman, M. and Padmarekha, A. (2024). Effect of rest period on the fatigue characteristics of unmodified and modified bitumen. *International Journal of Pavement Research and Technology*, pages 1–13.

Kim, Y. R. (1988). *Evaluation of healing and constitutive modeling of asphalt concrete by means of the theory of nonlinear viscoelasticity and damage mechanics*. Texas A&M University.

Klug, A., Ng, A., and Faxina, A. (2022). Application of the viscoelastic continuum damage theory to study the fatigue performance of asphalt mixtures—a literature review. *Sustainability*, 14(9):4973.

Leahy, R., Hicks, R., Monismith, C., and Finn, F. (1995). Framework for performance-based approach to mix design and analysis (with discussion). *Journal of the Association of Asphalt Paving Technologists*, 64.

Lee, H.-J., Daniel, J. S., and Kim, Y. R. (2000). Continuum damage mechanics-based fatigue model of asphalt concrete. *Journal of materials in Civil Engineering*, 12(2):105–112.

Leegwater, G., Scarpas, A., and Erkens, S. (2018). The influence of boundary conditions on the healing of bitumen. *Road Materials and Pavement Design*, 19(3):571–580.

Leegwater, G., Scarpas, T., and Erkens, S. (2016). Direct tensile test to assess healing in asphalt. *Transportation Research Record*, 2574(1):124–130.

Li, J., Li, H., Jiao, Y., Liu, Y., Xia, X., and Yu, C. (2014). Analysis for oblique wave propagation across filled joints based on thin-layer interface model. *Journal of Applied Geophysics*, 102:39–46.

Li, Y., Hao, P., and Zhang, M. (2021). Fabrication, characterization and assessment of the capsules containing rejuvenator for improving the self-healing performance of asphalt materials: A review. *Journal of Cleaner Production*, 287:125079.

Little, D., Bhasin, A., and Darabi, M. (2015). Damage healing in asphalt pavements: Theory, mechanisms, measurement, and modeling. In *Advances in asphalt materials*, pages 205–242. Elsevier.

Liu, G., Liang, Y., Chen, H., Wang, H., Komacka, J., and Gu, X. (2019). Influence of the chemical composition and the morphology of crumb rubbers on the rheological and self-healing properties of bitumen. *Construction and Building Materials*, 210:555–563.

Lv, Q., Huang, W., Zhu, X., and Xiao, F. (2017). On the investigation of self-healing behavior of bitumen and its influencing factors. *Materials & Design*, 117:7–17.

Lv, S., Ge, D., Wang, Z., Wang, J., Liu, J., Ju, Z., Peng, X., Fan, X., Cao, S., Liu, D., et al. (2023). Performance assessment of self-healing polymer-modified bitumens by evaluating the suitability of current failure definition, failure criterion, and fatigue-restoration criteria. *Materials*, 16(6):2488.

Mangiafico, S., Sauzeat, C., Di Benedetto, H., Pouget, S., Olard, F., and Planque, L. (2015). Quantification of biasing effects during fatigue tests on asphalt mixes: non-linearity, self-heating and thixotropy. *Road Materials and Pavement Design*, 16(sup2):73–99.

Mannan, U. A. and Tarefder, R. A. (2018). Investigating different fatigue failure criteria of asphalt binder with the consideration of healing. *International Journal of Fatigue*, 114:198–205.

Mateos, A., Ayuso, J. P., and Jáuregui, B. C. (2011). Shift factors for asphalt fatigue from full-scale testing. *Transportation research record*, 2225(1):128–136.

Moghaddam, T. B. and Baaj, H. (2016). The use of rejuvenating agents in production of recycled hot mix asphalt: A systematic review. *Construction and Building Materials*, 114:805–816.

Moghaddam, T. B., Karim, M. R., and Abdelaziz, M. (2011). A review on fatigue and rutting performance of asphalt mixes. *Scientific Research and Essays*, 6(4):670–682.

Moreno-Navarro, F., Sol-Sánchez, M., García-Travé, G., and Rubio-Gámez, M. C. (2018). Fatigue cracking in asphalt mixtures: the effects of ageing and temperature. *Road Materials and Pavement Design*, 19(3):561–570.

Oshone, M., Dave, E. V., and Sias, J. E. (2019). Asphalt mix fracture energy based reflective cracking performance criteria for overlay mix selection and design for pavements in cold climates. *Construction and Building Materials*, 211:1025–1033.

Pierce, L. M., Jackson, N. C., and Mahoney, J. P. (1993). Development and implementation of a mechanistic, empirically based overlay design procedure for flexible pavements. *Transportation Research Record*, (1388).

Planche, J. P., Anderson, D., Gauthier, G., Le Hir, Y., and Martin, D. (2004). Evaluation of fatigue properties of bituminous binders. *Materials and Structures*, 37:356–359.

Prowell, B. D. (2010). Estimate of fatigue shift factors between laboratory tests and field performance. *Transportation research record*, 2181(1):117–124.

Qiu, J. (2012). Self healing of asphalt mixtures: towards a better understanding of the mechanism.

Qiu, J., Van de Ven, M., Wu, S., Yu, J., and Molenaar, A. (2009). Investigating the self healing capability of bituminous binders. *Road Materials and Pavement Design*, 10(sup1):81–94.

Qiu, J., Van de Ven, M., Wu, S., Yu, J., and Molenaar, A. (2012). Evaluating self healing capability of bituminous mastics. *Experimental mechanics*, 52:1163–1171.

Qiu, X., Cheng, W., Xu, W., Xiao, S., and Yang, Q. (2022). Fatigue evolution characteristic and self-healing behaviour of asphalt binders. *International Journal of Pavement Engineering*, 23(5):1459–1470.

Ragni, D., Ferrotti, G., Petit, C., and Canestrari, F. (2020). Analysis of shear-torque fatigue test for bituminous pavement interlayers. *Construction and Building Materials*, 254:119309.

Safaei, F. and Castorena, C. (2016). Temperature effects of linear amplitude sweep testing and analysis. *Transportation Research Record*, 2574(1):92–100.

Safaei, F., Lee, J.-s., Nascimento, L. A. H. d., Hintz, C., and Kim, Y. R. (2014). Implications of warm-mix asphalt on long-term oxidative ageing and fatigue performance of asphalt binders and mixtures. *Road Materials and Pavement Design*, 15(sup1):45–61.

Said, S. F. (1997). *Variability in roadbase layer properties conducting indirect tensile test*. Statens väg-och transportforskningsinstitut., VTI särtryck 278.

Santagata, E., Baglieri, O., Dalmazzo, D., and Tsantilis, L. (2017). Investigating cohesive healing of asphalt binders by means of a dissipated energy approach. *International Journal of Pavement Research and Technology*, 10(5):403–409.

Santagata, E., Baglieri, O., Tsantilis, L., and Chiappinelli, G. (2015). Fatigue and healing properties of nano-reinforced bituminous binders. *International Journal of Fatigue*, 80:30–39.

Sarsam, S. I. and Mahdi, M. S. (2020). Enhancing the service life of aged asphalt concrete by micro crack healing and recycling. In *Sustainable Thoughts in Ground Improvement and Soil Stability: Proceedings of the 3rd GeoMEast International Congress and Exhibition, Egypt 2019 on Sustainable Civil Infrastructures–The Official International Congress of the Soil-Structure Interaction Group in Egypt (SSIGE)*, pages 57–69. Springer.

Schapery, R. A. (1984). Correspondence principles and a generalized j integral for large deformation and fracture analysis of viscoelastic media. *International journal of fracture*, 25:195–223.

Shan, L., Tan, Y., and Kim, Y. R. (2013). Establishment of a universal healing evaluation index for asphalt binder. *Construction and Building Materials*, 48:74–79.

Shan, L., Tan, Y., Underwood, S., and Kim, Y. R. (2010). Application of thixotropy to analyze fatigue and healing characteristics of asphalt binder. *Transportation research record*, 2179(1):85–92.

Shen, S., Chiu, H.-M., and Huang, H. (2010). Characterization of fatigue and healing in asphalt binders. *Journal of Materials in Civil Engineering*, 22(9):846–852.

Shen, S., Lu, X., Zhang, Y., and Lytton, R. (2013). Fracture and viscoelastic properties of asphalt binders during fatigue and rest periods. *Journal of Testing and Evaluation*, 42(1):109–117.

Si, Z., Little, D., and Lytton, R. (2002). Characterization of microdamage and healing of asphalt concrete mixtures. *Journal of materials in civil engineering*, 14(6):461–470.

Stimilli, A., Hintz, C., Li, Z., Velasquez, R., and Bahia, H. U. (2012). Effect of healing on fatigue law parameters of asphalt binders. *Transportation research record*, 2293(1):96–105.

Subhy, A., Menegusso Pires, G., Jiménez del Barco Carrión, A., Lo Presti, D., and Airey, G. (2019). Binder and mixture fatigue performance of plant-produced road surface course asphalt mixtures with high contents of reclaimed asphalt. *Sustainability*, 11(13):3752.

Sun, D., Lin, T., Zhu, X., Tian, Y., and Liu, F. (2016). Indices for self-healing performance assessments based on molecular dynamics simulation of asphalt binders. *Computational Materials Science*, 114:86–93.

Sun, D., Sun, G., Zhu, X., Guarin, A., Li, B., Dai, Z., and Ling, J. (2018). A comprehensive review on self-healing of asphalt materials: Mechanism, model, characterization and enhancement. *Advances in colloid and interface science*, 256:65–93.

Sun, D., Yu, F., Li, L., Lin, T., and Zhu, X. (2017). Effect of chemical composition and structure of asphalt binders on self-healing. *Construction and Building Materials*, 133:495–501.

Sun, G., Sun, D., Guarin, A., Ma, J., Chen, F., and Ghafooriroozbahany, E. (2019). Low temperature self-healing character of asphalt mixtures under different fatigue damage degrees. *Construction and Building Materials*, 223:870–882.

Sun, W. and Wang, H. (2020). Self-healing of asphalt binder with cohesive failure: Insights from molecular dynamics simulation. *Construction and Building Materials*, 262:120538.

Tan, Y., Shan, L., Kim, Y. R., and Underwood, B. S. (2012). Healing characteristics of asphalt binder. *Construction and Building Materials*, 27(1):570–577.

Varma, R., Balieu, R., and Kringos, N. (2021). A state-of-the-art review on self-healing in asphalt materials: Mechanical testing and analysis approaches. *Construction and Building Materials*, 310:125197.

Venudharan, V. and Biligiri, K. P. (2020). Conceptualization of three-stage fatigue failure in asphalt-rubber gap-graded mixtures using dynamic semi-circular bending test. *Transportation Research Record*, 2674(7):44–55.

Wang, C., Chen, Y., and Cao, W. (2019). A chemo-rheological approach to the healing characteristics of asphalt binders under short-and long-term oxidative aging. *Construction and Building Materials*, 221:553–561.

Wang, C., Gong, G., and Ren, Z. (2023a). Addressing the healing compensation on fatigue damage of asphalt binder using tsh and lash tests. *International Journal of Fatigue*, 167:107292.

Wang, C., Sun, Y., and Ren, Z. (2023b). Toward to a viscoelastic fatigue and fracture model for asphalt binder under cyclic loading. *International Journal of Fatigue*, 168:107479.

Wang, C., Xie, W., and Underwood, B. S. (2018). Fatigue and healing performance assessment of asphalt binder from rheological and chemical characteristics. *Materials and Structures*, 51:1–12.

Wang, H., Liu, X., van de Ven, M., Lu, G., Erkens, S., and Skarpas, A. (2020). Fatigue performance of long-term aged crumb rubber modified bitumen containing warm-mix additives. *Construction and Building Materials*, 239:117824.

Wang, R. and An, X. (2024). An optimized fatigue model of asphalt binder combining nonlinear viscoelastic and intrinsic healing characteristics. *Construction and Building Materials*, 424:135946.

Wool, R. and O'connor, K. (1981). A theory crack healing in polymers. *Journal of applied physics*, 52(10):5953–5963.

Xiang, H., He, Z., Chen, L., Zhu, H., and Wang, Z. (2019). Key factors and optimal conditions for self-healing of bituminous binder. *Journal of Materials in Civil Engineering*, 31(9):04019172.

Xie, W., Castorena, C., Wang, C., and Kim, Y. R. (2017). A framework to characterize the healing potential of asphalt binder using the linear amplitude sweep test. *Construction and Building Materials*, 154:771–779.

Yang, D.-G., Yoo, P.-J., and Hong, Y.-K. (2014). Study on polymer-modified self-healing asphalt. *Elastomers and Composites*, 49(2):134–143.

Yaseen, G. and Hafeez, I. (2020). Effect of cereclor as rejuvenator to enhance the aging resistance of reclaimed asphalt pavement binder. *Materials*, 13(7):1582.

Yu, J., Tsai, B.-W., Zhang, X., and Monismith, C. (2012). Development of asphalt pavement fatigue cracking prediction model based on loading mode transfer function. *Road materials and pavement design*, 13(3):501–517.

Zaumanis, M., Mallick, R. B., and Frank, R. (2015). Evaluation of different recycling agents for restoring aged asphalt binder and performance of 100% recycled asphalt. *Materials and Structures*, 48:2475–2488.

Zhang, C., Ren, Q., Qian, Z., and Wang, X. (2019). Evaluating the effects of high rap content and rejuvenating agents on fatigue performance of fine aggregate matrix through dma flexural bending test. *Materials*, 12(9):1508.

Zhang, H., Bai, Y., and Cheng, F. (2018a). Rheological and self-healing properties of asphalt binder containing microcapsules. *Construction and Building Materials*, 187:138–148.

Zhang, L., Liu, Q., Wu, S., Rao, Y., Sun, Y., Xie, J., and Pan, P. (2018b). Investigation of the flow and self-healing properties of uv aged asphalt binders. *Construction and Building Materials*, 174:401–409.

Zhang, Y. and Gao, Y. (2021). Predicting crack growth in viscoelastic bitumen under a rotational shear fatigue load. *Road materials and pavement design*, 22(3):603–622.

Zhang, Y., Zhang, J., Ma, T., Qi, H., and Chen, C. (2023). Predicting asphalt mixture fatigue life via four-point bending tests based on viscoelastic continuum damage mechanics. *Case Studies in Construction Materials*, 19:e02671.

Zhao, Y., Alae, M., and Fu, G. (2018). Investigation of mechanisms of top-down fatigue cracking of asphalt pavement. *Road Materials and Pavement Design*, 19(6):1436–1447.

Zhou, L., Huang, W., Zhang, Y., Lv, Q., Yan, C., and Jiao, Y. (2020). Evaluation of the adhesion and healing properties of modified asphalt binders. *Construction and Building Materials*, 251:119026.

7 Appendices

A. Materials and Methods

A.1. Mixture Properties

Table A.1 lists the percentage of materials used in the asphalt mixtures.

Table A.1.: Percentages of materials used in the studied asphalt mixtures.

Building Code	**Name of Material**	**Result matrix calculation [% m/m]**		
		M1	**M2**	**M3**
4630 (v1.3)	Bestone 11/16 Norway	19.23	10.84	10.84
4620 (v1.4)	Bestone 8/11 Norway	12.34	0.83	0.83
4600 (v1.3)	Bestone 2/5 Norway	8.19	1.23	1.23
4610 (v1.4)	Bestone 4/8 Norway	13.19	1.90	1.90
5030 (v1.3)	Scottish granite 0/2 Scotland	8.87	-	-
5120 (v1.2)	Coarse sand 0/2 Netherlands	26.59	13.98	13.98
6110 (v1.1)	Wigro 50K 0/0.1 Winterswijk	5.79	0.11	0.11
6190 (v1.0)	Own dust 0/0.1 AMI	1.50	0.10	0.10
7273TT (v1.3)	Anova 1817	-	-	0.20
7010 (v1.0)	Penetration bitumen 40/60	4.30	-	-
7030 (v1.0)	Penetration bitumen 70/100	-	-	0.81
7040 (v1.0)	Penetration bitumen 160/220	-	1.01	-
8023TT2310 (v1.1)	Recycled Asphalt Pavement 0/16 APN	-	70.00	70.00

Table A.2 shows the aggregate gradation of three asphalt mixtures.

Table A.2.: Aggregate gradation of the asphalt mixtures.

Sieve size [mm]	**min. [% m/m]**	**max. [% m/m]**	**Percentage passing [% m/m]**		
			M1	**M2**	**M3**
22.4	94.0	100.0	100	100	100
16.0	85.0	100.0	97.3	96.7	96.7
11.2	75.0	85.0	81.0	81.0	81.0
8.0	60.0	70.0	68.0	68.0	68.0
5.6	53.0	63.0	59.0	58.0	58.0
2.0	41.0	45.0	43.0	43.0	43.0
0.5	15.0	35.0	26.8	27.6	27.6
0.125	4.1	9.1	9.1	8.7	8.7
0.063	5.0	10.0	7.0	7.1	7.1

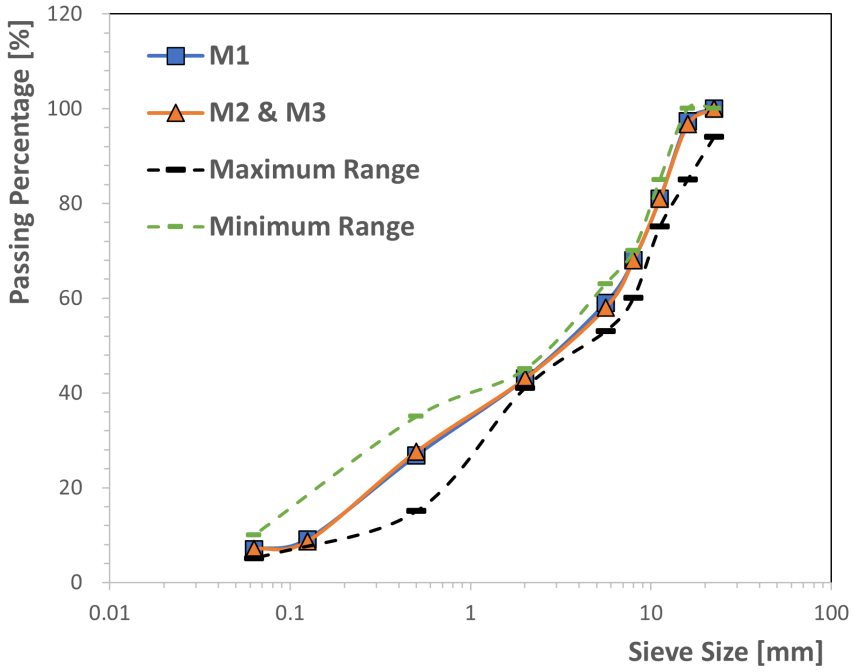

Figure A.1.: Aggregate gradation of the asphalt mixtures.

According to the information in the table, the gradation curves of the three asphalt mixtures are drawn in Figure A.1 The gradation of these asphalt mixtures is within the maximum and minimum permissible ranges.

A.2. Binder Composition Calculation

Binder content provided in the mixture design information:

- Binder 40/60: 4.3 % m/m
- Binder 160/220: 1.15 % m/m
- Binder 70/100: 0.95 % m/m & ANOVA: 0.2 % m/m

Binder-1:

Fresh binder 40/60: 100%

Binder-2:

- Fresh binder 160/220 ”in” the mixture = 1.15%
- Target binder content “in” the mixture = 4.3%
- Bitumen from RA “in” the mixture = 4.3% - 1.15% = 3.15%
- RA bitumen percentage in the binder 2:

$$\left[\frac{3.15\%}{4.3\%}\right] \times 100\% = 73.3\%$$

- Fresh bitumen percentage in the binder 2:

$$\left[\frac{1.15\%}{4.3\%}\right] \times 100\% = 26.7\%$$

Binder-3:

- Fresh binder 70/100 ”in” the mixture = 0.95%
- ANOVA ”in” the mixture = 0.2%
- Target binder content “in” the mixture = 4.3%
- Bitumen from RA “in” the mixture = 4.3% - 0.95% - 0.2% = 3.15%
- RA bitumen percentage in the binder 3:

$$\left[\frac{3.15\%}{4.3\%}\right] \times 100\% = 73.3\%$$

- ANOVA percentage in the binder 3:

$$\left[\frac{0.2\%}{4.3\%}\right] \times 100\% = 4.6\%$$

- Fresh bitumen percentage in the binder 3:

$$\left[\frac{0.95\%}{4.3\%}\right] \times 100\% = 22.1\%$$

B. Fatigue Test Results

B.1. Time Sweep Test Modulus Evolution Curves

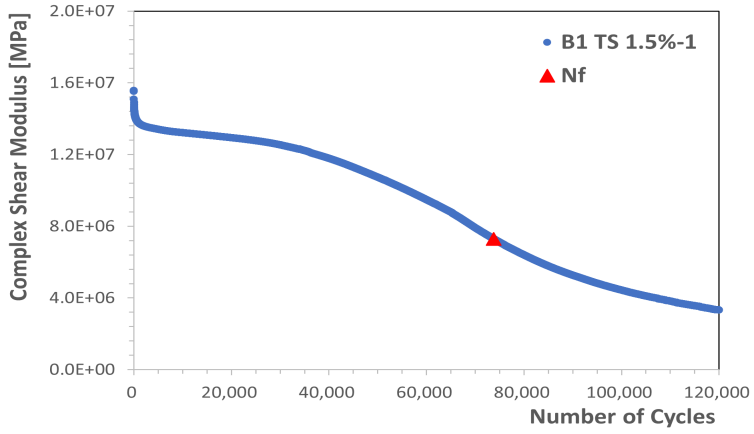

(a)

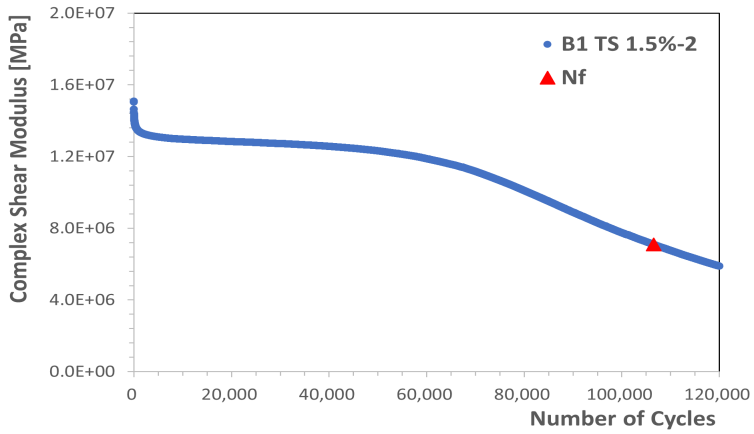

(b)

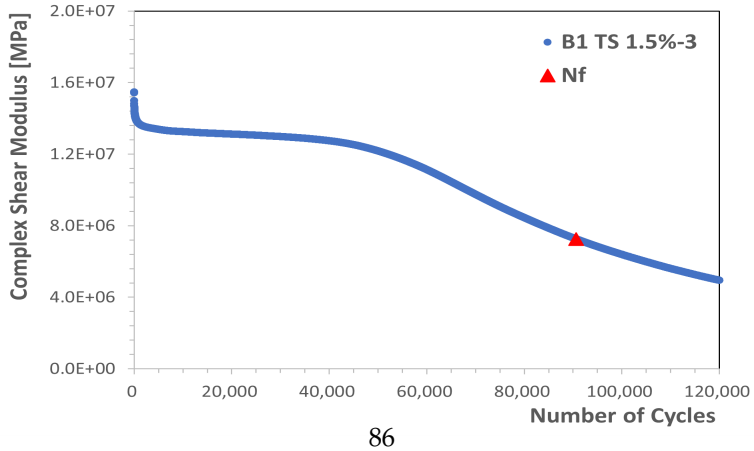

(c)

Figure B.1.: Binder 1 modulus evolution at 1.5% strain in TS test.

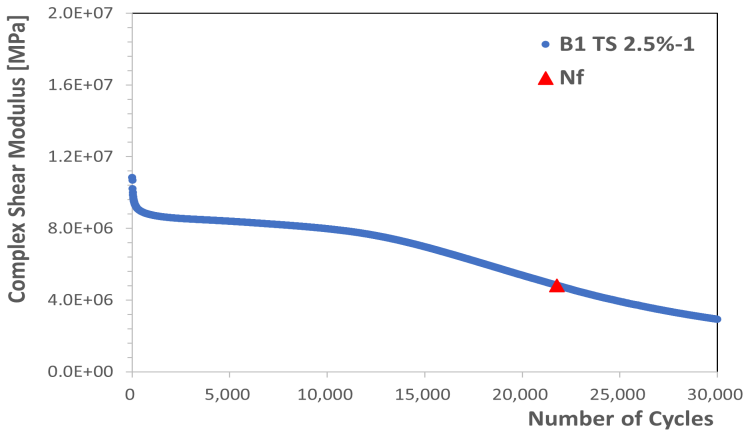

(a)

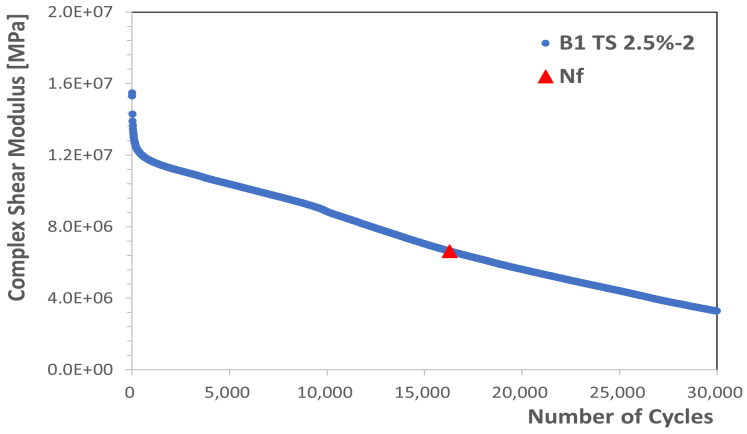

(b)

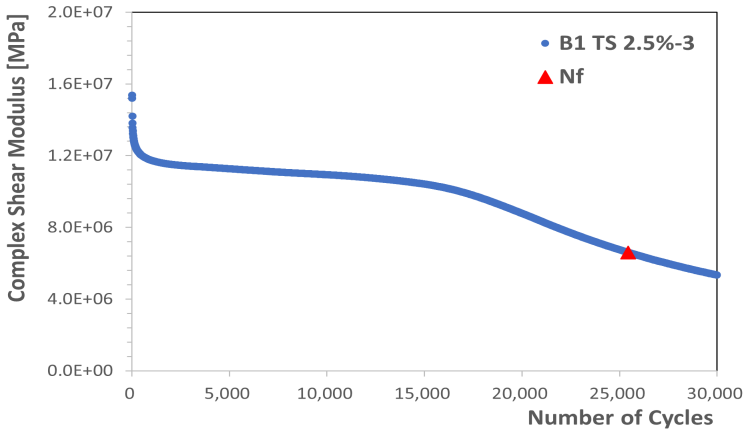

(c)

Figure B.2.: Binder 1 modulus evolution at 2.5% strain in TS test.

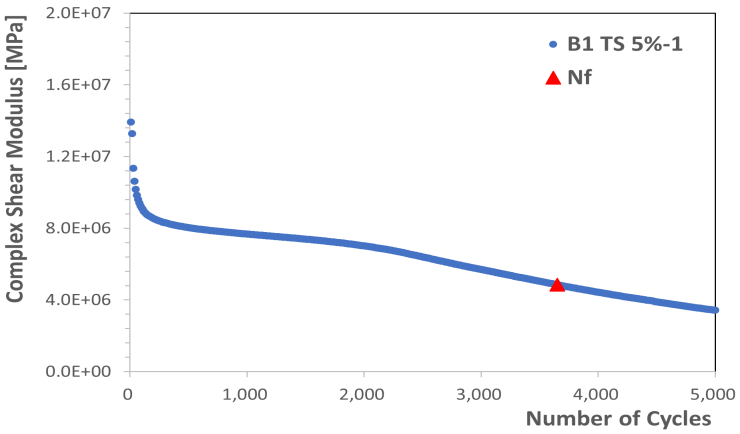

(a)

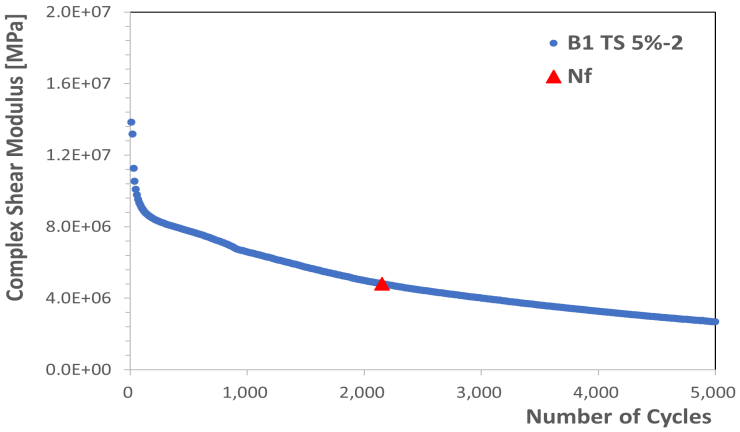

(b)

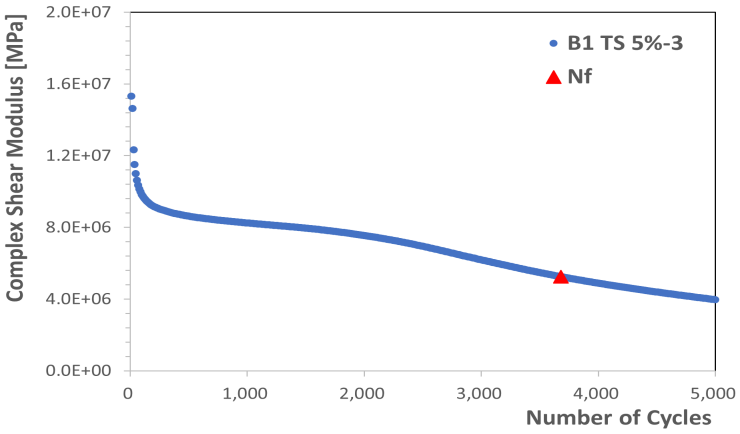

(c)

Figure B.3.: Binder 1 modulus evolution at 5% strain in TS test.

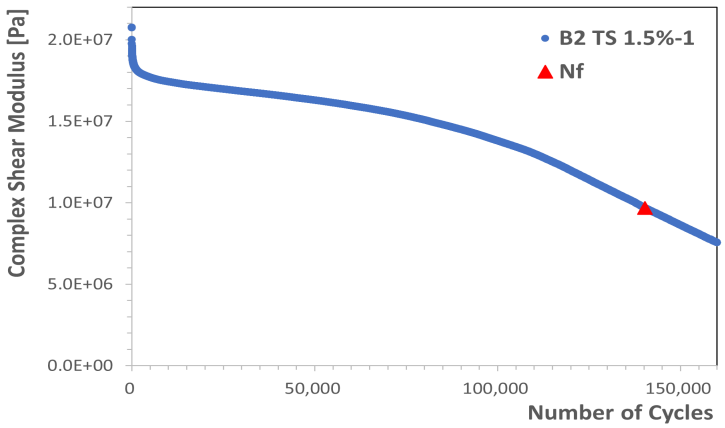

(a)

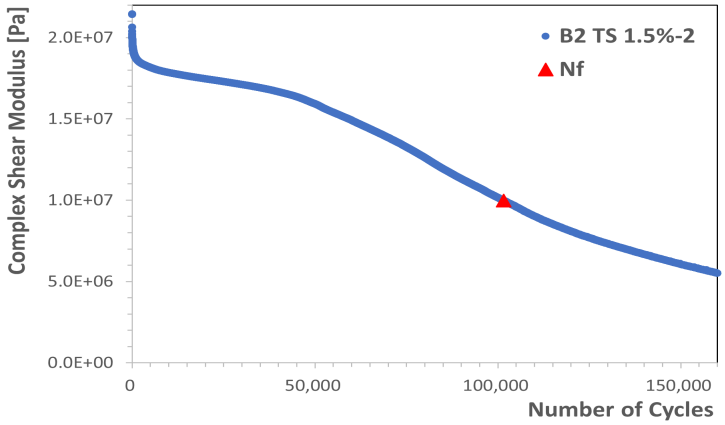

(b)

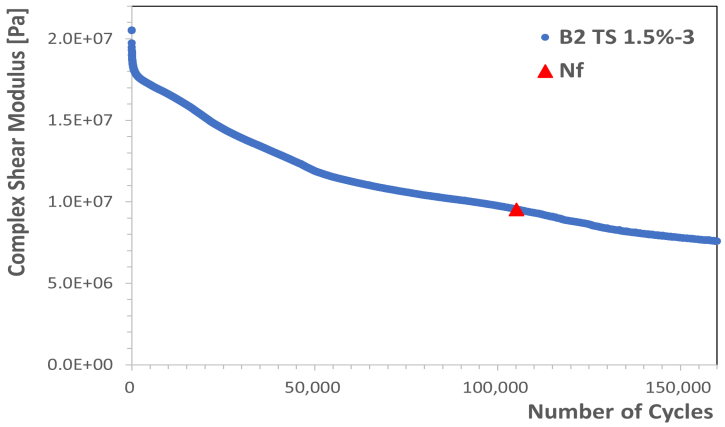

(c)

Figure B.4.: Binder 2 modulus evolution at 1.5% strain in TS test.

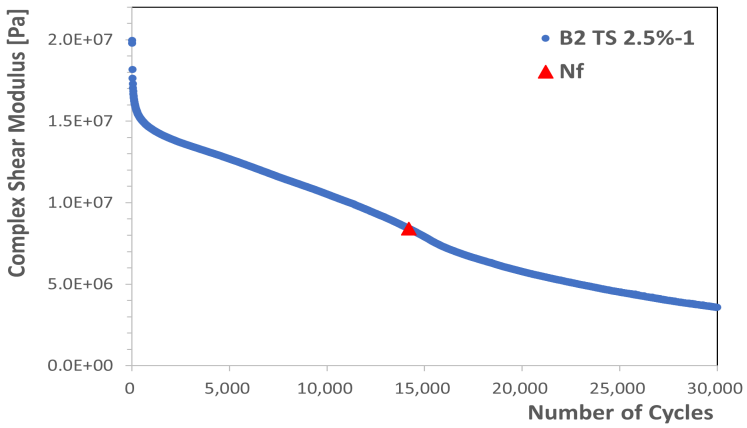

(a)

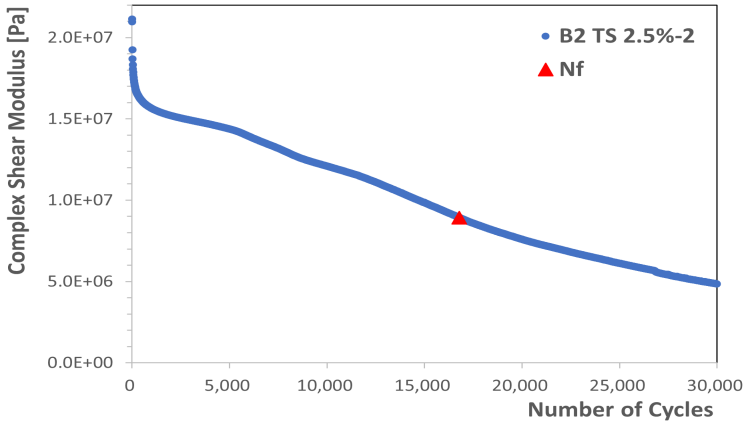

(b)

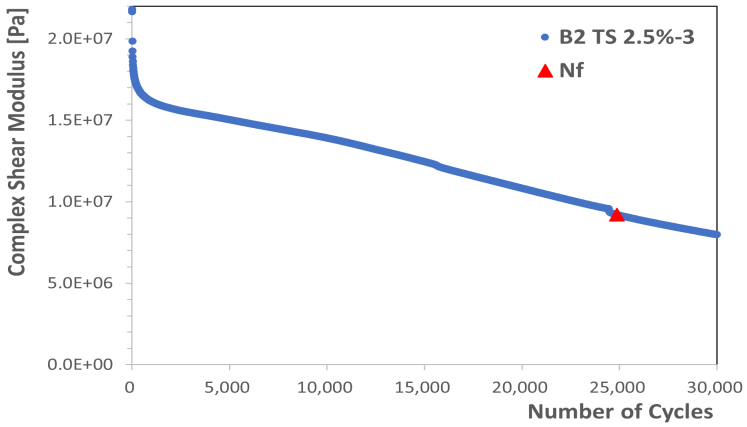

(c)

Figure B.5.: Binder 2 modulus evolution at 2.5% strain in TS test.

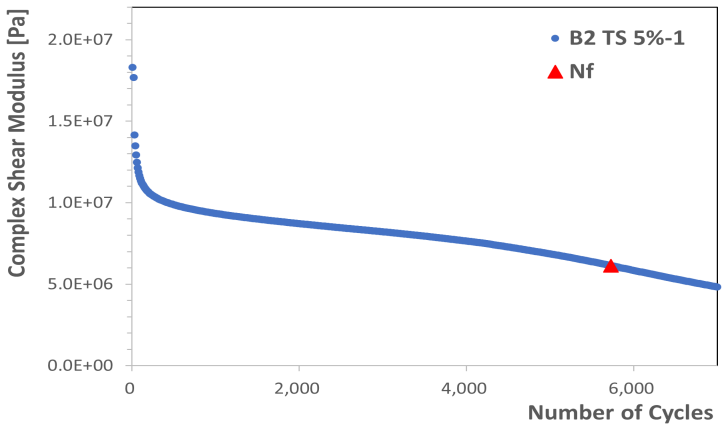

(a)

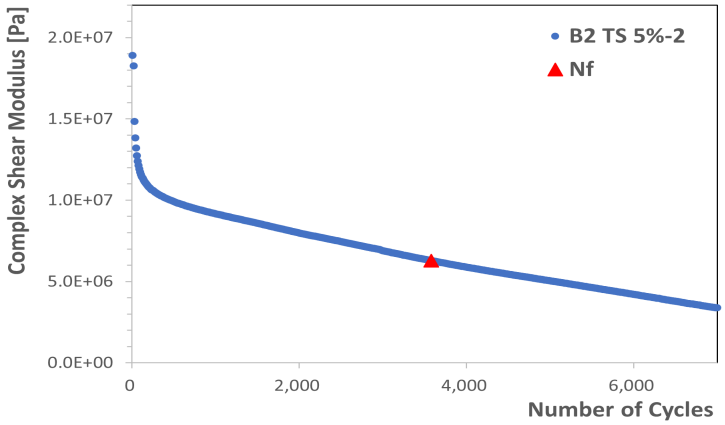

(b)

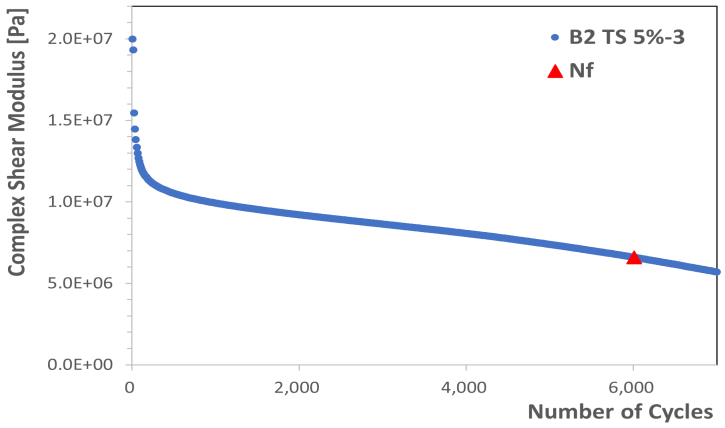

(c)

Figure B.6.: Binder 2 modulus evolution at 5% strain in TS test.

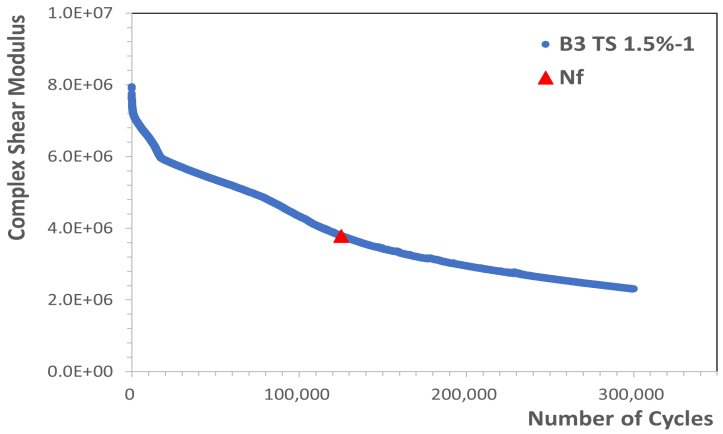

(a)

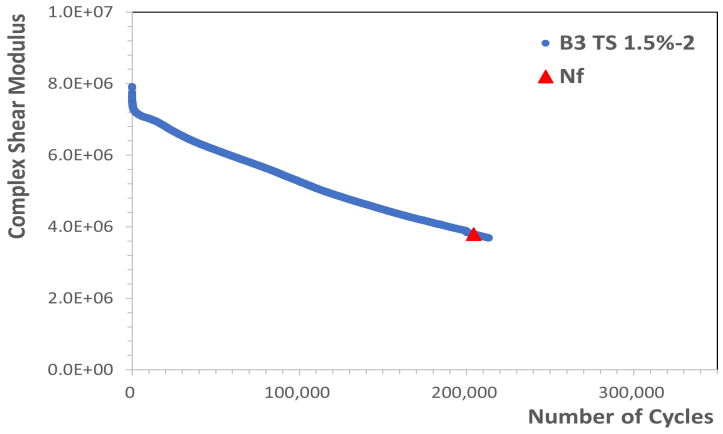

(b)

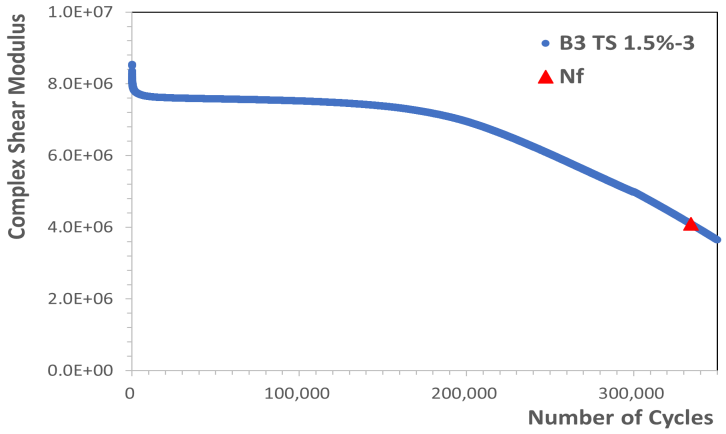

(c)

Figure B.7.: Binder 3 modulus evolution at 1.5% strain in TS test.

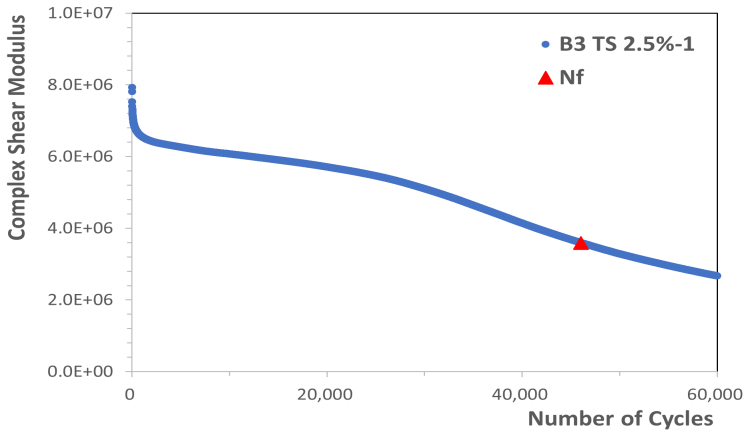

(a)

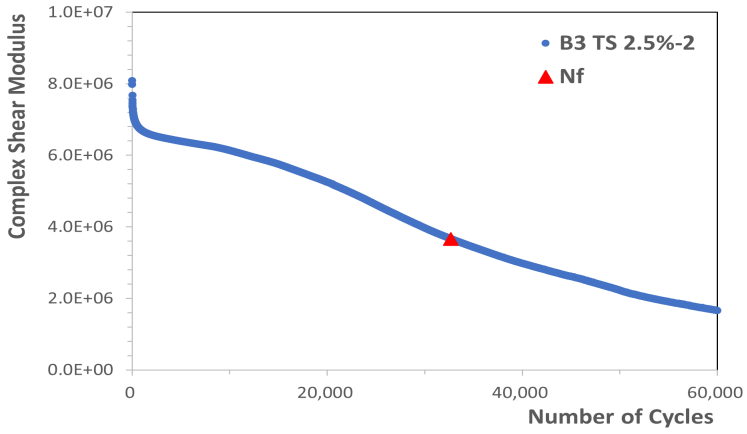

(b)

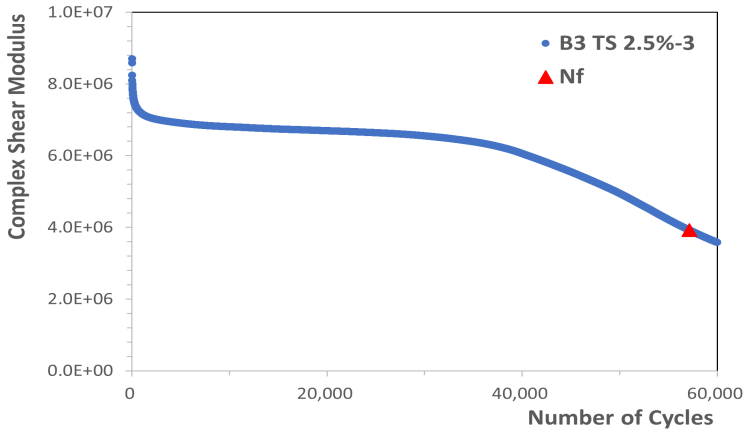

(c)

Figure B.8.: Binder 3 modulus evolution at 2.5% strain in TS test.

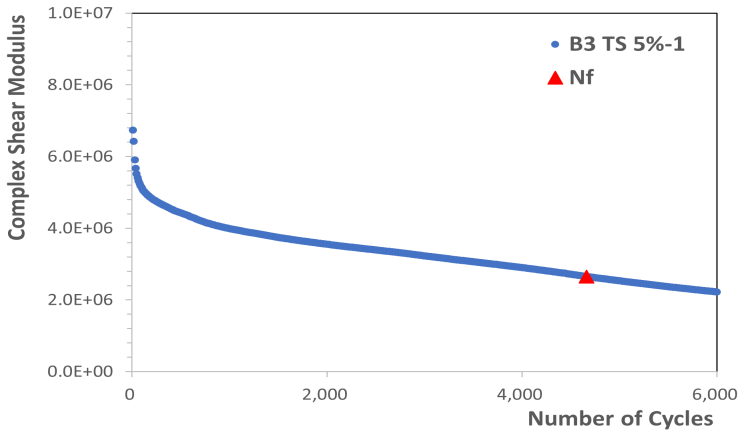

(a)

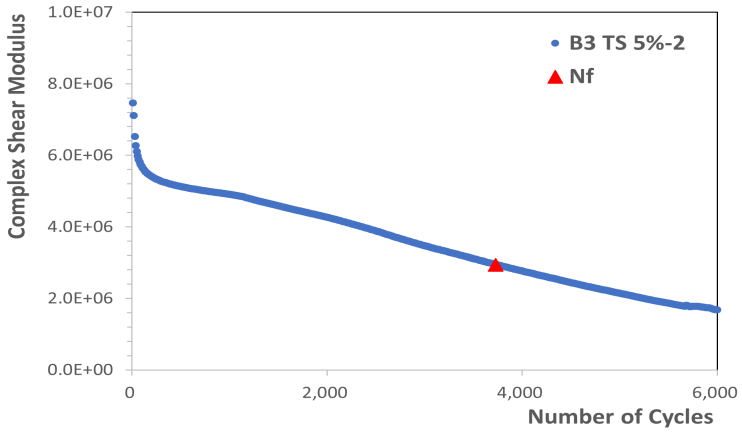

(b)

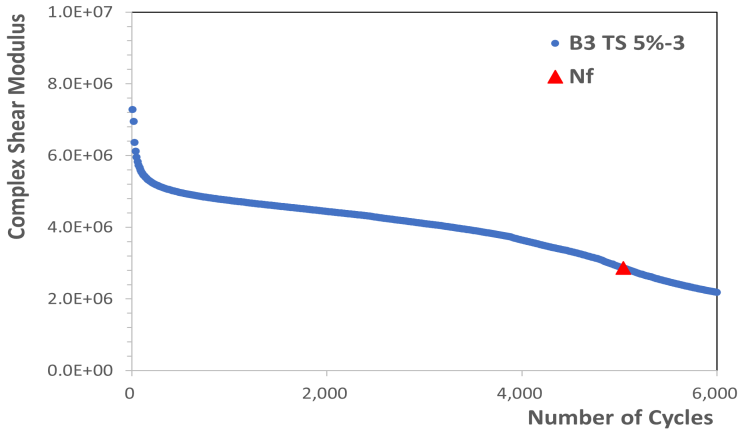

(c)

Figure B.9.: Binder 3 modulus evolution at 5% strain in TS test.

B.2. Linear Amplitude Sweep Test C-S Curves

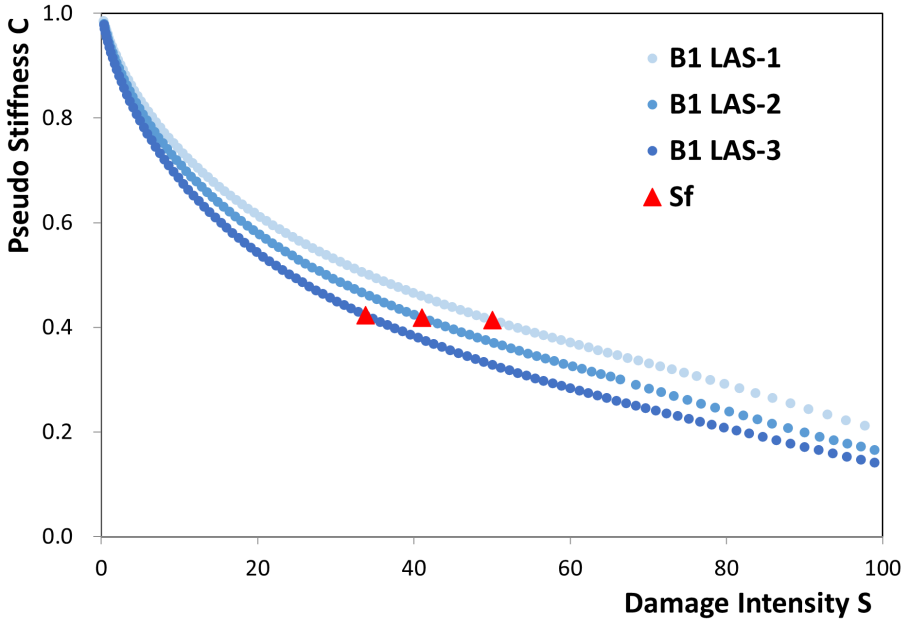

Figure B.10.: Binder 1 LAS test C-S curve.

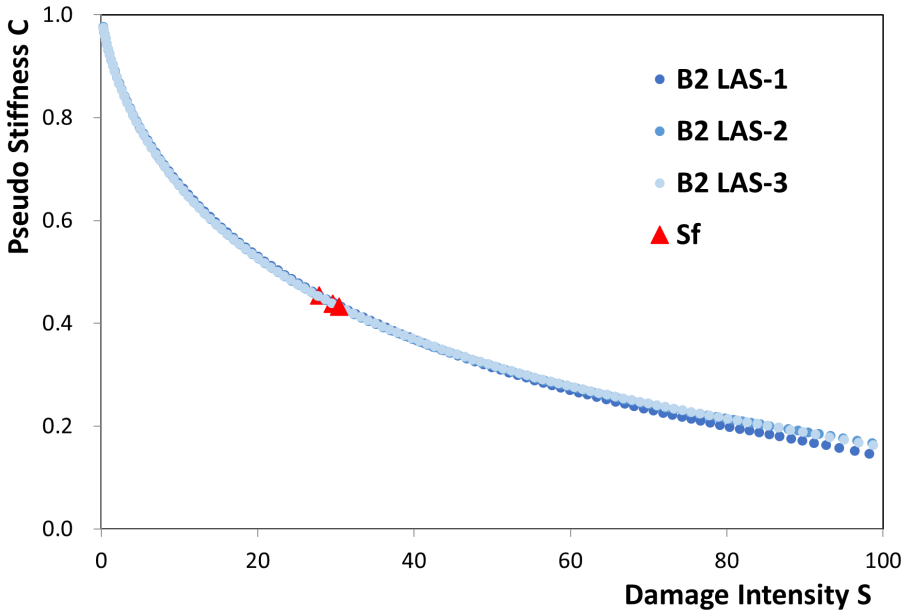

Figure B.11.: Binder 2 LAS test C-S curve.

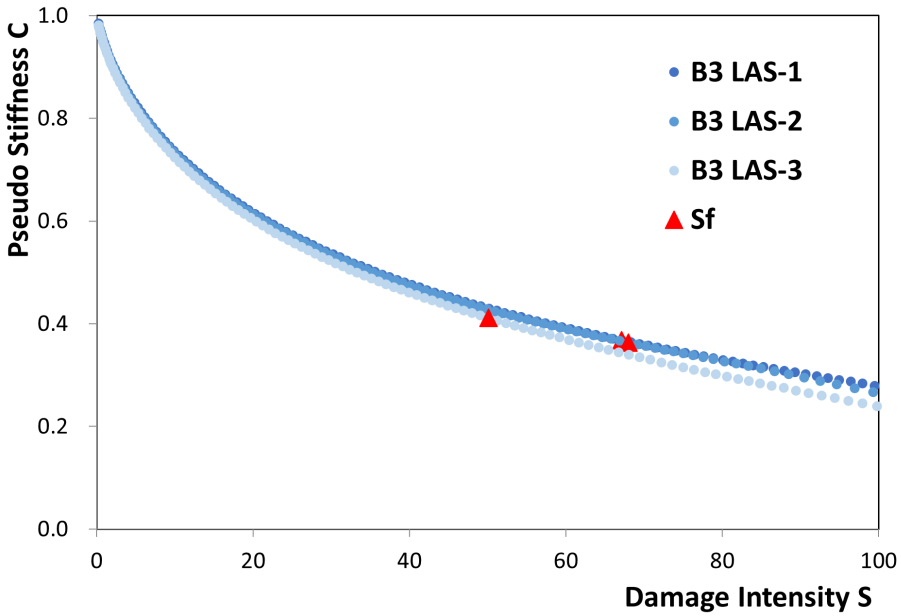

Figure B.12.: Binder 3 LAS test C-S curve.

C. Healing Test Results

C.1. TS-H Single Modulus Evolution Curves

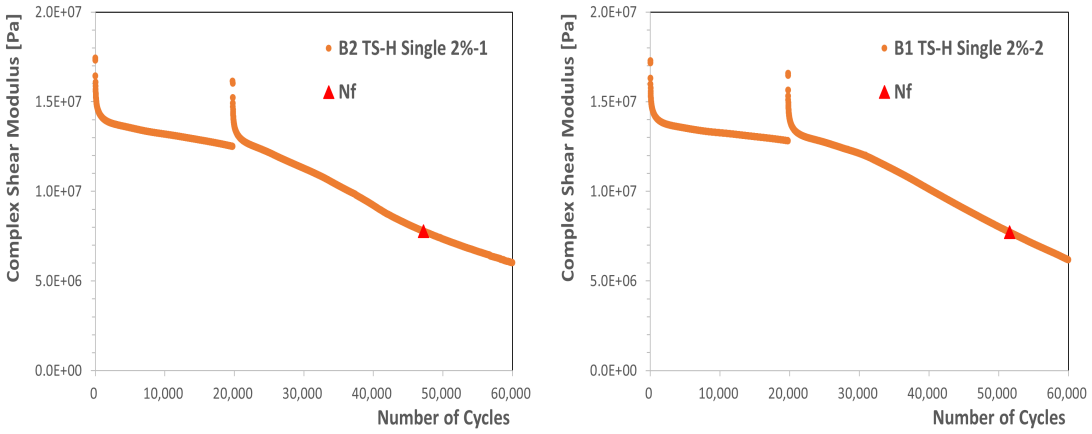

(a) (b)

Figure C.1.: Binder 1 modulus evolution at 2% strain in TS-H Single test.

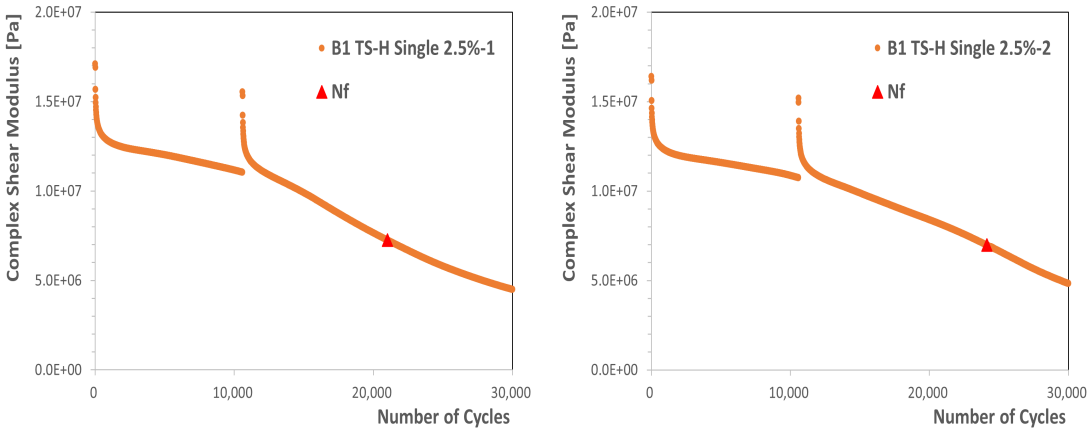

(a) (b)

Figure C.2.: Binder 1 modulus evolution at 2.5% strain in TS-H Single test.

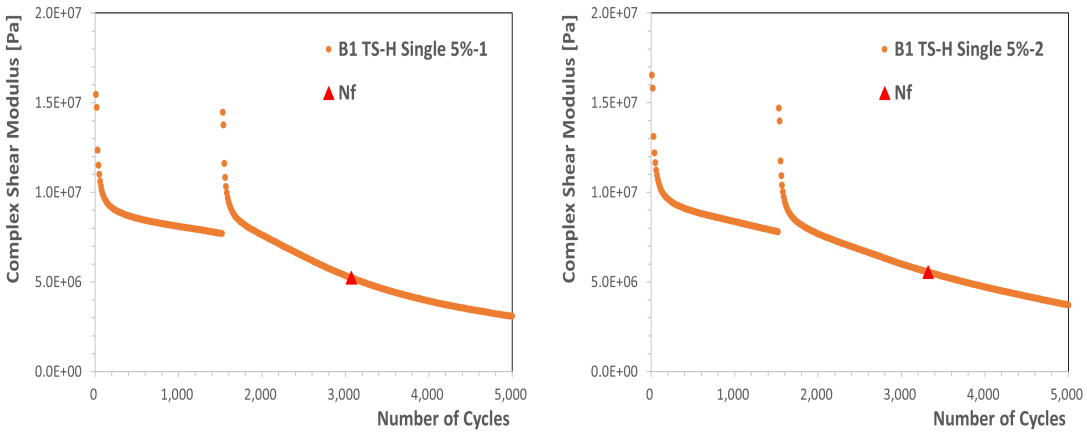

(a) (b)

Figure C.3.: Binder 1 modulus evolution at 5.0% strain in TS-H Single test.

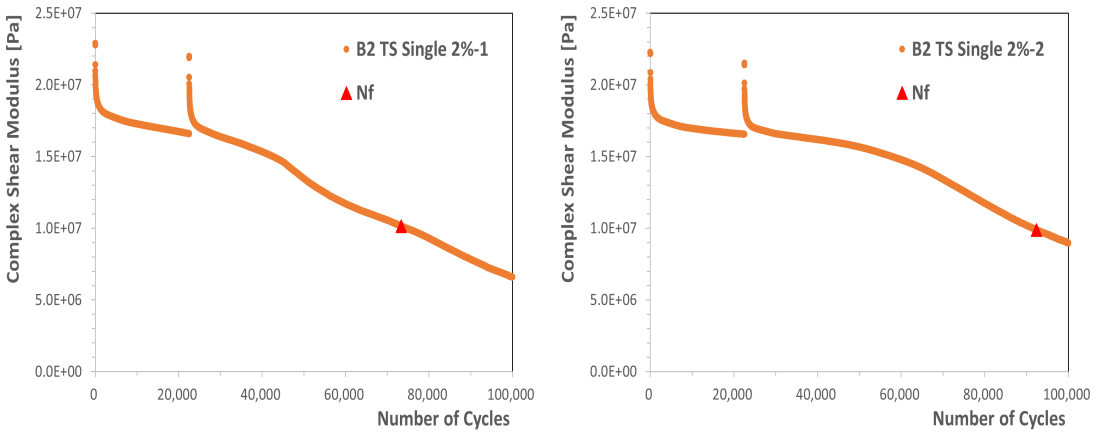

(a) (b)

Figure C.4.: Binder 2 modulus evolution at 2.0% strain in TS-H Single test.

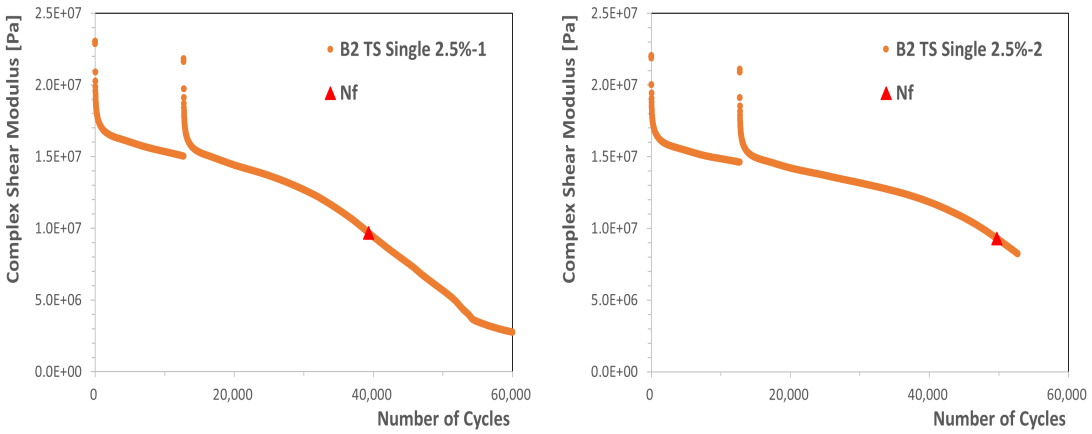

(a) (b)

Figure C.5.: Binder 2 modulus evolution at 2.5% strain in TS-H Single test.

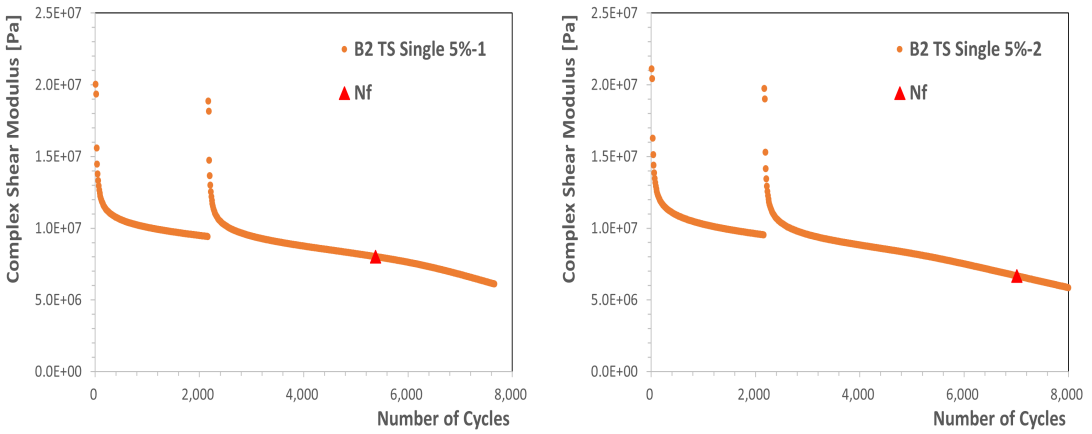

(a) (b)

Figure C.6.: Binder 2 modulus evolution at 5.0% strain in TS-H Single test.

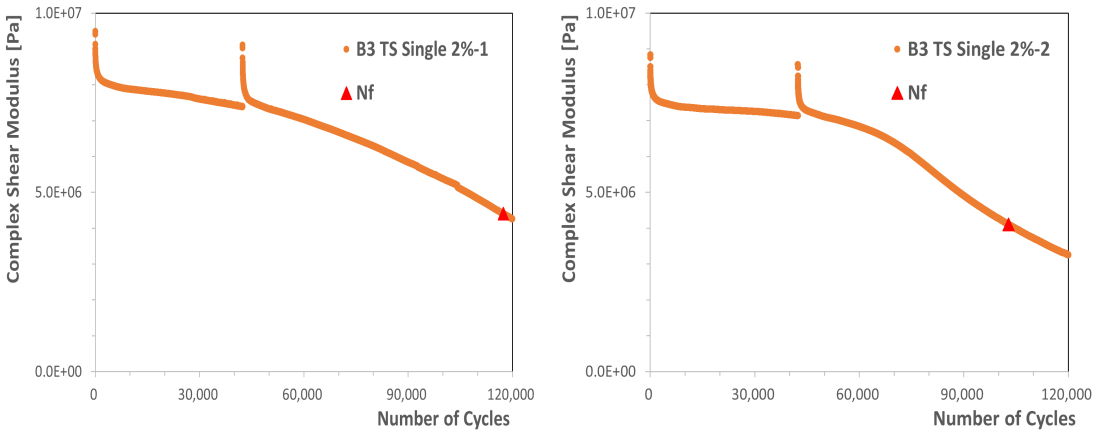

(a) (b)

Figure C.7.: Binder 3 modulus evolution at 2.0% strain in TS-H Single test.

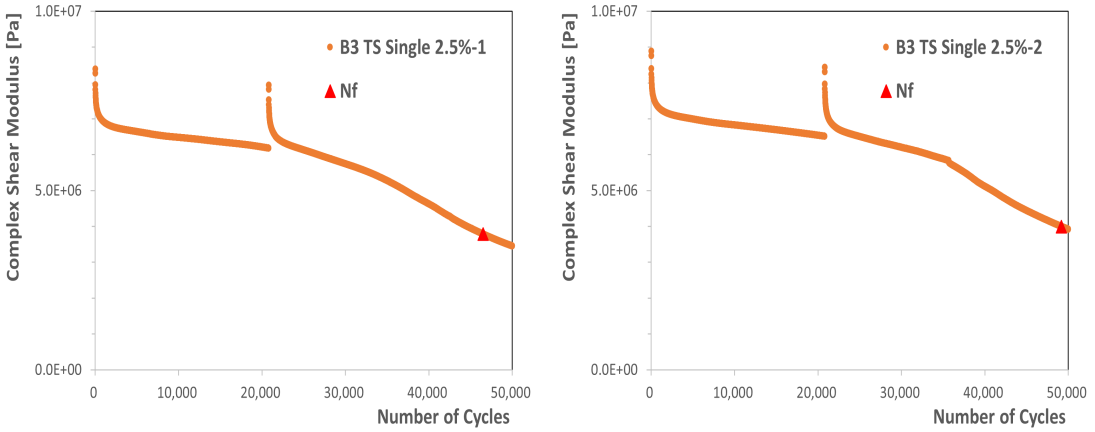

(a) (b)

Figure C.8.: Binder 3 modulus evolution at 2.5% strain in TS-H Single test.

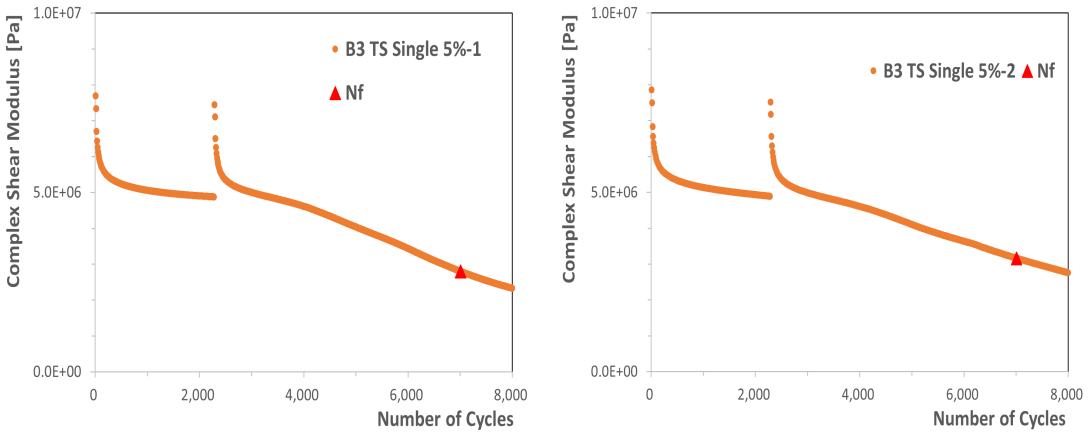

(a) (b)

Figure C.9.: Binder 3 modulus evolution at 5.0% strain in TS-H Single test.

C.2. TS-H Multi Modulus Evolution Curves

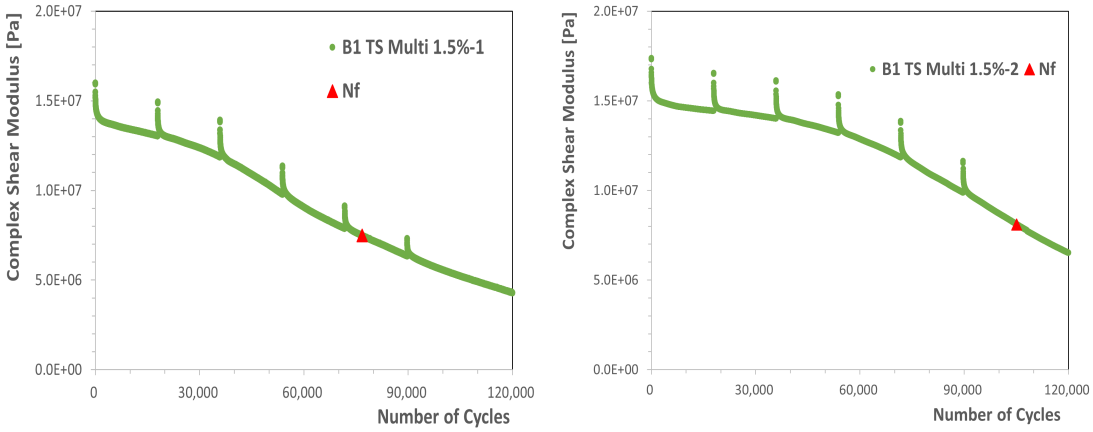

(a) (b)

Figure C.10.: Binder 1 modulus evolution at 1.5% strain in TS-H Multi test.

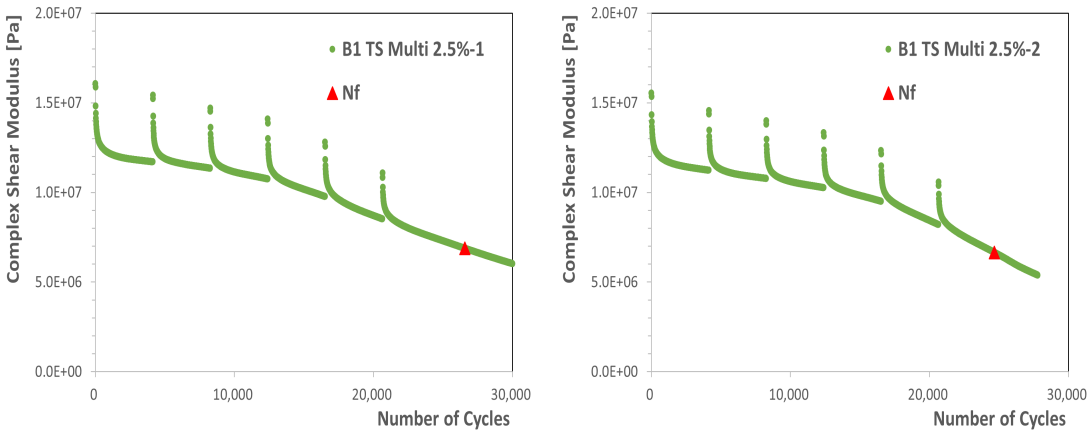

(a) (b)

Figure C.11.: Binder 1 modulus evolution at 2.5% strain in TS-H Multi test.

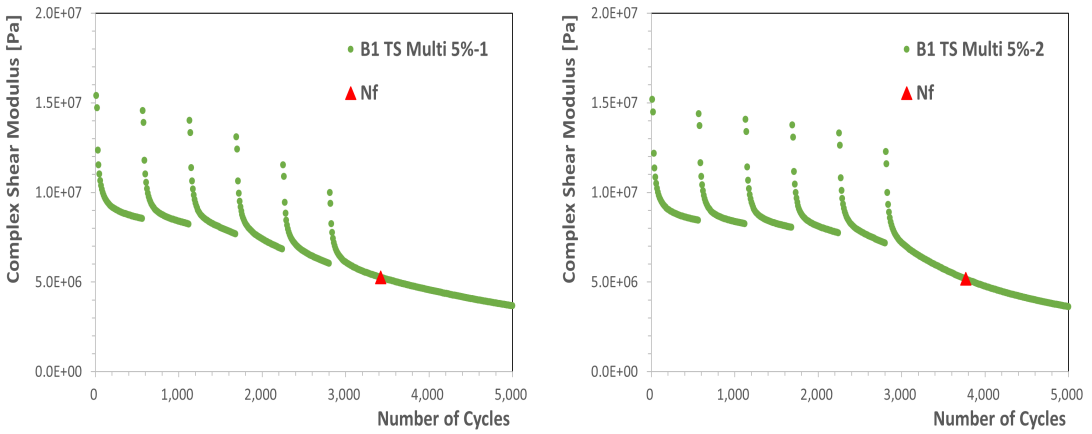

(a) (b)

Figure C.12.: Binder 1 modulus evolution at 5.0% strain in TS-H Multi test.

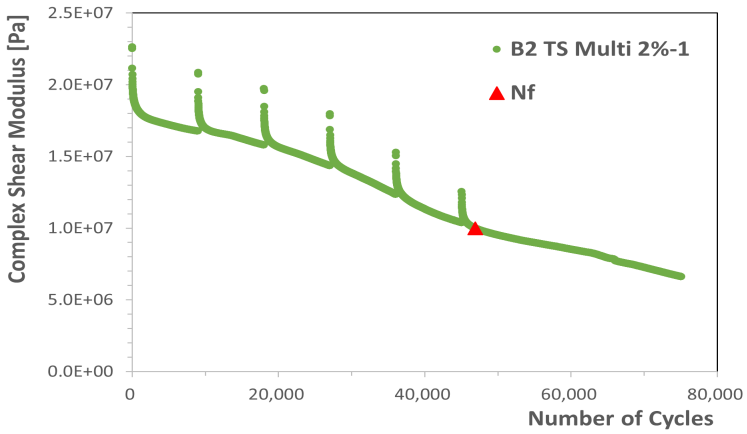

(a)

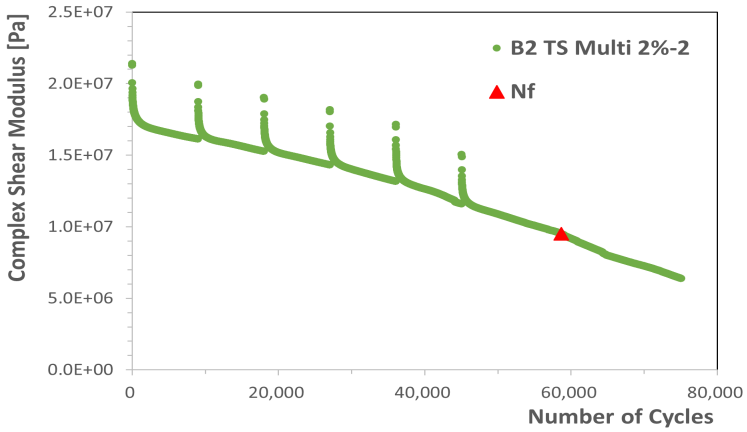

(b)

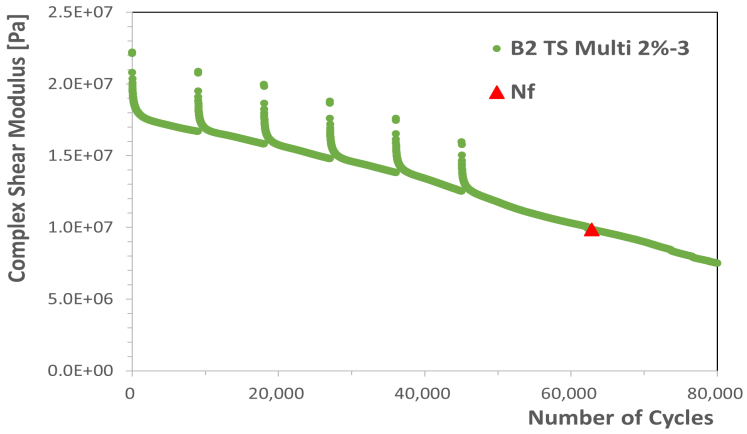

(c)

Figure C.13.: Binder 2 modulus evolution at 2.0% strain in TS-H Multi test.

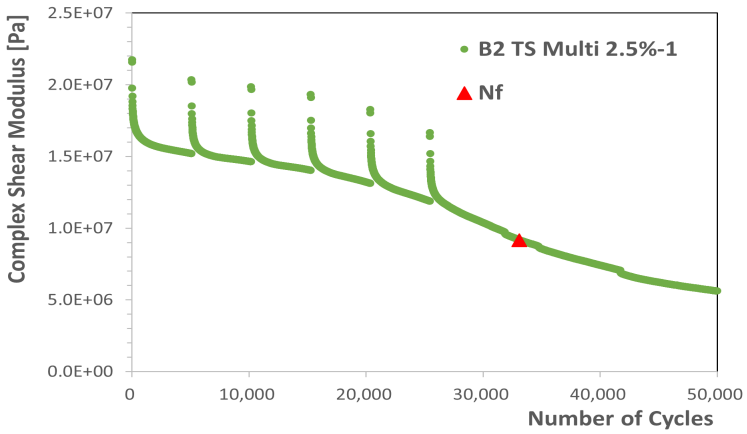

(a)

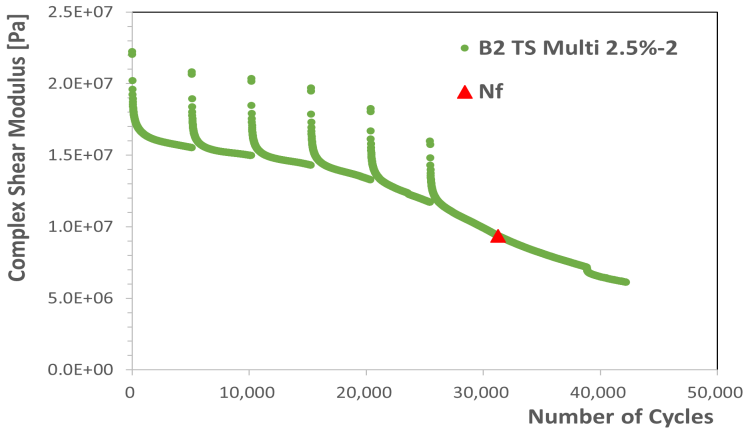

(b)

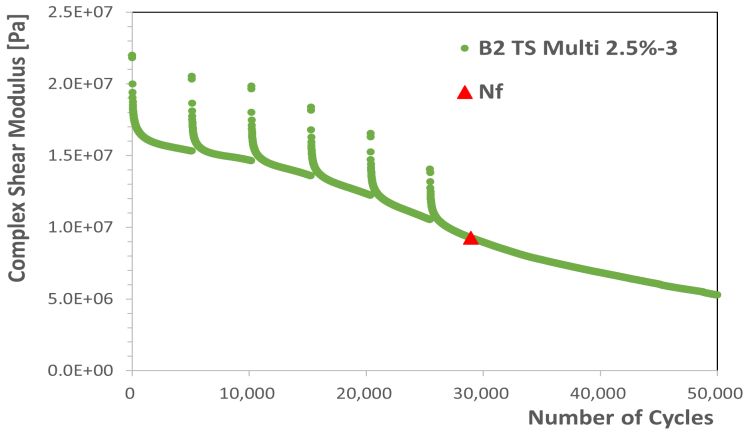

(c)

Figure C.14.: Binder 2 modulus evolution at 2.5% strain in TS-H Multi test.

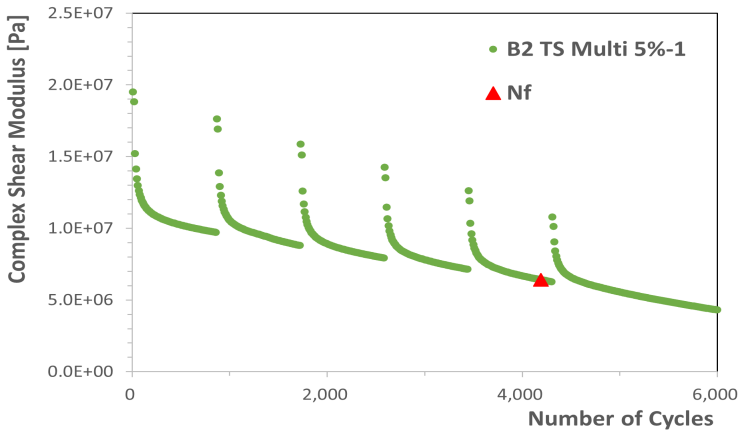

(a)

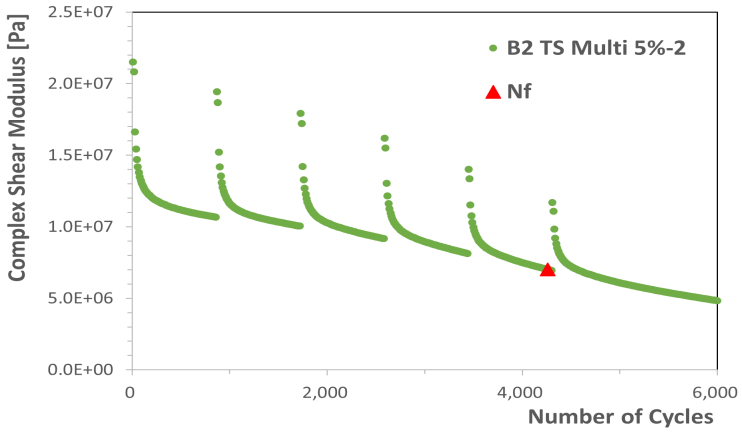

(b)

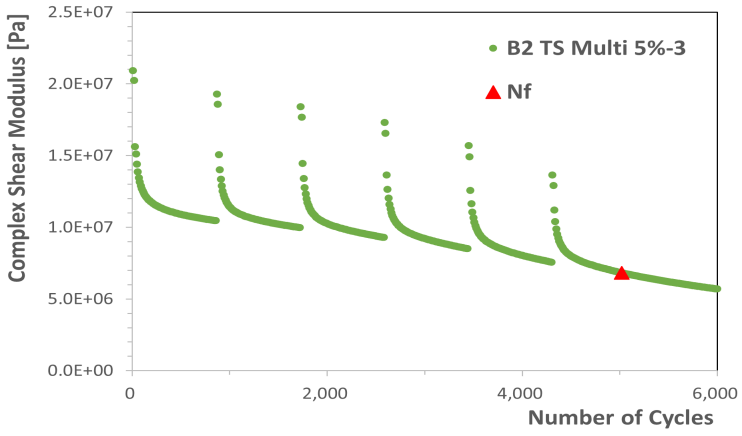

(c)

Figure C.15.: Binder 2 modulus evolution at 5.0% strain in TS-H Multi test.

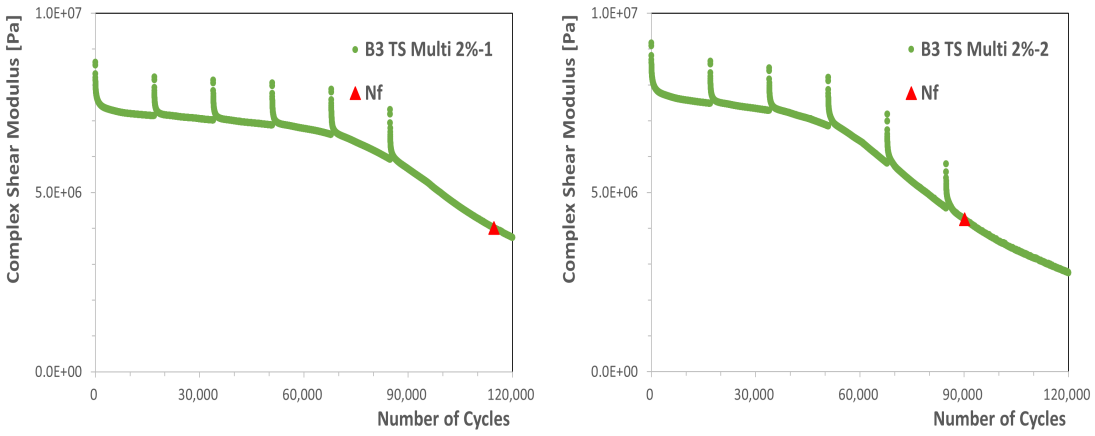

(a) (b)

Figure C.16.: Binder 3 modulus evolution at 2.0% strain in TS-H Multi test.

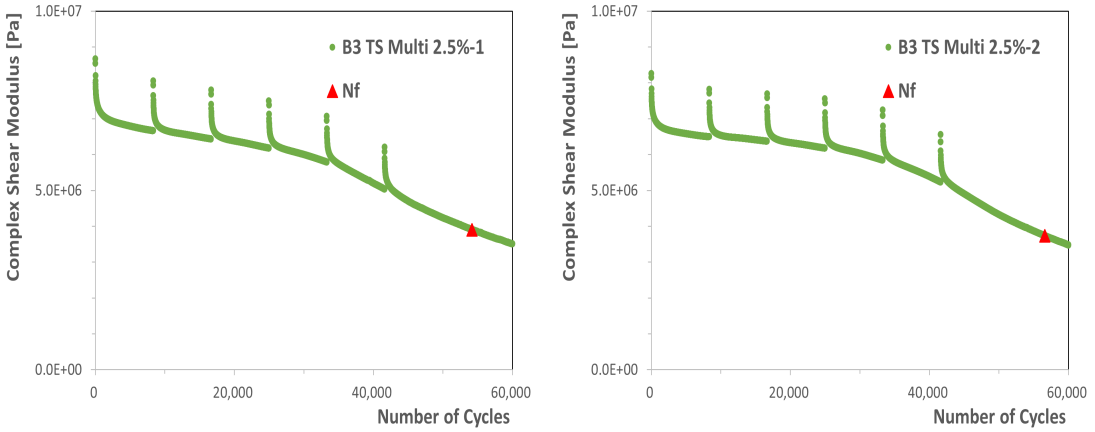

(a) (b)

Figure C.17.: Binder 3 modulus evolution at 2.5% strain in TS-H Multi test.

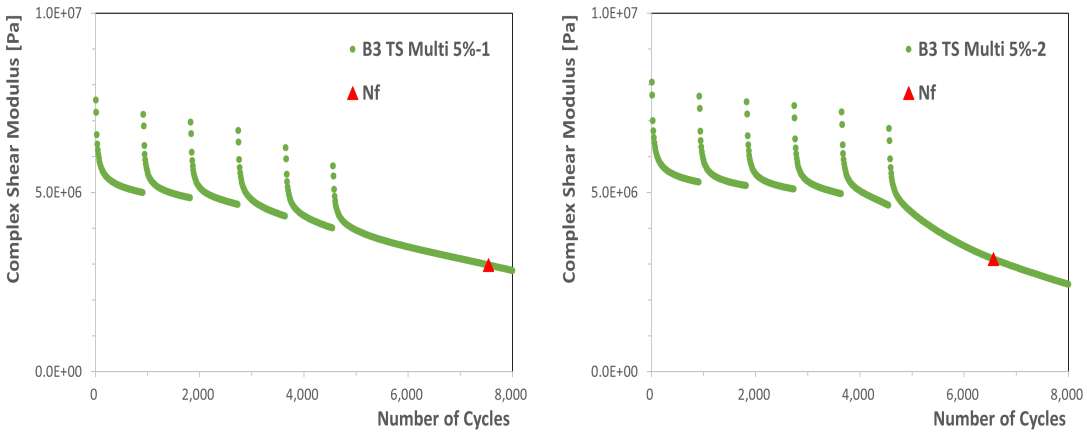

(a) (b)

Figure C.18.: Binder 3 modulus evolution at 5.0% strain in TS-H Multi test.

C.3. LAS-H Test Results

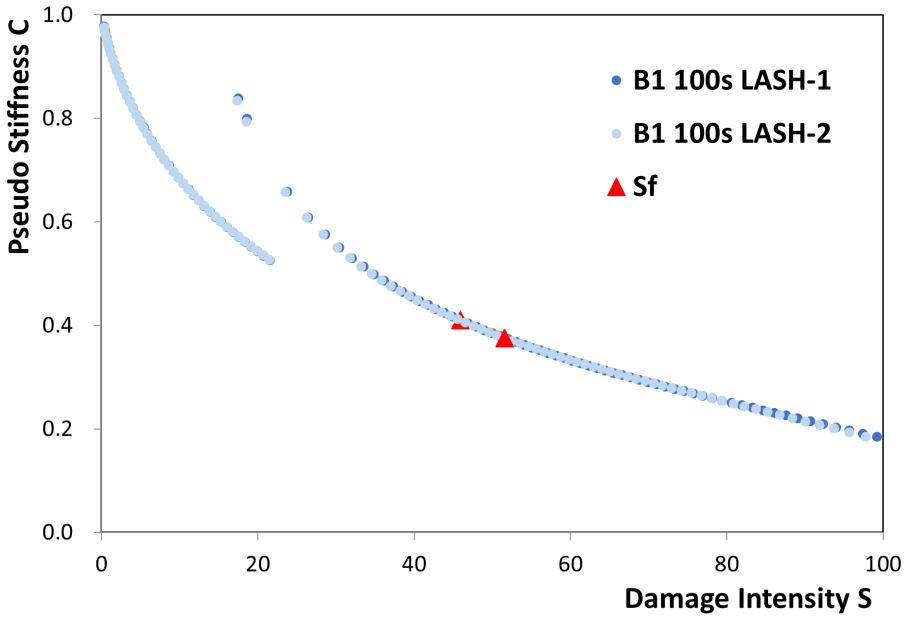

Figure C.19.: Binder 1 LASH 100s test C-S curve.

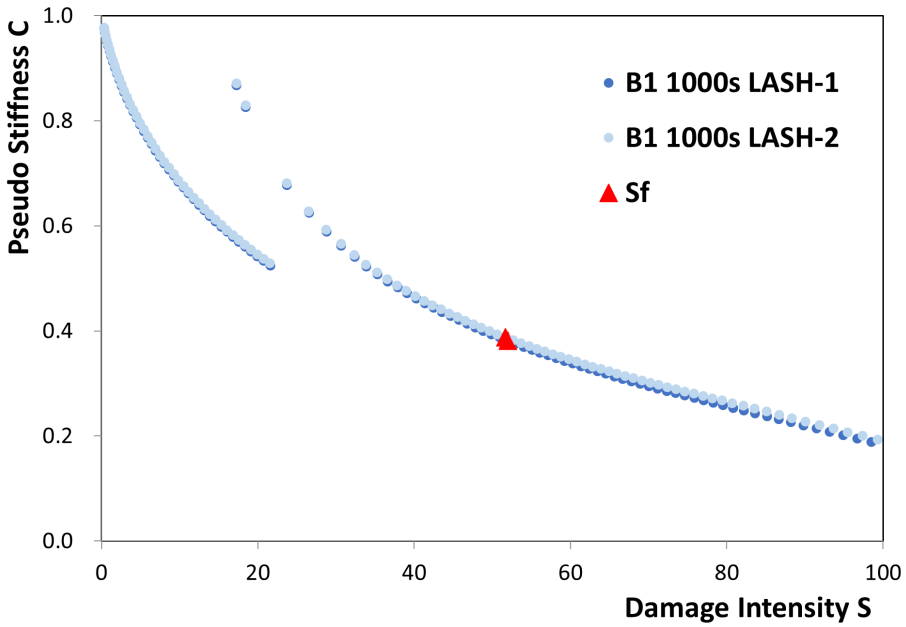

Figure C.20.: Binder 1 LASH 1000s test C-S curve.

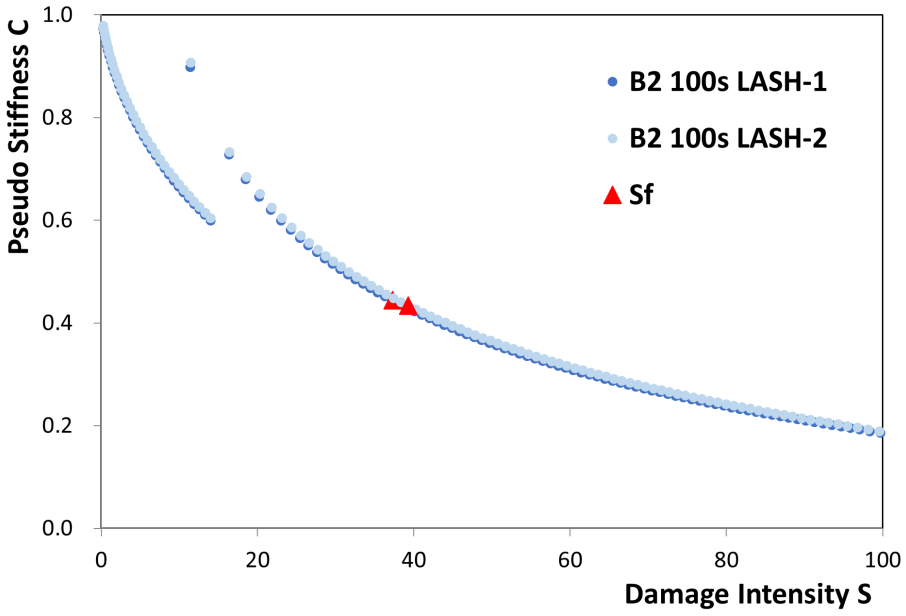

Figure C.21.: Binder 2 LASH 100s test C-S curve.

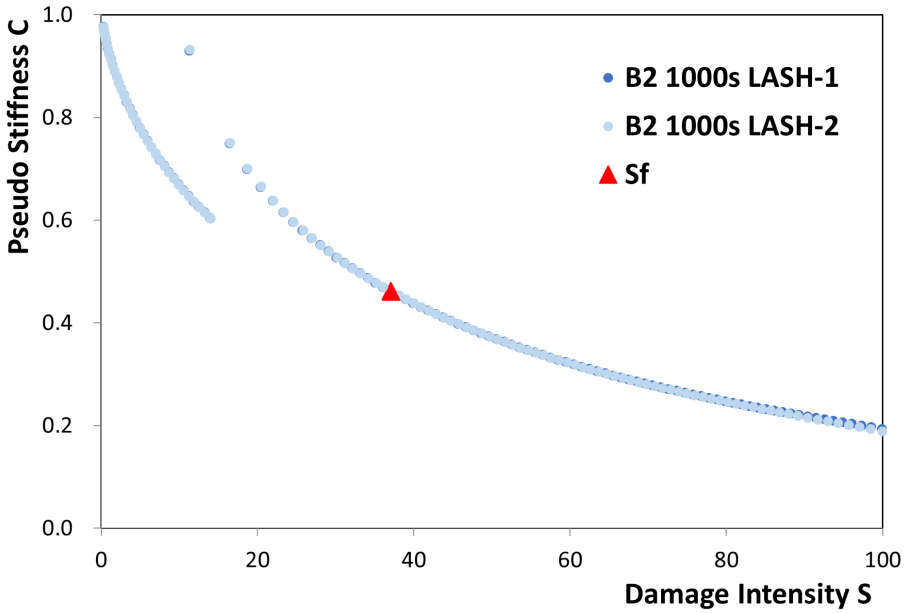

Figure C.22.: Binder 2 LASH 1000s test C-S curve.

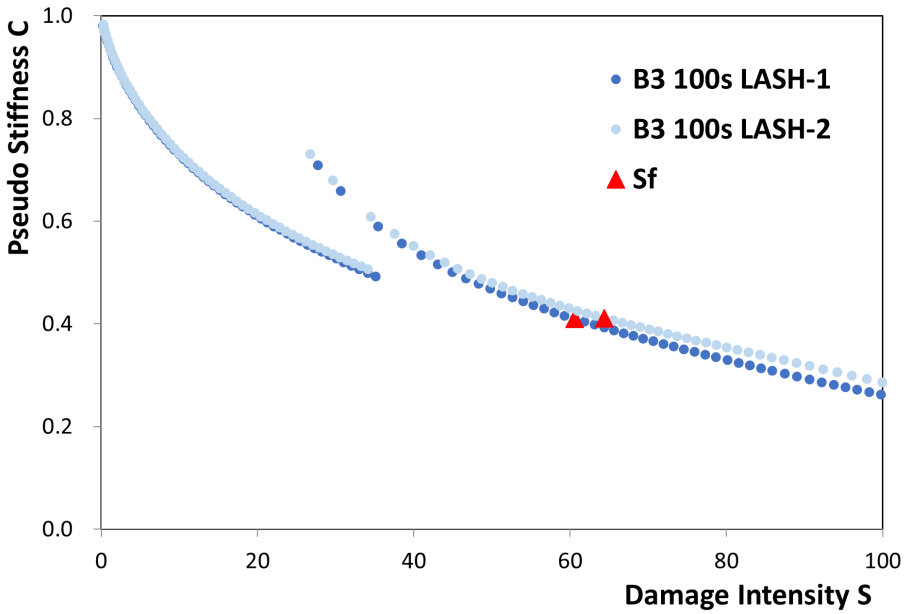

Figure C.23.: Binder 3 LASH 100s test C-S curve.

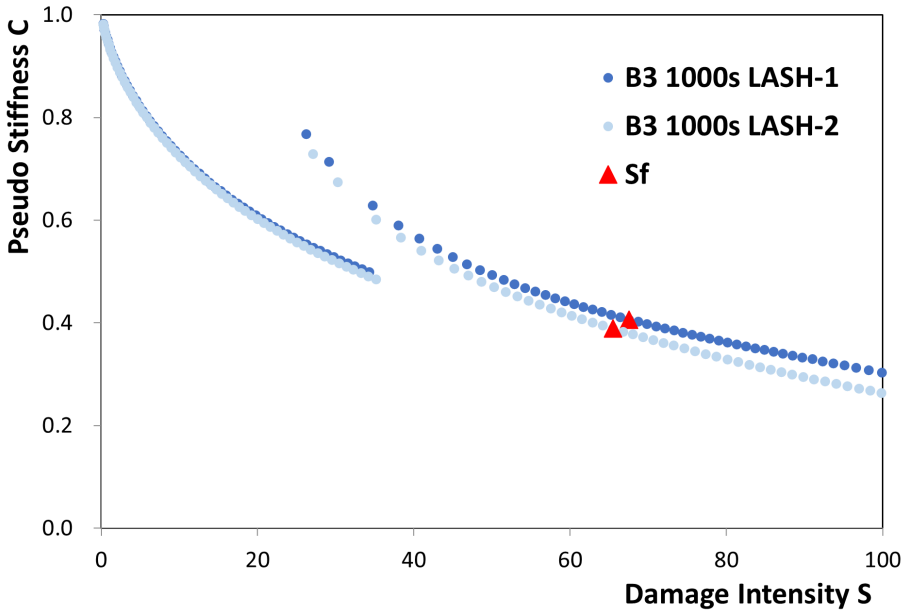

Figure C.24.: Binder 3 LASH 1000s test C-S curve.

Table C.1.: LAS Healing index of three binders under 100s and 1000s rest period.

Healing period (s)	Binder 1	Binder 2	Binder 3
100	19.12%	18.53%	21.45%
1000	19.86%	19.18%	23.22%